NTNU

Norwegian University of
Science and Technology

Optimal Operation of a Distributed System with High Share of Power Electronic Loads

Nadeem Jelani

Master of Science in Electric Power Engineering
Submission date: July 2010
Supervisor: Marta Molinas, ELKRAFT

Norwegian University of Science and Technology
Department of Electric Power Engineering

Problem Description

Reactive power producing power electronic interfaces for loads can always be used to support the voltage and reduce the losses in the power system in which they are connected. The design of control structure plays an important role in the performance of the converter control system. The understanding and development of the tuning rules for the optimal performance is one of the tasks in the thesis. The stability of a power electronic load needs to analytically investigated and verified by simulation studies. Several probable sources of instability in the distribution system and the impact of distributed reactive injection by parallel converters is to be investigated. At the same time, optimization of the network from the power flow point of view will be analyzed by injecting / absorbing an amount of reactive current that will minimize overall distribution losses.

Assignment given: 15. February 2010
Supervisor: Marta Molinas, ELKRAFT

Abstract

The tendency of connecting the loads to the three phase AC system through power electronic interfaces is increasing with time. These interfaces greatly affect the performance of the power system when properly operated. The injection of reactive power by these interfaces provides the possibility to support the voltage, increase the stability margins and decrease the power losses in the power system.

The power electronic loads when tightly regulated consume constant power from the grid and therefore exhibit negative resistance instability behavior. A fast control system with high stability margins is desirable for the converters. This thesis deals with the control of power electronic loads and the stability of the AC distribution system. One of the objectives of the work is to understand the basic control structure of the converters and establish the tuning rules for the PI regulators of the converter controllers.

A basic power electronic converter is considered and vector control method is implemented. A mathematical model of the control system for the converter is described and transfer functions are analyzed in frequency domain for different values of grid voltage. The simulations in time domain are performed in PSCAD/EMTDC software. The simulation results validate the results from the frequency domain analysis. The simulation analysis also shows that the stability of the converter in generation mode is higher as compared to when it acts as a load.

A larger model of AC distribution system with different shares of loads is investigated for the transient stability. It has been observed through simulations that the injection of reactive power during contingency greatly improve the stability limits of the system. However this increase in the stability margins comes at the cost of an increase in converter current rating. A comparison between the distributed injection by parallel converter and centralized injection through STATCOM confirms the advantages of the distributed injection.

The simulations for power flow optimization show that the reactive injection by constant power loads decreases the total current in the distribution line. A methodology is developed for loss minimization based on the dispersed injection of reactive current by the power electronic loads. This methodology helps to reduce the power losses to 50% of the initial value.

Preface

This master's thesis is written at the Department of Electric Power Engineering in the Norwegian University of Science and Technology (NTNU) during the Spring Semester, 2010. This thesis is a continuation of my work in specialization project during the Fall Semester, 2009.

First of all, I would like to thank my supervisor Professor Marta Molinas for her timely advices, continuous support and encouragement. From the point of origin to the point of completion of my thesis, I never found a single moment when my questions were not answered. I would like to mention that it would not be possible for me to write a paper in connection to the thesis work without her guidance and ideas. This paper is included in the appendix of this report and is presented in IEEE-ISIE (July 4-7, 2010 Bari, Italy).

I am also grateful to the Higher Education Commission (HEC) of Pakistan for funding my studies in Norway.

I am thankful to my mother, Khadija Bibi and my brothers for being there always for me to keep my moral high, regardless of being thousands of miles away from me. I would also like to thank my friends who supported me and encouraged me whenever I felt alone.

I hope that the reader will find my work interesting, and that my contributions in this thesis can play a part for the further research.

_____

Nadeem Jelani
Trondheim, July 2010

Contents

Abbreviations

AC	:	**A**lternating **C**urrent
DC	:	**D**irect **C**urrent
CPL	:	**C**onstant **P**ower **L**oad
VSC	:	**V**oltage **S**ource **C**onverter
PWM	:	**P**ulse **W**idth **M**odulation
IGBT	:	**I**nsulated **G**ate **B**ipolar **T**ransistor
PLL	:	**P**hase **L**ocked **L**oop
PCC	:	**P**oint of **C**ommon **C**oupling
DER	:	**D**istributed **E**nergy **R**esources
IG	:	**I**nduction **G**enerator
IM	:	**I**nduction **M**otor

Chapter 1: Introduction

This chapter describes the problem to be solved and outline of this thesis as reader's guide. But first it discusses the motivation behind it.

1.1 Motivation

In response to the public concern about possible global warming and climate change, there is a growing interest in the development of environmentally friendly distributed generation technologies in recent years [1]. Deregulation of the power market will contribute to an increased use of distributed generation from renewable energy sources. Some other advantages like the reduction of power demand from the grid, the backup power function, the potential of improving the local power quality, and provision of ancillary services to the grid, are impelling the development of associated technologies, making possible to connect the distributed power systems to the utility grid [2].

The expansion of solid-state devices in ac power systems to improve the performance and flexibility resulted in extensive use of power electronic converters and motor drives in distribution systems. Consequently, power electronic converters are emergent interfaces for the loads in AC distribution systems [3]. Most of the loads in AC distribution systems have positive incremental impedance characteristic. However, power electronic loads, when tightly regulated, consume constant power and therefore exhibit negative incremental impedance characteristic. This can cause negative impedance instability. Power electronic loads usually have a controlled or uncontrolled rectifier at the front end. Different ways of handling these power electronic interfaces greatly affect the operation of AC distribution systems. By allowing injection of reactive current by power electronic interfaces would give the possibility to support the system voltage and increase the stability margins [4].

The role of power electronic interfaces for loads in AC distribution systems from the system stability point of view has not been systematically investigated. The stability of power electronic loads compared to traditional passive loads has for long time been a subject of interest in DC distribution systems [5][6]. For DC distribution systems, several criteria have been investigated to ensure stability with high share of CPLs. On the other hand similar

stability criteria have not yet become common subject of research for AC distribution system with high share of power electronic loads.

1.2 Scope of the Thesis Work

The thesis work is mainly focused on how the power electronic interfaces for loads can be used to optimize the overall performance of an AC distribution system. The objectives of the work are mentioned as follows:

- Analytical investigation of the control system for VSC based power electronic loads
- Development and understanding of tuning rules for converter controllers
- Frequency domain analysis of the transfer functions of converter controllers for reduced values of the grid voltage
- Verification of the converter control system stability through simulations
- Understanding the impact of reactive injection on transient stability margins of the AC distribution system
- Identification of the impact of generation and grid parameters on the transient stability margins
- Understanding the parallel operation of the converters in distribution system and impact of reactive injection on the current rating of the converter
- Identification of optimal operating point for the converters in distribution system
- Development of a methodology for the power flow optimization in distribution system

1.3 Report Outline

This thesis is structured as follows:

Chapter 1: Introduction presents the motivation behind this thesis. It gives an overview of the report and the problem to be solved.

Chapter 2: Background describes the theoretical background regarding the concepts relevant to the work done in this thesis.

Chapter 3: AC Distribution system: Case Study describes the basic distribution system model implemented in PSCAD/EMTDC software package and provides the details about the converter control system and tuning rules for the controllers.

Chapter 4: Stability Analysis of the Converter Control System presents the analytical investigation of the transfer functions of the converter controllers and verification of the stability through simulations.

Chapter 5: Transient Stability analysis of AC Distribution System presents the impact of reactive injection by CPL on stability margins and discusses the parallel operation of the converters.

Chapter 6: Power Flow Optimization of AC Distribution System presents a methodology for the reduction of losses in distribution system.

Chapter 7: Discussion presents a discussion on the accuracy of the results and some shortcomings in the implemented models.

Chapter 8: Conclusion and Future Work concludes the thesis by summing up the results and proposing the future work.

Appendix A: presents the mathematical expressions for park and clark transformations.

Appendix B: shows some figures about the simulation results obtained in transient stability analysis.

Appendix C: shows the implemented PSCAD/EMTDC models for converter stability

Appendix D: shows the implemented PSCAD/EMTDC models for transient stability

Appendix E: shows the paper presented in ISIE-IEEE 4-7 July, 2010 Bari

Chapter 2: Background

This chapter introduces the theoretical background regarding the concepts which are relevant to the work done in this thesis. It begins by describing the basics of distributed energy systems. Then it explains the different types of loads present in AC distribution system. More focus is put on the constant power loads and the instability associated with them. It also provides information of reactive power compensation technologies in distributed systems. It highlights shortly the losses in the AC distribution system and the methods to reduce them. In the end, it discusses briefly the impact of dispersed generation on AC distribution systems.

2.1 Basics of Distributed Power Systems

Distributed power system is a small source of electric power generation or storage (typically ranging from less than a kW to tens of MW) that is not a part of a large central power system and is located close to the point of utilization [7]. In the last few years technological advances in the development of small-scale generation have led Distributed Generation (DG) to play a major role on the future development of distribution systems [8].

There are broad range of prospective benefits to distributed generation both to the customer and the electrical supplier. For the user these benefits incorporate: reduced price volatility, greater reliability and improved power quality [9]. There are many potential benefits for the power supplier. Firstly, being DG located close to the loads, there is a reduction in both losses and voltage drops. Furthermore, the ability of DG system to provide ancillary services to the grid such as voltage support and stability is of immense advantage for the power supplier [10].

DG technologies include solar energy photovoltaics, wind turbines, fuel cells, small and micro sized turbine packages, stirling-engine based generators, and internal combustion engine-generators. These technologies are ingoing a period of rapid growth and commercialization [11].

Distributed power systems do not use a conventional grid coupled synchronous generator to convert primary energy into electricity. Instead, they use a squirrel cage or doubly fed induction generator or a synchronous or squirrel cage induction generator that is grid connected through a power electronic converter. In the case of solar panels and fuel cells, it is not the mechanical power that is converted into electricity. Because of the low power

production capabilities, DG are often connected to low and medium voltage grids and not to the high voltage transmission grid [12].

2.2 Composition of AC Distribution System

Distributed AC system is composed of both generation and different types of loads. It is generally beneficial to have generation of electrical energy as close to the point of consumption as possible. An example of generation unit is wind farm or a solar panel or a small hydropower plant. Basic structure of a distributed power system is shown in figure 2.1.

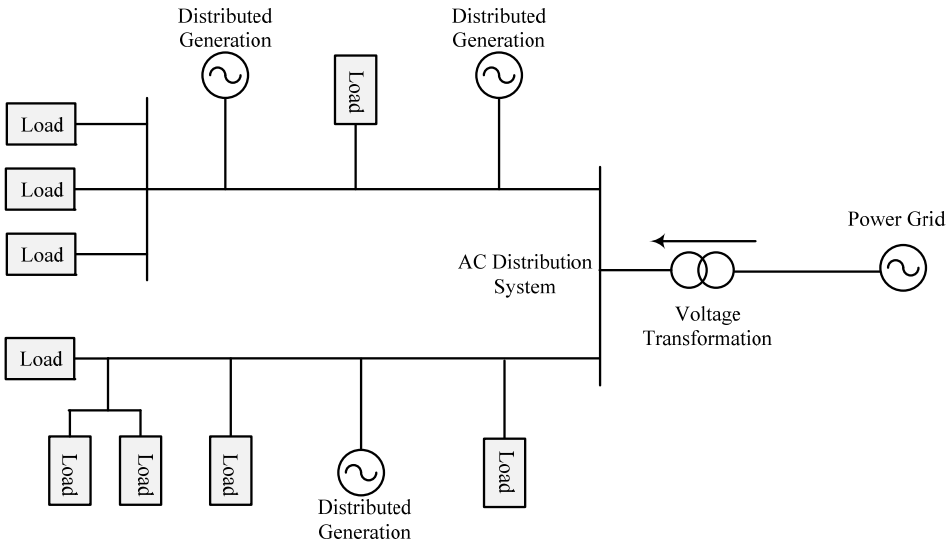

Figure 2.1 – Basic configuration of a distributed system

Solar energy photovoltaics (PV) systems convert solar energy into electric power. PV modules produce DC power. This DC power is then converted into AC power compatible with the electric power system by a power electronic (PE) inverter.

Wind energy systems on the other hand use three different design technologies. The wind systems using induction generators are connected directly to the grid without any PE interface. However wind system designs using double-fed induction generator (DFIG) or permanent magnet synchronous generators do not produce power at a voltage and frequency that is compatible with the electric power system. A PE based rectifier and inverter are therefore used to convert the full rated output of the machine to power that is compatible with the electric power system [9].

Small hydro systems are used where the resource is available. Most of the present applications use synchronous generators or induction generators connected directly to the electric power system without any PE interface [10].

The loads used in distribution system can be classified into passive or active loads. Passive loads consume power from the utility without taking into account the stability of the system. However an active load can be used to enhance the system stability if required. A load using power electronic interface is an example of active load. The main focus of this work is to investigate the operation of these power electronic interfaces for the loads in distribution system. These types of loads normally show a static characteristic and categorized as follows [13].

- **Constant impedance load:** The active and reactive powers vary with the square of the load voltage magnitude. It is also referred to as a constant admittance load. An incandescent lamp is an example of such kind of loads.
- **Constant current load:** The active and reactive powers are directly proportional to the load voltage magnitude.
- **Constant power load:** The active and reactive powers are independent of the load voltage magnitude. Controlled loads with Power electronic interface and motor drives when tightly regulated behave as constant power load [14].

Among electric loads, Constant Power Loads (CPLs) interfaced to the grid by power electronic converters are one of the most destabilizing types of loads under abnormal voltage conditions [4].

2.3 Power Electronic Loads in AC Distribution System

Figure 2.2 shows several loads connected to each bus in a distribution system. The responsibility of the source subsystem is to maintain the amplitude and frequency of the bus voltage fixed. It is assumed that some of the loads, which are fed from the source subsystem, are tightly regulated power electronic converters. Therefore, these power electronic loads, which may be voltage regulators or motor drives, behave as constant power loads [3].

Most of the power electronic loads have a rectifier at their front end. Therefore, generally, constant power loads are connected to AC distribution systems via a controlled or

uncontrolled rectifier. These loads consume constant active power from the generation system irrespective of any abnormalities in the system. In a CPL, input current decreases/increases when the input voltage increases/decreases. As a result, CPLs have negative impedance characteristics at the input terminals [14].

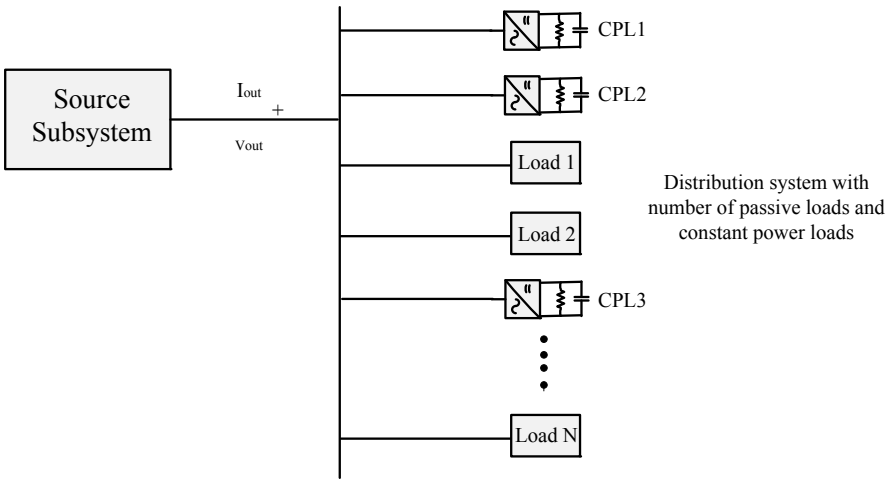

Figure 2.2 - Power electronic controlled constant power loads connected to a typical bus [3]

2.3.1 Absolute and Differential Impedance

The V-I characteristics of two typical loads are shown in figure 2.3. The left side figure represents an incandescent lamp, where the blue dashed line is the absolute impedance for a certain operating point that depends on the applied RMS voltage, and the red line represents the positive differential impedance, in that operating point. The right side figure can be that of a DC power supply, which shows negative differential impedance. In most cases it can be assumed that loads or sources connected to the grid with power electronic converters have the possibility to demonstrate negative differential impedance (NDI). This can lead to voltage instability [15].

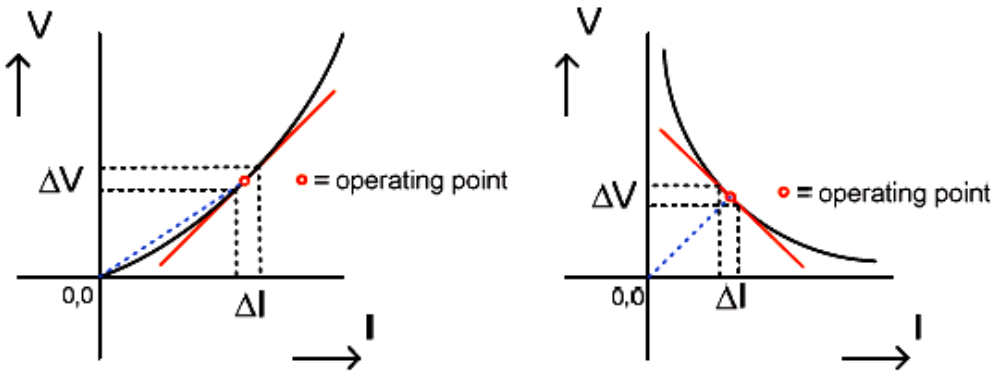

Figure 2.3 – Absolute and differential impedance [15]

2.3.2 Negative Resistance Behaviour of a Constant Power Load

Negative incremental resistance behaviour is typical feature of a constant power load. A constant power load is represented by figure 2.4.

R_{CPL} demonstrate the negative resistance seen from the AC distribution system. This small signal non-linear input resistance can be calculated by considering the input power equal to output power that is $P_{in}=P_o=v\cdot i$ and $v=\frac{P}{i}$ [16].

Differentiating the voltage with respect to the current yields negative input resistance:

$$\frac{dv}{di}=-i^{-2}\cdot P=-\left|\frac{P}{i^2}\right|=-\left|\frac{v^2}{P}\right|=-R_{CPL} \qquad (2.1)$$

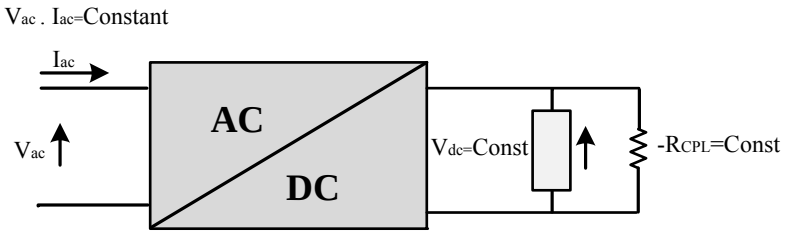

Figure 2.4 – Constant Power Load

In practice a lot of home appliances are loads with AC/DC converters inside, feeding an internal part that works on a constant dc voltage feeding the internal load. The control system of these AC/DC converters controls the direct voltage V_{dc} in a way that it is independent of the applied grid voltage v. This implies that the AC power is independent of the value of grid voltage [15]. Under reduced grid voltage the operation of the internal controller demands the AC/DC converter to draw more grid current to maintain the active power input to the converter at a constant value and the other way around.

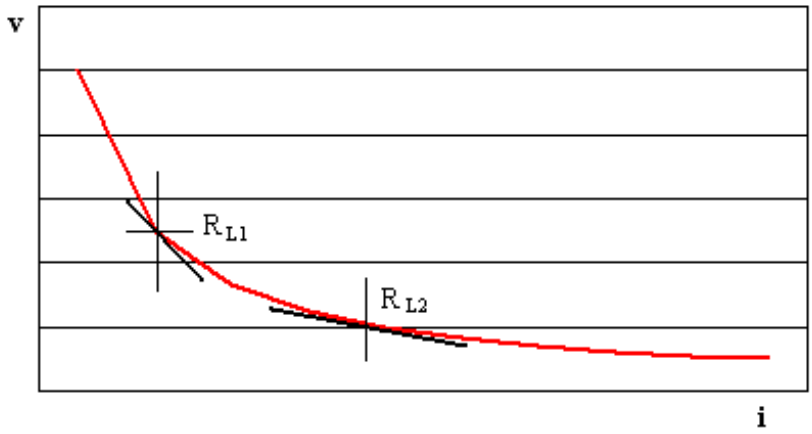

Figure 2.4 – Negative resistance behavior of a CPL [16]

The static input voltage *v-i* characteristic for the load is shown in figure 2.4; since P_{in} is a constant therefore plot is a hyperbola. This diagram shows two different values of input impedance, R_{LI} and R_{L2} at two different operating points. The slope of this characteristic is negative, therefore the resistance of the converter is known as a negative input resistance where, any increment in input voltage will cause a decrease in the input current and vice versa [16]. The constant power and negative input resistance characteristic potentially have destabilizing effects on the electrical supply system.

2.4 Reactive Power Compensation Technologies in Distributed Power Systems

Reactive power compensation is defined as the management of reactive power to improve the performance of AC power systems [17]. Reactive power compensation is viewed from three aspects:

- Load compensation for power factor improvement, to balance the real power drawn from the ac supply, to compensate voltage regulation, and to eliminate current harmonic components produced by large and fluctuating nonlinear industrial loads.
- Voltage support, to reduce voltage fluctuation at a given terminal of a transmission line [17].
- Stability improvement of the ac power system by increasing the maximum power transfer capacity.

Conventionally, the easiest and least-expensive method of providing the reactive power required by distributed systems based on squirrel-cage induction generator is to install capacitor banks at the generator terminals [18]. There are two approaches in installing capacitor banks:

- Connecting a fixed-capacitor bank at the generator terminals at all times
- Connecting multiple capacitor banks that are switched in and out based on the requirements.

An alternative approach to reactive power compensation is the use of static Var compensator (SVC), which in its simplest form, consists of a Thyristor Controlled Reactor (TCR) connected in parallel with a fixed-capacitor bank. SVC acts as a shunt-connected variable capacitive or inductive reactance, which generates or absorbs reactive power in order to regulate the voltage magnitude at the point of connection to the electric network [12].

The third reactive power compensation scheme is voltage source converter based STATCOM, which is composed of a converter with a capacitor or a dc voltage source on its DC side, a coupling transformer, and a control block. STATCOM is a controlled reactive-power source/sink that delivers or consumes the desired amount of reactive power entirely by means of electronic processing of voltage and current waveforms in a voltage-sourced converter [18]. However a STATCOM does not perform as a load cannot draw active power from the system.

In this work an ac distribution system model with voltage source converters controlling constant power loads will be investigated as provider of reactive power for improving the stability margins and minimizing the overall losses in the distribution system. These electronically controlled constant power loads behave like distributed STATCOMs and provide reactive power ancillary service to the grid [4][19].

2.5 Power Losses in AC Distribution System

Energy losses take place as power flows through the network to meet customer load demands. Some of the input energy is dissipated in the conductors and transformers along the delivery route. These losses are inherent in the processing and delivery of power but can be minimized. Losses represent a considerable operating cost, estimated to add 6 to 10 percent to the cost of electricity and some 25 percent to the cost of delivery [20].

Power losses in distribution systems vary with many factors depending on the system composition, such as level of losses through transmission and distribution lines, transformers, capacitors, insulators, etc. Power losses can be divided into two categories: real power loss and reactive power loss. The resistance of lines causes the real power loss, while reactive power loss is produced due to the reactive elements. Normally, the real power loss draws more attention for the utilities, as it reduces the efficiency of transmitting energy to customers [21]. However, reactive power loss is clearly not less significant. This is due to the fact that reactive power flow in the system needs to be maintained at a certain amount for satisfactory voltage level. Therefore reactive power makes it possible to transfer real power through transmission and distribution lines to consumers. The total real and reactive power losses in a distribution system can be expressed by,

$$P_{Loss} = \sum_{p=1}^{n} |I_p|^2 R_p$$
$$Q_{Loss} = \sum_{p=1}^{n} |I_p|^2 X_p \qquad (2.2)$$

Where n is the total number of branches in the distribution system. $|I|$ is the magnitude of the current in branch p. R_p and X_p are the resistance and reactance of branch p.

2.6 Distribution System Loss Minimization Methods

There are many alternatives available for the loss minimization at the distribution level. These methods include network reconfiguration, capacitor installation, load balancing, voltage optimization and reconductoring [22]. These methods are briefly discussed in the following subsections.

2.6.1 Network Reconfiguration

Network reconfiguration is a process of changing the topological structures of distribution feeders by changing the open/closed states of the sectionalizing and tie switches. This important operating practice is normally used to reduce the system real power loss and to improve system security [23].

The development of Distributed Generation has increased the complexity of the network reconfiguration problem since the power distribution systems will no longer remain passive radial networks with unidirectional power flows, but they will support bi-directional power flows and will contain meshes. However, the recent advances in the distribution system automation have made much easier the remote real-time control of sectionalizing and tie switches. It therefore provides power system utilities with the opportunity to reconfigure their distribution networks in response to load variations for significant loss reduction and reliability improvement.

2.6.2 Capacitor Installation

This concept is well known and widely considered to be one of the most economical loss reduction measures [24]. Systematically switching capacitors to better match system reactive requirements to minimize reactive current flow can decrease losses.
Many different capacitor control schemes are in use. Var controls on capacitors often yield the best results for distribution system loss minimization. Some other types of control include current, voltage, time, and power factor.

2.6.3 Phase Balancing

In power distribution systems, single or two-phase laterals and unbalanced loading are common phenomena. Unbalanced feeders not only increase energy losses and the risk of overload situations, but they also affect system power quality and electricity price. Power system utilities therefore always practice balanced operating conditions in their distribution systems. A balanced system has smaller peak load voltage drops and power losses enabling a utility to provide power service with higher quality and lower cost [25].

2.6.4 Voltage Optimization

Voltage variation in three-phase circuits is equally undesirable because it introduces power losses and reduces the stability of the distribution system [26]. Voltage optimization is therefore a process of optimizing the user voltage to reduce both system losses and end-use consumption without any adverse effect on the customers.

There are a number of new equipment configurations available to mitigate voltage-level problems. These include:

- Autotransformer with multiple excitation windings and AVR
- Semiconductor-controlled tap changers replacing mechanical switches
- Series Compensators

2.6.5 Re-conductoring

Optimal selection of conductors in a distribution system has considerable impact on the reduction of active power losses [27]. Re-conductoring to a larger conductor generally decreases the I^2R losses in a distribution line. Another approach is to choose a conductor with a lower value of per meter resistance.

2.7 Impact of Dispersed Generation on AC Distribution System

Dispersed, or distributed, generation (DG) affects the electric power system at the system and more directly at the distribution level [28]. Recent technological advances in dispersed generation have drawn serious attention for the electrical utilities to change in the electric infrastructure for adapting dispersed generation in distribution systems. Employment of DG technologies makes it more likely that electricity supply system will depend on DG systems and will be operated in deregulated environment to achieve a variety of benefits [21]. As DG systems generate power locally to fulfill client demands, appropriate size and placement of DG can significantly reduce power losses in the system. DG inclusion also improves supply quality and reliability and reduces green house effects.

2.7.1 Impact on Reliability

DG units when properly coordinated can have a positive impact on distribution system reliability. The most common application of DG is for backup generation. After experiencing an interruption, backup generators are started to supply electricity to the critical loads. For critical and sensitive loads, backup generators can be combined with batteries and inverters to ensure uninterruptible power. After an interruption occurs, loads are immediately transferred to the batteries and inverter. The batteries are sized to serve the critical loads until the generator can accelerate to full speed [29].

Another DG application that is gaining popularity is referred as net metering, where on-site generation can exceed local load demand and result in power being fed back into the distribution system.. The energy that is injected in the network is measured and the customer only has to pay for the difference between the energy consumed from the distribution utility and the amount injected in the network [30].

The next most common application for DG is peak shaving. During time periods of high energy demand or high energy prices, local generators come into play and start supplying part of the local loads. In addition to reducing the consumer energy bills, peak shaving can improve system reliability by reducing overall feeder loading [29].

.

2.7.2 Impact on Voltage Regulation and Losses

The distribution systems are usually regulated through tap changing at substation transformers and by the use of voltage regulators and capacitors on the feeders based on radial power flow [11]. DG unit introduce the meshed power flow and therefore unsuitable DG allocation may result in low or over voltages in the distribution system. However by enabling reactive compensation for voltage control and loss reduction DG unit will have positive overall impact on the distribution system.

DG units also cause an impact on loss reduction due to their proximity to the point of consumption. By placing DG units at optimal locations the impact on the losses will be even more prominent. This process of DG allocation is similar to capacitor allocation for reactive compensation to minimize losses. The main difference is that the DG units cause impact on both the active and reactive power, while the capacitor banks only have impact on the reactive

power flow. For a distribution system with high losses, a small DG unit strategically placed supplying only 20 % of total load demand can cause considerable reduction of losses.

In this thesis work an investigation of power loss reduction will be carried out in a system with several DG units and power electronic loads at the distribution level. The dispersed injection of reactive current by the PE interfaces of the DG units and by the power electronic loads will be one of the features of the loss minimization technique.

Chapter 3: AC Distribution System: Case Study

This chapter provides the details of the basic AC distribution system implemented in PSCAD/EMTDC simulation software. It describes the parameters of different components of the distribution system. Then it explains in detail the design of control system for the power electronic loads. It presents an in depth study for the derivation of transfer functions and develops the tuning rules for the converter controllers for optimal performance.

3.1 AC Distribution System

The basic schematic system diagram is shown in figure 3.1. This system is based on the work done by author in [12]. This basic distribution system will be extended to a larger system with multiple constant power loads where appropriate. The AC distribution system is composed of an asynchronous machine, a distribution grid, two transformers with voltage levels at 690 V and 22 kV, a constant power load and electrical lines to connect the components together. The generation and the load are operating at 690 V and are connected to the distribution grid through two transformers.

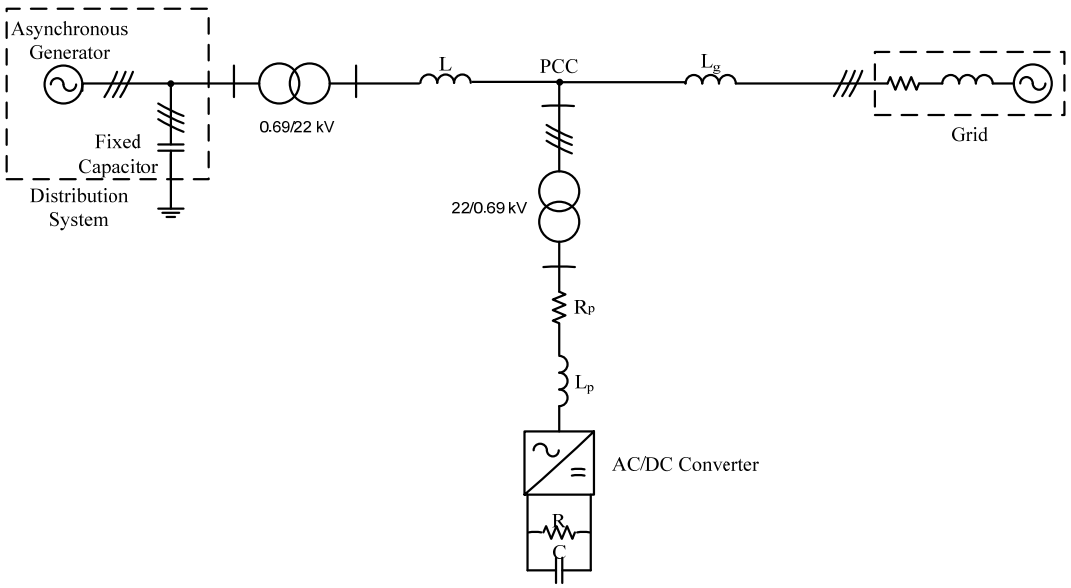

Figure 3.1 - Schematic system

3.2 PU System

The design and implementation of controllers of the VSC based constant power loads becomes easy by using the per unit (pu) system. In this way it is easy to determine the real value of a generic quantity by multiplying it with a reference value. First of all it is necessary to choose a reference power and reference voltages. Then the reference currents and impedances can be calculated. This is very common method to select the base values in the electric drives research area [31]. The following reference values are chosen:

$$\begin{aligned} S_b &= 800\ [kVA] \\ V_{b1} &= \sqrt{\frac{2}{3}}.690 = 563.38\ [V] \\ V_{b2} &= \sqrt{\frac{2}{3}}.22000 = 17962.92\ [V] \\ \omega_b &= 314.159[\text{rad/s}] \end{aligned} \tag{3.1}$$

Where S_b is the nominal power V_{b1} and V_{b2} are the primary and secondary side voltages of the main transformer and ω_b is the base frequency.
The base impedance and current referred to the primary side are given as:

$$\begin{aligned} Z_{b1} &= \frac{V_{b1}^2}{S_b} = 0.595\ [\Omega] \\ I_{b1} &= \frac{V_{b1}}{\sqrt{3} \cdot Z_{b1}} = 669.5\ [A] \end{aligned} \tag{3.2}$$

The values referred to the secondary side are the following:

$$\begin{aligned} Z_{b2} &= \frac{V_{b2}^2}{S_b} = 605\ [\Omega] \\ I_{b2} &= \frac{V_{b2}}{\sqrt{3} \cdot Z_{b2}} = 21\ [A] \end{aligned} \tag{3.3}$$

In order to prevent the over-modulation, the DC link voltage must always be greater than twice the value of base voltage [31].

$$V_{dc} = 2 \cdot V_{b1} = 1126.77\ [V] \tag{3.4}$$

The lower value of the DC link voltage will result in serious instabilities in the VSC operation.

DC side base current is given by:

$$I_{dc.base} = \frac{3}{4} \cdot I_{b1} = 710\ [A] \tag{3.5}$$

DC base impedance is calculated as:

$$Z_{dc.base} = \frac{V_{dc}}{I_{dc.base}} = 1.587\ [\Omega] \tag{3.6}$$

3.3 Asynchronous Machine

An asynchronous machine can operate in either generation or motoring mode. The mode of operation is dictated by the sign of the mechanical torque, positive for motoring, negative for generation. A squirrel cage asynchronous generator also called induction generator, and a fixed capacitor for magnetization, form the distributed generation in the system of figure 3.1. Because of the need for a separate source of magnetizing reactive power induction generators are not commonly used as sources of electrical power [19]. Synchronous generators are the widespread means of electric power generation. However, small generators used to supply a farm or residence or an industry from wind energy can be induction generators. These generators draw their magnetizing reactive power from the utility system and generate electrical power for the local load and/or supply power to the utility system. The parameters of induction generator are given in Table 3.1.

The capacitor bank provides the magnetization to induction generator for the smooth operation. Its value is adjusted in such a way that nominal voltage at the generator terminal can be fixed to1.0 pu for the operation in steady state. The value found is 260 kVar. This value along with the generator power gives the apparent value of 794 kVA, which is very close to the chosen reference value. The value of power factor is therefore 0.944.

Parameters of the Induction Generator	
Nominal power	750000 [W]
Nominal voltage	690 [V_{rms}] line to line
Nominal current	628 [A_{rms}]
Nominal frequency	50 [Hz]
Pole pairs	2
Stator resistance	R_s = 0.0092 pu
First cage resistance	R_r = 0.0076 pu
Second cage resistance	10 pu
Second cage reactance	10 pu
Mutual inductance	3.8693 pu
Stator leakage inductance	0.1580 pu
Rotor mutual inductance	0.0651 pu
Polar moment of inertia[32]	H = 0.5 s
Mechanical damping	F = 0.008

Table 3.1 – Induction Generation parameters

3.4 Three Phase Transformer

Two transformers in Y-Δ configuration are shown in figure 3.1. This configuration produces a phase shift. Y-winding is a primary winding with a voltage level of 690 V while Δ-winding is secondary winding and operates at 22 kV. Star point of the Y-winding is grounded. Magnetization and saturation currents are neglected. Table 3.2 presents the transformer parameters.

Parameters of the Three Phase Transformer	
Nominal power	800000 [VA]
Nominal frequency	50 [Hz]
Winding 1 type	Y
Winding 1 nominal voltage	690 [$V_{3ph\,rms}$]
Winding 2 type	Δ
Winding 2 nominal voltage	22000 [$V_{3ph\,rms}$]
Δ lags or leads Y	Lags
Positive leakage reactance	0.06 [pu]
Ideal transformer model	Yes
No load losses	0.001 [pu]
Copper losses	0.01 [pu]
Saturation enabled	No

Table 3.2 – Transformer parameters

3.5 Distribution Grid

The generator is connected to the distribution grid through a three-phase line. Implemented grid is a weak 22 kV grid represented by a three-phase voltage source behind a resistance and an inductance. Parameters of distribution grid are given in Table 3.3.

Parameters of the Power Grid	
Nominal voltage	22000 [V_{rms}] line to line
Nominal frequency	50 [Hz]
Resistance	2 [Ω]
Inductance	0.2 [H]

Table 3.3 – Grid parameters

3.6 Lines

Resistances of the transmission lines are small compared to reactance so they are neglected. The reactance *Lp* from distribution grid to load is much smaller and resistance of the distribution line is neglected. Capacitances between lines and the earth are neglected. Following values of line reactance per kilometer of length are used in the system under consideration [19].

L	1 [mH]
L_p	0.1 [mH]
L_g	1 [mH]

3.7 Constant Power Load

The constant power load is a power electronic AC/DC voltage source converter as shown in figure 3.2. The control system of AC/DC voltage source converter controls the direct voltage V_{dc} in a way that the voltage is independent of the AC grid voltage. This implies that the AC power remains constant if the grid voltage varies. If the grid voltage increases, the grid current will decrease and if the grid voltage decreases, the grid current will increase [15].

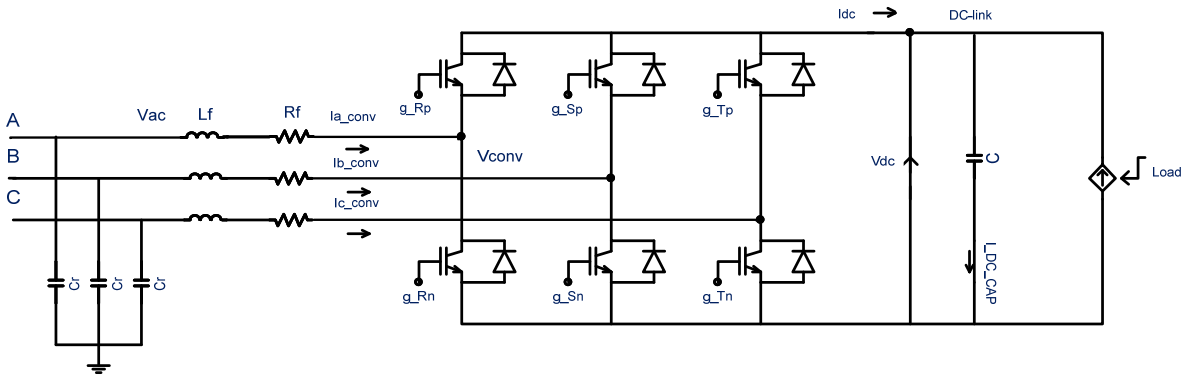

Figure 3.2 – Implemented converter as constant power load

The voltage source converter uses six IGBTs switches with anti-parallel diodes for reverse current conduction. Switching of IGBTs is done by using pulse width modulation (PWM) third harmonic injection technique at a frequency of 5 [kHz]. A DC-link capacitor with a value of 4000 μF is connected in parallel to the load. This capacitor reduces the voltage ripple on the dc side. The implementation of load is done by using a dependent current source that use a manually specified value of power divided by measured dc voltage as shown in figure 3.3. A negative value of the power indicates that the converter is acting as a load while the positive power represents the generation mode for the converter.

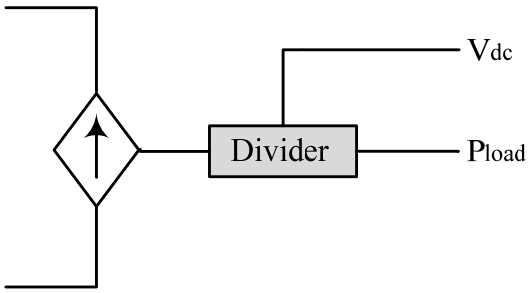

Figure 3.3 – Load representation

Lf and *Rf* are chosen to be 5 % and 1% of the base impedance Z_{b1} respectively. The value of high pass filtering capacitor *Cf* is taken as 100µF [31]. It prevents the harmonics caused by switching of the IGBTs from entering into the grid side.

3.8 Control of Power Electronic Load

The most commonly used method for control of voltage source converters these days is vector control method. This method is generally utilized to achieve an independent control of the active and reactive powers. The three phase AC system is modeled with the help of axis transformation. An interesting feature of vector control is that the ac currents and voltages appear as dc quantities in steady state and therefore static errors in the control system can be removed by using PI controllers [33].

The control configuration of the power electronics converter is represented by figure 3.4 and the explanation on the operation is given in the succeeding subsections.

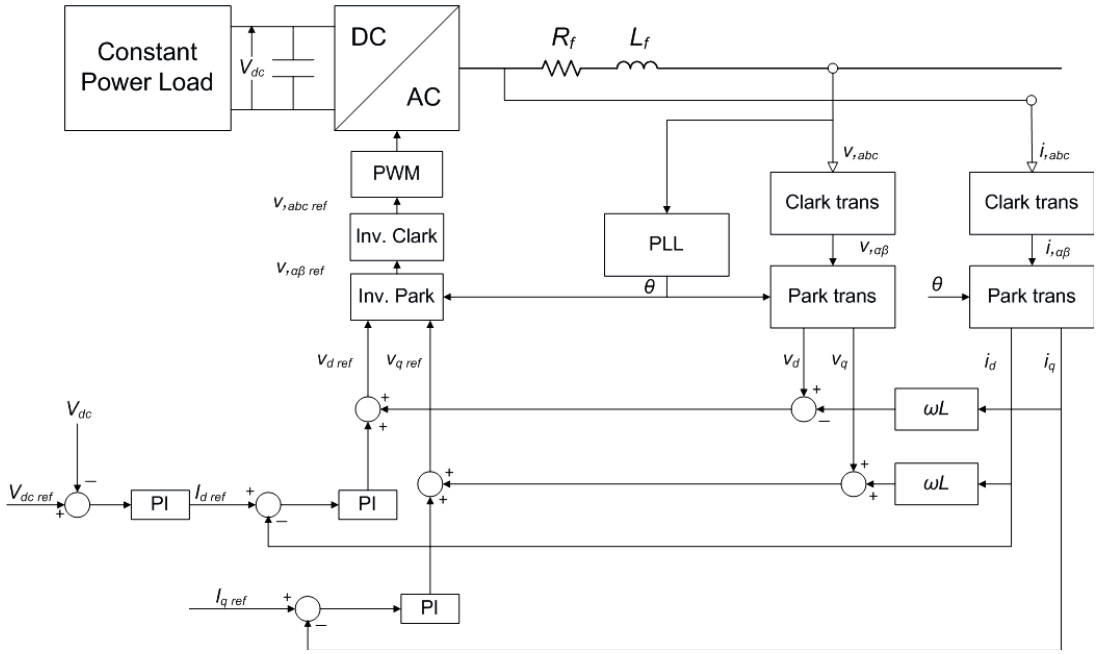

Figure 3.4 – Converter control scheme

3.8.1 Clark and Inverse Clark Transformation

Clark and Inverse-Clark transformations are used to convert the three phase values of voltages and currents into stationary α-β complex reference frame and vice-versa. Figure 3.5 explains this stationary two coordinates system.

For simplification stationary α -axis is aligned with the three phase a-axis. The zero sequence vector is not shown in the diagram because it has non zero value only when there is any unbalanced condition. It is assumed that the system under treatment is in three phase balance. The matrix form of Clark and Inverse-Clark transformation is presented in Appendix A.1.

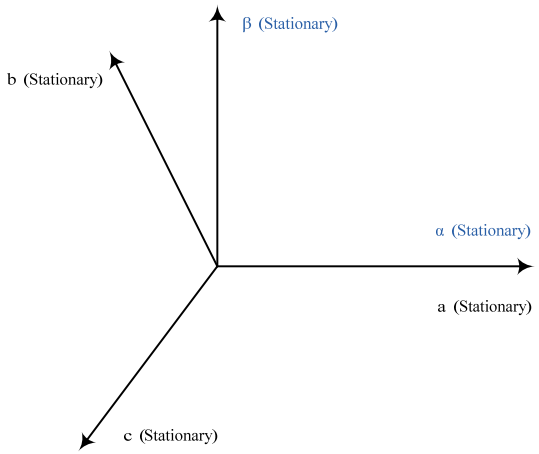

Figure3.5 – Stationary complex reference frame

3.8.2 Park and Inverse Park Transformation

Park and Inverse-Park transformations convert the values from stationary α-β reference frame to rotating d-q reference frame, and vice versa. The d-q reference frame is rotating at a speed ω with respect to the stationary α-β reference frame. The d-q frame is synchronized to the grid, the voltage and current vectors appear to be constant in the d-q reference frame in steady state. The position of d-axis at any instant is presented by angle θ as shown in figure 3.6. The matrix form of park and inverse park transformation is given in the Appendix A.2.

3.8.3 Phase-Locked Loop

A phase-locked loop (PLL) is a control system that generates a signal that has a fixed relation to the phase of a reference signal. It is a closed loop control that controls the angle θ [34]. The schematic representation of PLL is shown in figure 3.7

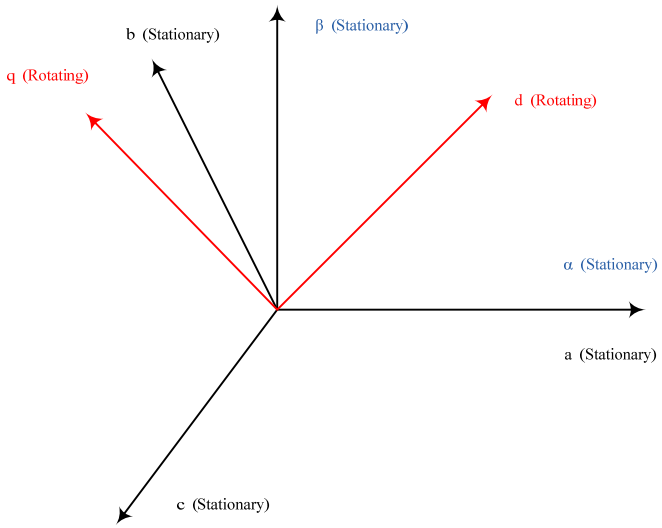

Figure 3.6 – Stationary reference frame along with rotating reference frame

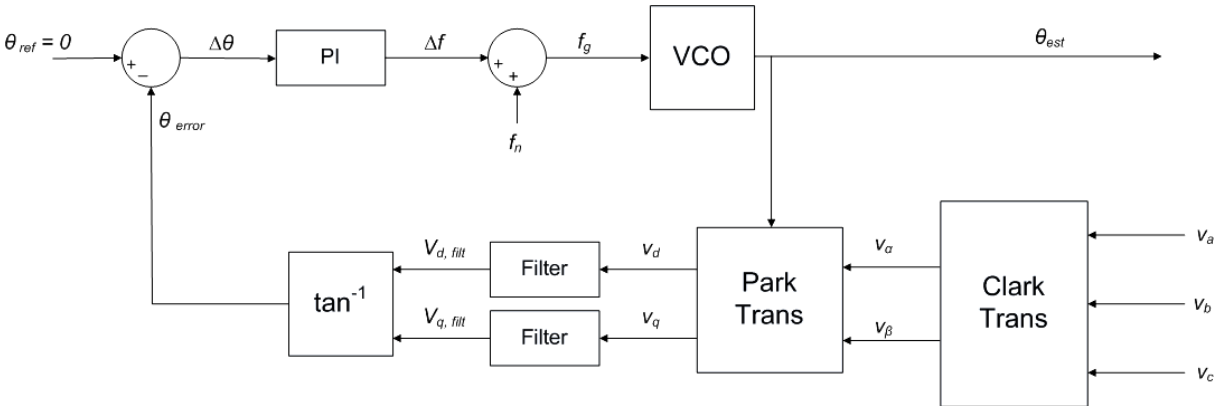

Figure 3.7 – PLL structure

The PLL detects the phase of the grid voltage by transforming measured phase voltages to a rotating dq-reference frame referred to the grid voltage space vector. The d and q components of the voltage are smoothed by a filter. An arc tangent function then calculates the phase of the voltage in all four quadrants. The reference angle θ_{ref} is set to zero and the deviation from this reference value is fed into a PI controller that outputs a deviation from the base frequency Δf. The actual grid frequency f_g is obtained by adding the base frequency. The grid frequency is fed to a Voltage Controlled Oscillator (VCO). The VCO is an integrator that outputs a triangle waveform between 0 and 2π with a period corresponding to the grid frequency [19]. This output angle estimate is used as an input to the dq-transform, closing the loop. When the estimated angle output is correct, the input to the PI-controller is constant and the integral part

of the controller outputs a constant value that corresponds to the real frequency of the grid, keeping the loop in lock. If the output angle differs from the grid angle, the frequency is adjusted by the PI-controller, and the grid angle estimate is changed until the loop is in lock again.

3.8.4 Current Control

This block controls the current flowing through the load to define the voltage that it needs to generate. The current control consists of two PI regulators separately for active and reactive current control, decoupling factors and the feed-forward terms [35]. The basic structure of the current control is shown in figure 3.8.

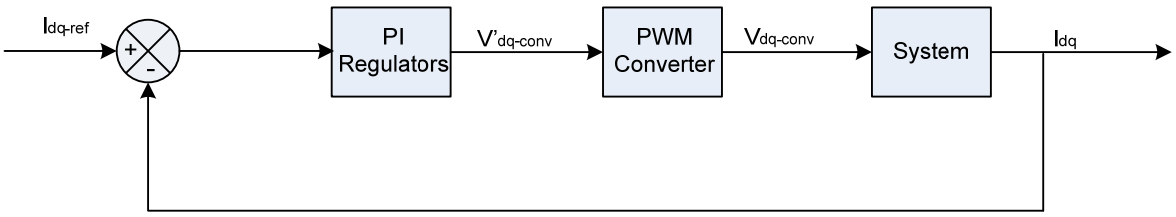

Figure 3.8 – Block Diagram of Current Controller

3.8.4.1 PI Regulator

PI regulators convert the error between the active and reactive current components into respective voltage signal. The general expression for the regulators is given by:

$$P(s) = K_{pc} + \frac{K_{ic}}{s} = K_{pc}.\left(\frac{1 + T_{ic}.s}{T_{ic}.s}\right) \tag{3.7}$$

Where the subscript ‘c’ represents the current regulator.

K_{pc} is the proportional gain and $T_{ic} = \frac{K_{pc}}{K_{ic}}$ is the integral time constant. These parameters will be defined in the next sections. The regulator block transfer function is then:

$$\left(I_{dq-ref}(s) - I_{dq}(s)\right).\left(K_{pc} + \frac{K_{ic}}{s}\right) = V'_{dq-conv}(s) \tag{3.8}$$

3.8.4.2 PWM Converter

PWM converter acts as an ideal power transformer with an average time delay equal to half of the switching cycle as a result of IGBTs switching [36]. The time delay is given by:

$$T_a = \frac{T_{switch}}{2} \tag{3.9}$$

The equation of PWM converter therefore is represented by:

$$Q(s) = \left(\frac{1}{1 + T_a.s} \right) \tag{3.10}$$

Therefore the converter block is:

$$V'_{dq-conv}(s).\left(\frac{1}{1 + sT_a} \right) = V_{dq-conv}(s) \tag{3.11}$$

Using the result of equation 3.8 in equation 3.11

$$\left(I_{dq-ref}(s) - I_{dq}(s) \right).\left(K_{pc} + \frac{K_{ic}}{s} \right).\left(\frac{1}{1 + sT_a} \right) = V_{dq-conv}(s) \tag{3.12}$$

3.8.4.3 The System

V_{AC} is the reference voltage for PLL and current reference for the control system is $I_{abc\text{-}conv}$ as shown in the figure 3.2. V_{AC} is written as:

$$V_{AC} = V_{AC-conv} + R_f.I_{abc-conv} + L_f \frac{dI_{abc-conv}}{dt} \tag{3.13}$$

Transforming the equation 3.13 into dq-reference frame

$$\begin{pmatrix} v_d \\ v_q \end{pmatrix} = \begin{pmatrix} v_{d-conv} \\ v_{q-conv} \end{pmatrix} + R_f \begin{pmatrix} i_d \\ i_q \end{pmatrix} + L_f \frac{d}{dt} \begin{pmatrix} i_d \\ i_q \end{pmatrix} + L_f \begin{pmatrix} 0 & -\omega \\ \omega & 0 \end{pmatrix}.\begin{pmatrix} i_d \\ i_q \end{pmatrix} \tag{3.14}$$

Separating equation 3.14 into d and q axis we get:

$$v_d - v_{d-conv} = R_f i_d + L_f \frac{di_d}{dt} - \omega L_f i_q$$
$$v_q - v_{q-conv} = R_f i_q + L_f \frac{di_q}{dt} + \omega L_f i_d \quad (3.15)$$

The transformed voltage equations have the frequency terms that provide cross coupling between the two axis. The cross coupling terms are compensated by the feed-forward terms in the controller.

Using the equation 3.12 in equation 3.15 for the d and q axis separately:

$$V'_{d-conv} = -\left(i_{d-ref} - i_d\right).\left(K_{pc} + \frac{K_{ic}}{s}\right) + \omega L_f i_q + v_d$$
$$V'_{q-conv} = -\left(i_{q-ref} - i_q\right).\left(K_{pc} + \frac{K_{ic}}{s}\right) - \omega L_f i_d + v_q \quad (3.16)$$

Equating the system equation 3.15 with equation 3.12 we get:

$$R_f i_d + L_f \frac{di_d}{dt} = V_{d-conv}$$
$$R_f i_q + L_f \frac{di_q}{dt} = V_{q-conv} \quad (3.17)$$

For both the axis the equations are same. Therefore taking the Laplace transform of the equation 3.15 for d axis only we get:

$$i_d(s) = \left(\frac{1}{R_f + sL_f}\right).V_{d-vonv}(s) \quad (3.18)$$

The system transfer function hence becomes:

$$H(s) = \frac{1}{R_f}.\left(\frac{1}{1 + s.\tau}\right) \quad (3.19)$$

Where $\tau = L_f/\omega_b R_f$ is the time constant of the distribution line.

The complete block diagram of d and q axis current controllers is given in the figure 3.9. However as the cross coupling terms are cancelled out by the feed forward terms therefore the block diagram reduces to two separate loops in the d and q axis as shown in figure 3.10.

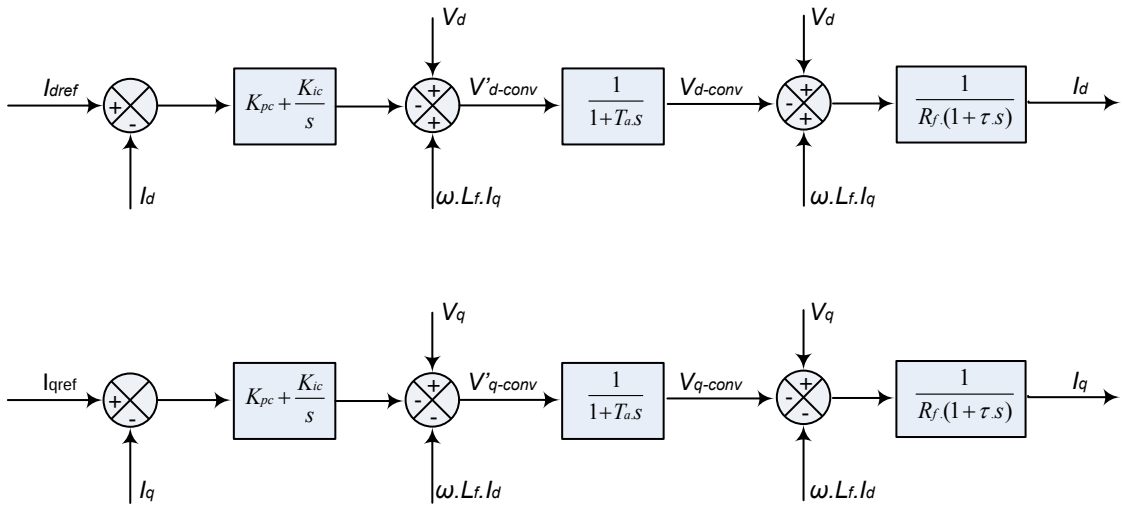

Figure 3.9 – Complete Block Diagram of Current Controller

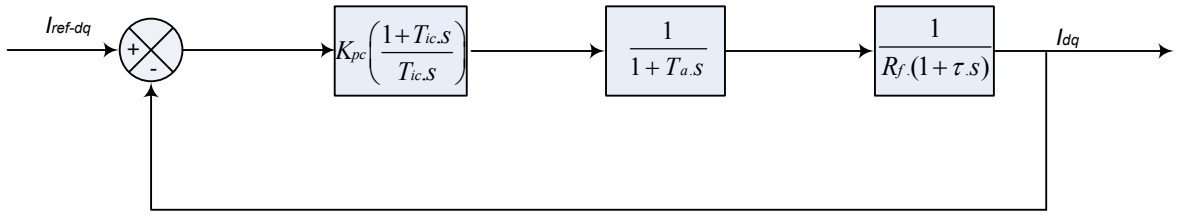

Figure 3.10 – Reduced Block Diagram of Current Controller

The q-axis current controller controls the reactive power while the d-axis current controller is used to control the flow of active power. All the values are in pu referred to the respective axis.

3.8.5 DC-Link Voltage Control

The DC-link control keeps the dc voltage constant to a specified value. This value is given by equation 3.4 for the given distribution system. This reference value is compared with the measured value and the difference is fed to a PI regulator. The general block diagram of the DC link voltage controller is given in the figure 3.11. Each block is discussed in detail in the following subsections.

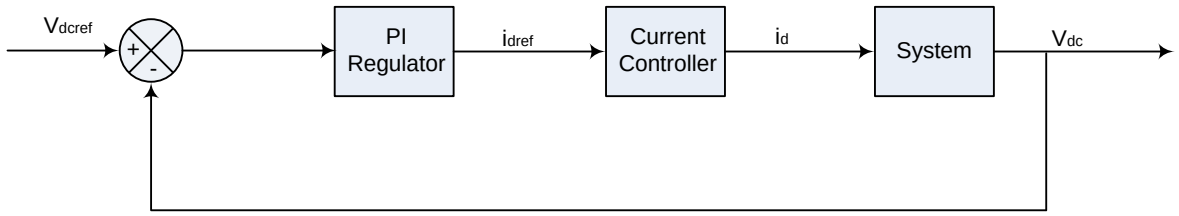

Figure 3.11 – Block Diagram of DC Link Voltage Controller

3.8.5.1 PI regulator

PI regulator converts the voltage error into current signal. The general expression for the regulator is given by:

$$P(s) = K_{pv} + \frac{K_{iv}}{s} = K_{pv}.\left(\frac{1 + T_{iv}.s}{T_{iv}.s}\right) \tag{3.20}$$

Where K_{pv} is the proportional gain and $T_{iv}=K_{pv}/K_{iv}$ is the integral time constant. The regulator block therefore is represented by:

$$\left(V_{dcref}(s) - V_{dc}(s)\right).\left(K_{pv} + \frac{K_{iv}}{s}\right) = i_{dref}(s) \tag{3.21}$$

3.8.5.2 Current Controller

As discussed in section 3.8.4 in detail the current controller provides the relation between i_{dref} and i_d. For the design of DC link voltage controller the current controller is generally assumed as ideal and represented by unity. In this case a simplified representation of the second order closed loop transfer function of the current controller by the equivalent first order approximation is assumed based on the work done in [36].

$$Q(s) = \left(\frac{1}{1 + T_{eq}.s}\right) \tag{3.22}$$

Where $T_{eq}=2.T_a$

3.8.5.3 The System

In the system of figure 3.2 the active power drawn by the load is always constant. The power balance relationship between the input and output of the converter is given as

$$P = \frac{3}{2}\left(v_d.i_d + v_q.i_q\right) = V_{dc}.I_{dc} = Const \tag{3.23}$$

Expression for the reactive power is given in the equation below:

$$Q = \frac{3}{2}\left(v_d.i_q + v_q.i_d\right) \tag{3.24}$$

The dc side current is therefore:

$$I_{dc} = C.\frac{dV_{dc}}{dt} + I_L \tag{3.25}$$

The d axis is always directed along the grid voltage vector. Therefore $v_q=0$. The instantaneous active and reactive powers on the ac side of the system are reduced to:

$$P = \frac{3}{2}.v_d.i_d = V_{dc}.I_{dc}$$

$$Q = \frac{3}{2}.v_d.i_q \tag{3.26}$$

The active component of the current defines the active power absorbed or delivered by the load while the reactive current corresponds to the injected or absorbed reactive power.

From equation 3.26 the relation between the active component of ac current and the dc side current I_{dc} is then:

$$I_{dc} = \frac{3}{2}.\frac{v_d}{V_{dc}}.i_d \tag{3.27}$$

Using this value of dc current into equation 3.25:

$$C.\frac{dV_{dc}}{dt} = \left(\frac{3}{2}.\frac{v_d}{V_{dc}}.i_d\right) - I_L \tag{3.28}$$

The dc link current equation is non linear equation. The linearization of this equation is done based on Taylor series expansion and it is observed that I_L acts as a disturbance and only significant input is the active component of ac current i_d [36].

After linearization equation 3.28 reduces to:

$$C.\frac{d\Delta V_{dc}}{dt} = \frac{3}{2}.\frac{v_{d,0}}{V_{dc,ref}}.\Delta i_d \tag{3.29}$$

By taking the Laplace transform the system is represented by the equation 3.30:

$$\frac{\Delta V_{dc}(s)}{\Delta i_d(s)} = \frac{3}{2}.\frac{v_{d,0}}{V_{dc,ref}}.\frac{1}{s.C} \tag{3.30}$$

In per unit the final system transfer function of equation 3.30 reduces to [36]:

$$\frac{\Delta V_{dc}(s)}{\Delta i_d(s)} = \frac{v_{d,0}}{V_{dc,ref}}.\frac{\omega_b.C}{s} \tag{3.31}$$

In order to maintain the power balance the DC link voltage controller controls the capacitor current such as I_c=0 and therefore I_{dc}=I_L. Using this value of I_{dc} in equation 3.27:

$$i_d = \frac{2}{3}.\frac{V_{dc}}{v_d}.I_L \tag{3.32}$$

This is the feed forward term used to minimize the slow dynamic response of the controller and to compensate for the variation in the load. In per unit the equation 3.32 becomes:

$$i_d = \frac{V_{dc}}{v_d}.I_L \tag{3.33}$$

The complete block diagram of the DC link voltage controller using the derived expressions is shown in the figure 3.12. All the values are in given in per unit.

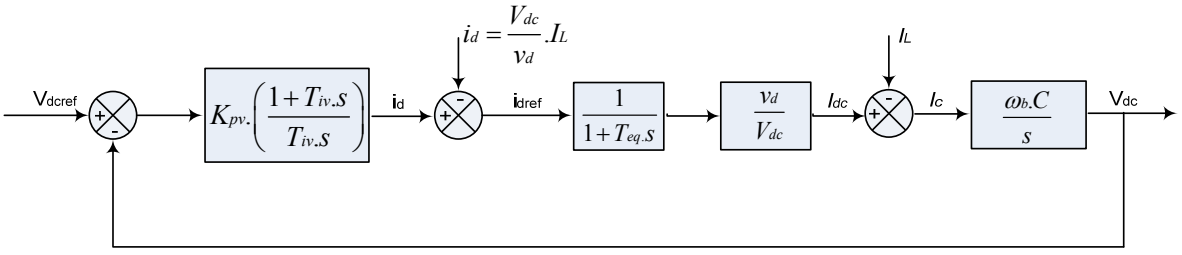

Figure 3.12 – Complete Block Diagram of DC Link Voltage Controller

3.8.6 Tuning of Controllers

The controllers must be tuned to obtain the optimal performance of the control loops. The optimal operation of the control loops is based on the following factors.

- Swift response of the system which can be achieved by keeping the cut-off frequency high.
- To achieve the lowest possible overshoot, or to get a good damping of oscillations.

In order to obtain the described objectives *modulus optimum* and *symmetrical optimum* tuning techniques are applied to tune the current controller and DC link voltage controller respectively [37].

3.8.6.1 Tuning of Current Controllers by Modulus Optimum Method

Modulus optimum technique is used for plants with low order transfer functions and makes the cutoff frequency as high as possible. When the system has one dominant and another minor pole in the transfer function, the integral time constant of the PI controller is selected to cancel out the dominant pole.

From the block diagram of current controller shown in figure 3.10 the open loop transfer function is represented as:

$$H_{C,OL}(s) = K_{pc}.\left(\frac{1+T_{ic}.s}{T_{ic}.s}\right).\left(\frac{1}{1+T_a.s}\right).\left(\frac{1}{R_f.(1+s.\tau)}\right) \tag{3.34}$$

The zero of the PI controller is cancelled out by defining $T_{ic}=\tau$. The open loop transfer function hence reduces to:

$$H_{C,OL}(s) = \frac{K_{pc}}{\tau.R_f}.\frac{1}{s.(1+T_a.s)} \tag{3.35}$$

The open loop transfer function is used to find the closed loop transfer function as:

$$H_{C,CL}(s) = \frac{H_{C,OL}(s)}{1+H_{C,OL}(s)} = \frac{\frac{K_{pc}}{\tau.R_f.T_a}}{s^2+\frac{1}{T_a}.s+\frac{K_{pc}}{\tau.R_f.T_a}} \tag{3.36}$$

The controller gain is calculated from the unity gain condition at cutoff frequency such as:

$$\left|H_{C,CL}(j\omega)\right| = \left|\frac{K_{pc}}{\tau.R_f.T_a.(j\omega)^2+\tau.R_f.(j\omega)+1}\right| = 1 \tag{3.37}$$

After the evaluation of equation 3.37 the controller gain K_{pc} comes out to be:

$$K_{pc} = \frac{\tau.R_f}{2.T_a} \tag{3.38}$$

Hence the closed loop transfer function is given as:

$$H_{C,OL}(s) = \frac{1}{2{T_a}^2.s^2+2T_a.s+1} \tag{3.39}$$

3.8.6.2 Tuning of DC Link Voltage Controller by Symmetrical Optimum Method

When one pole of the open loop transfer function is close to the origin or at the origin itself, the modulus optimum criterion can not be applied. Instead, symmetrical optimum tuning technique is used for tuning the PI controllers. The method has the advantage of maximizing the phase margin and optimizing the control system behaviour with respect to disturbance input [37].

From the DC link voltage block diagram shown in figure 3.12 the open loop transfer function is given as:

$$H_{V,OL}(s) = K_{pv}.\left(\frac{1+T_{iv}.s}{T_{iv}.s}\right).\left(\frac{1}{1+T_{eq}.s}\right).\left(\frac{v_d}{V_{dc}}.\frac{\omega_b.C}{s}\right) \tag{3.40}$$

Simplification of equation 3.40 is done by defining the $T_c=1/\omega_b.C$ and $K=v_d/V_{dc}$

$$H_{V,OL}(s) = K_{pv}.\left(\frac{1+T_{iv}.s}{T_{iv}.s}\right).\left(\frac{K}{1+T_{eq}.s}\right).\left(\frac{1}{s.T_c}\right) \tag{3.41}$$

According to the tuning criteria derived in [37], the parameters for tuning the DC link voltage controller by symmetrical optimum found as:

$$K_{pv} = \frac{T_c}{a.K.T_{eq}} \quad \text{and} \quad T_{iv} = a^2 T_{eq} \tag{3.42}$$

$$\text{Phase Margin, } \Phi_M = \tan^{-1}\sqrt{\frac{T_{iv}}{T_{eq}}} - \tan^{-1}\sqrt{\frac{T_{eq}}{T_{iv}}}$$

$$a = \sqrt{\frac{1+\sin\Phi_M}{1-\sin\Phi_M}} \tag{3.43}$$

Where a is a constant number. A value of a between 2 and 4 is recommended in [37].

Using the values of these converter parameters in equation 3.41 the open and closed loop transfer functions are obtained as:

$$H_{V,OL}(s) = \frac{1}{a^3.T_{eq}^2.s^2} \cdot \left(\frac{1 + a^2.T_{eq}.s}{1 + T_{eq}.s} \right) \tag{3.44}$$

$$H_{V,CL}(s) = \frac{1 + a^2.T_{eq}.s}{1 + a^2.T_{eq}.s + a^3.T_{eq}^2.s^2 + a^3.T_{eq}^3.s^3} \tag{3.45}$$

3.8.7 AC Voltage Control

AC voltage controller is implemented as shown in figure 3.13 and will be used occasionally to provide voltage support by reactive compensation under abnormal voltage conditions. The reference value of the voltage on ac side of the converter is compared with the actual value of ac voltage *vd*. The difference is fed to a PI regulator. The output of the PI regulator is the reference value of reactive component of current *Iq* in the current control. The reactive current is related to the reactive power produced by the CPL. This reactive power provides voltage support during the fault and helps to reduce the instability caused by the negative resistance effects of the CPL.

A programming logic is implemented in the software to ensure that controller activates and injects reactive current only during the fault and it deactivate automatically when the fault ends. This control is very important in order to investigate precisely the stability margins of the system.

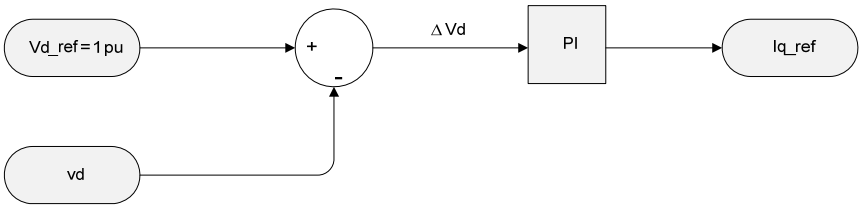

Figure 3.13– AC voltage control block

3.8.8 Measurements

Distributed Generation

Mechanical and electrical torque, rotor speed, and real and reactive internal generator powers are measured from "internal output variables" in the induction generator implemented in the

PSCAD software. Phase voltages and currents, and real and reactive power from the distribution system are measured on the lines between the capacitor bank and the transformer.

CPL

Real and reactive power are measured over L_f and at the point of common coupling to know the amount of power active and reactive power delivered or consumed by the load.. Current is measured in front of the converter before it is filtered and voltage measurement is done at the terminal of the capacitive filter. These voltages and currents are used as input to the converter control. The DC link voltage measured between capacitor and load is another input to the converter control. Active and reactive components of the converter currents and voltages are measured at the output of the two park transformations.

Grid

The amount of power that is transported to the grid or supplied from the grid is measured across grid inductance L_g.

Chapter 4: Stability Analysis of Converter Control System

In this chapter the converter control system presented in the previous chapter is analyzed. A theoretical study is performed to investigate the effects of reduced grid voltage on the stability of converter control system. The stability of the system under reduced voltage conditions is a very important part of this thesis work. This chapter focuses only on the instability originated by the converter control system. A simulation analysis of the system is also done and it is expected that it will validate the results obtained from the theoretical study. The stability of the converter control system in generation mode is also investigated through simulations.

4.1 Current Controller Tuning By Modulus Optimum Method

As discussed in the section 3.8.6.1. The modulus optimum tuning method is widely used because of its simplicity and fast response. Therefore different controller parameters are selected on the basis of modulus optimum tuning criteria for the current controllers. The converter used for this purpose is shown in figure 3.2. The system parameters as described in section 3.7 are

Inductance of the converter filter, L_f = 0.05 pu
Capacitance of the converter filter, C= 1.34 pu
Resistance of the converter filter, R_f = 0.01 pu
Base frequency of the system, ω_b = 314.1592
The switching frequency of the converter block is 5kHz. Therefore average time delay of converter is,

$$T_a = \frac{T_{sw}}{2} = \frac{1}{2.f_{sw}} = 100\mu s$$

Integral time Constant, $\tau = T_{ic} = \frac{L_f}{\omega_b . R_f} = 0.016$

Controller Gain as given by equation 3.38, $K_{pc} = \frac{\tau . R_f}{2.T_a} = 0.8$

$$K_{ic} = \frac{K_{pc}}{T_{ic}} = 50$$

By using the calculated converter control parameters in equation 3.35 we get the open loop transfer function for the current controller,

$$H_{C,OL}(s) = \frac{5000}{100 \times 10^{-6} s^2 + s}$$

Thus the closed loop transfer function by using the equation 3.36 is given by,

$$H_{C,CL}(s) = \frac{5000}{100 \times 10^{-6} s^2 + s + 5000}$$

4.1.1 Frequency Domain Analysis

The bode plot for the second order open loop transfer function is shown in figure 4.1. The gain margin is infinite and the phase margin is 65°. Therefore from the frequency domain stability criteria the closed loop system is stable and robust [38].

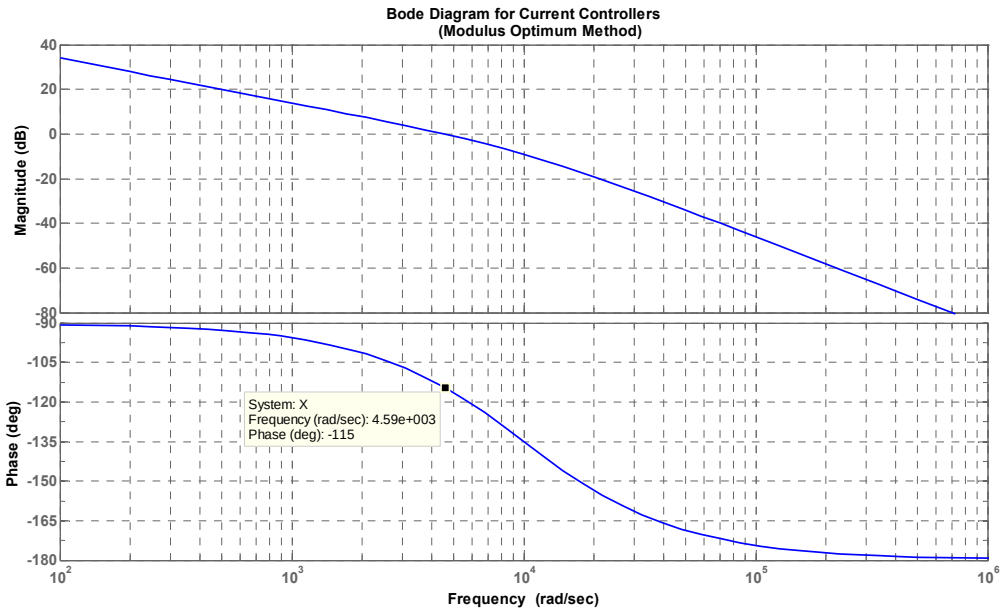

Figure 4.1 – Bode plot for open loop transfer function of current controller

4.2 DC Link Voltage Controller Tuning By Symmetrical Optimum Method

Tuning of the DC link voltage controller is done by the symmetrical optimum method. The value of a is chosen to be 3 in this case. The recommended value of a is between 2 and 4 [37]. The higher value of a results in higher phase margins however the response of the system becomes slower. The open loop transfer function of the DC link voltage controller as given by equation 3.41 is

$$H_{V,OL}(s) = K_{pv.}\left(\frac{1+T_{iv}.s}{T_{iv}.s}\right).\left(\frac{K}{1+T_{eq}.s}\right).\left(\frac{1}{s.T_c}\right)$$

The controller parameters are selected as given below

$$T_{eq} = 2.T_a = 200\mu s$$
$$T_{iv} = a^2.T_{eq} = 0.0018s$$

For the steady state operating conditions v_d=V_{dc}= 1 pu

Therefore, $$K = \frac{v_d}{V_{dc}} = 1$$

$$T_c = \frac{1}{\omega_b.C} = 0.0024$$

Controller Gain, $$K_{pv} = \frac{T_c}{3.K.T_{eq}} = 4$$

$$K_{iv} = \frac{K_{pv,\,pu}}{T_{iv}} = 2222.22$$

Using the calculated controller parameters the open loop transfer function is given by,

$$H_{V,OL}(s) = \frac{0.0018s+1}{0.216\times10^{-9}s^3 + 1.08\times10^{-6}s^2}$$

The closed loop transfer function is therefore,

$$H_{V,CL}(s) = \frac{0.0018s + 1}{0.216 \times 10^{-9} s^3 + 1.08 \times 10^{-6} s^2 + 0.0018s + 1}$$

4.2.1 Frequency Domain Analysis for Steady State

The open loop bode plot is shown for the DC link voltage controller in figure 4.2. The phase margin is 53˚ and it occurs at a frequency of 1.69e+3 rad/s. The gain margin is infinite. Therefore the margins to instability are sufficiently high. This ensures the stable operating limits of the system. The phase margin is maximum at the cross over frequency. The bode plot shows that the response of the transfer function is similar to a band pass filter. Therefore the tuning of the dc link voltage controller by symmetrical optimum method looks to be effective.

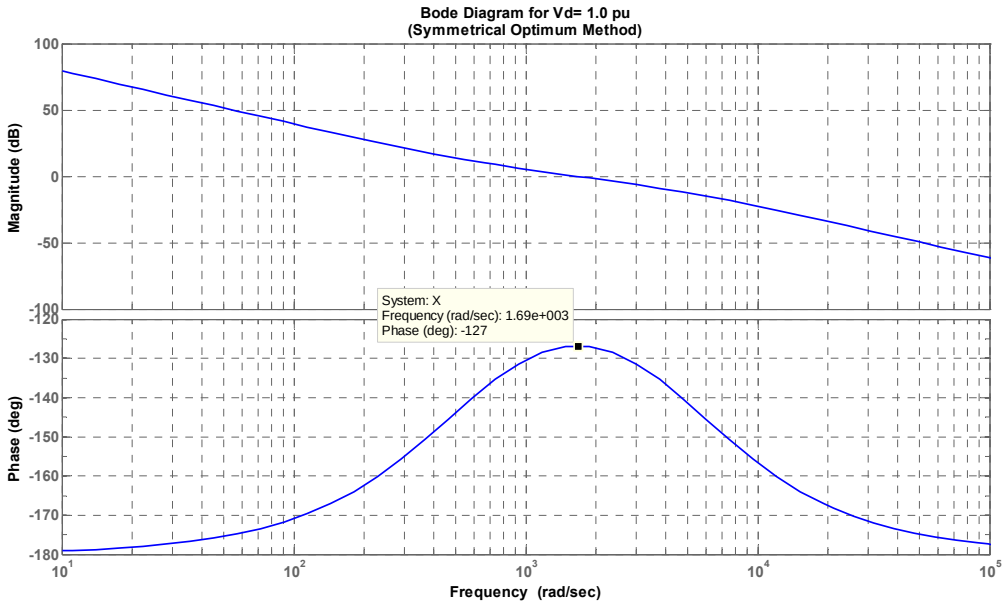

Figure 4.2 – Open loop bode plot for DC link voltage controller for steady state

4.2.2 Frequency Domain Analysis for v_d = 0.8 pu

The final expression of the open loop transfer function of the DC link voltage controller is independent of the value of the grid voltage as given by equation 3.44. However in the real systems there are always delays in the control system and the changes in the converter control

parameters are not modified instantaneously. Therefore the transfer functions are now found for reduced value of grid voltage to investigate its impact on the stability of the control system. The controller parameters are kept the same as in the previous section with steady state operating conditions. Only the values of K will be modified.

$$\text{Therefore,} \quad K = \frac{v_d}{V_{dc}} = 0.8$$

The transfer functions for this condition then become,

$$H_{V,OL}(s) = \frac{0.0018s + 1}{0.27 \times 10^{-9} s^3 + 1.35 \times 10^{-6} s^2}$$

$$H_{V,CL}(s) = \frac{0.0018s + 1}{0.27 \times 10^{-9} s^3 + 1.35 \times 10^{-6} s^2 + 0.0018s + 1}$$

Bode plot for this case is shown in figure 4.3. There is a small reduction in the phase margin compared to the steady state operating conditions. The value of phase margin is 52˚ and it occurs at a frequency of 1.38e+3 rad/s. The cross over frequency has also decreased from the previous case. The operation of the system however is still stable under reduced voltage conditions. The high value of the phase margin suggests that the system is robust as well.

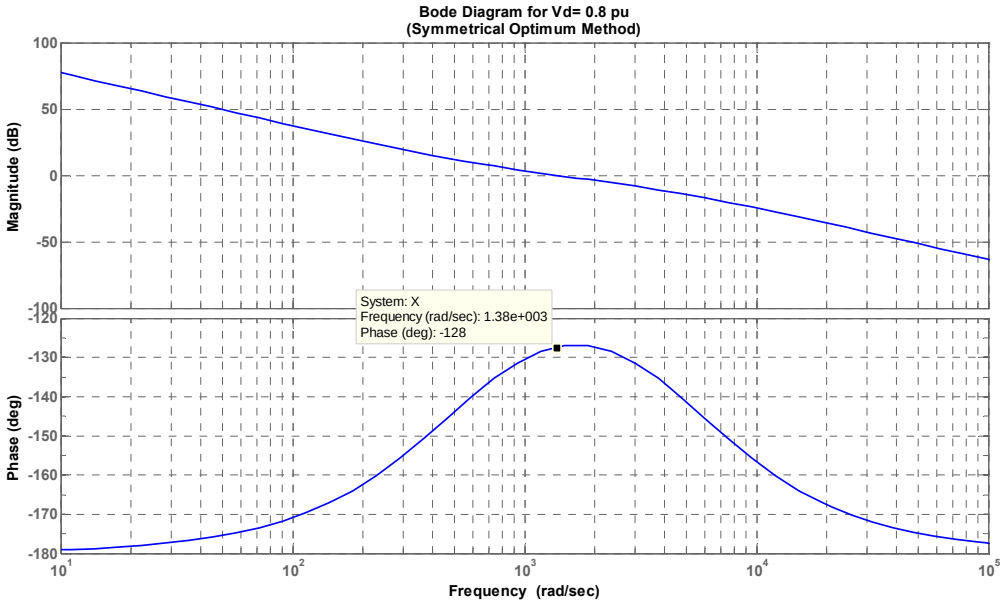

Figure 4.3 – Open loop bode plot for DC link voltage controller for v_d=0.8 pu

4.2.3 Frequency Domain Analysis for v_d = 0.6 pu

It is expected that the phase margin will decrease with the further decrease in the grid voltage. Now the grid voltage is set to 0.6 pu and the transfer functions of the dc link voltage controller are found. All the other controller parameters remain unchanged.

The value of K is then, $K = \frac{V_d}{V_{dc}} = 0.6$

$$H_{V,OL}(s) = \frac{0.0018s + 1}{0.36 \times 10^{-9} s^3 + 1.8 \times 10^{-6} s^2}$$

$$H_{V,CL}(s) = \frac{0.0018s + 1}{0.36 \times 10^{-9} s^3 + 1.8 \times 10^{-6} s^2 + 0.0018s + 1}$$

The figure below shows that the phase margin of the open loop transfer function is reduced to 50˚ and it occurs at a frequency of 1.09e+3 rad/s. The gain margin of the system is infinity. The margins to instability are within the acceptable limit and still indicate the stable operation of the converter control system.

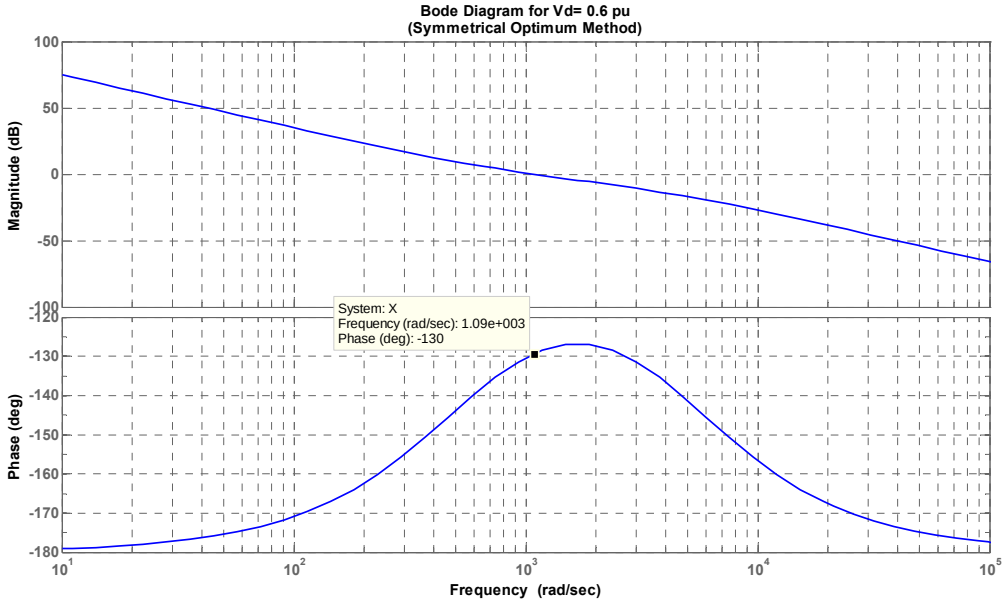

Figure 4.4 – Open loop bode plot for DC link voltage controller for v_d=0.6 pu

4.2.4 Frequency Domain Analysis for v_d = 0.4 pu

For this new value of the grid voltage the calculated transfer functions of the DC link voltage controller are found as:

$$H_{V,OL}(s) = \frac{0.0018s + 1}{0.54 \times 10^{-9} s^3 + 2.7 \times 10^{-6} s^2}$$

$$H_{V,CL}(s) = \frac{0.0018s + 1}{0.54 \times 10^{-9} s^3 + 2.7 \times 10^{-6} s^2 + 0.0018s + 1}$$

Frequency response of the open loop transfer function of the DC link voltage controller is shown in figure 4.5. The phase margin is further reduced to 46˚ and is just greater than the acceptable limit of 45˚ [39]. The margins show that system is still within the stable operating conditions. However any further drop in voltage will result the system to be unstable and a voltage crash is eminent.

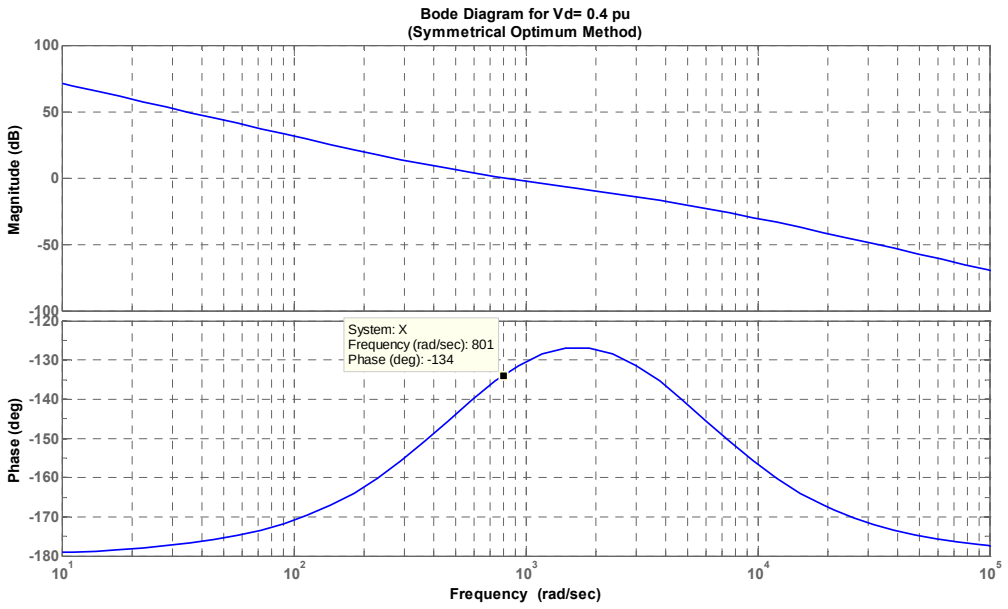

Figure 4.5 – Open loop bode plot for DC link voltage controller for v_d=0.4 pu

4.2.5 Frequency Domain Analysis for v_d = 0.3 pu

The grid voltage is now reduced to 0.3 pu. The value of K is 0.3 pu. All the other controller parameters are kept fixed to the values obtained in section 4.2.1. The transfer functions of the DC link voltage controllers are found to be,

$$H_{V,OL}(s) = \frac{0.0018s + 1}{0.72 \times 10^{-9} s^3 + 3.6 \times 10^{-6} s^2}$$

$$H_{V,CL}(s) = \frac{0.0018s + 1}{0.72 \times 10^{-9} s^3 + 3.6 \times 10^{-6} s^2 + 0.0018s + 1}$$

Bode plot of the open loop transfer function shows that the phase margin is 42˚ and the gain margin is infinite. The value of the phase margin is lower than the acceptable value for the control system to be stable [39]. It is obvious that the stability of the system is compromised with the reduction in grid voltage to this level.

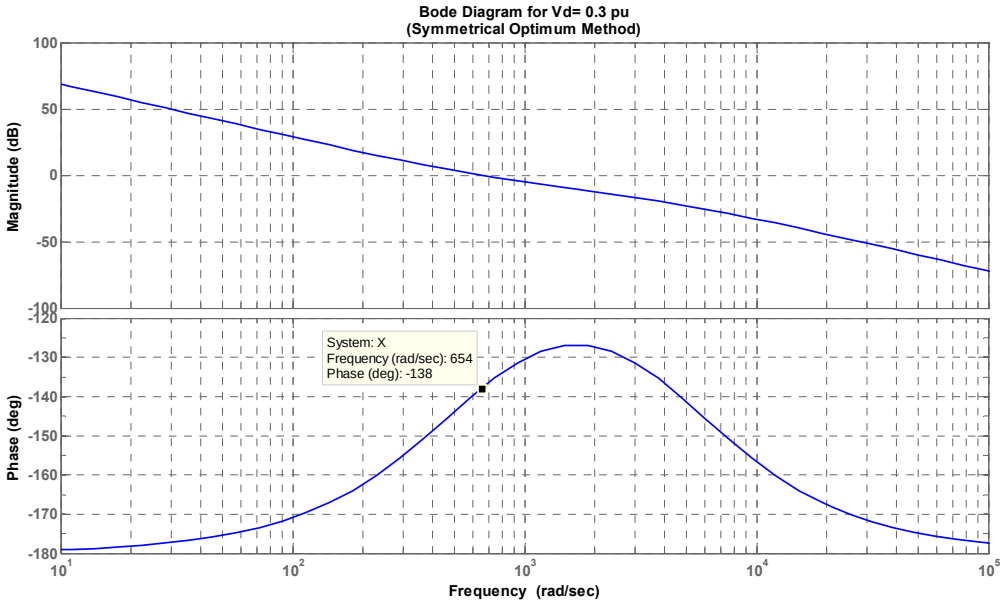

Figure 4.6 – Open loop bode plot for DC link voltage controller transfer function for v_d=0.3 pu

4.3 Simulation Analysis of the Converter Control System

The controller parameters found from the tuning methods are incorporated in the control system of the power electronic load. A simulation study is done to verify the results from the analytical study. The system used for the simulation analysis is shown in figure 4.7. It consists of a converter and an ideal grid. The induction generator shown in the system of figure 3.1 is removed for this analysis. The presence of induction generator makes it impossible to distinguish between the instability caused by the converter control strategy and the instability provoked by the induction generator itself. Another important source of instability in the distribution system is the grid inductance. The presence of grid inductance makes the system highly vulnerable to instabilities as will be further discussed in details in chapter 5. Therefore an ideal grid is used for this system. The effectiveness of the converter control strategy and its impact on the system stability can only be judged through simulations when all the other destabilizing factors are removed from the system. The simulation models implemented in PSCAD/EMTDC software are given in Appendix C.

For these simulations the converter is behaving as a load and draws 300 kW of active power from the ideal grid. The converter can also be used as a generator or a smart grid delivering power to the system.

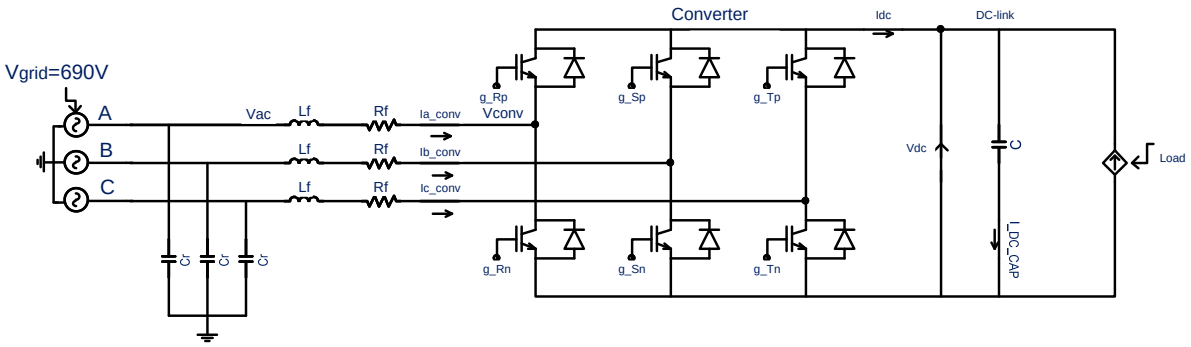

Figure 4.7 – Power Electronic Converter with an Ideal Grid

4.3.1 Simulations for Steady State Operation

Simulations are performed for the rated value of the grid voltage. The total duration of the simulation is 8 seconds. The results are shown in figure 4.8. The grid voltage is 1 pu and the corresponding value of the DC link voltage is also maintained to 1 pu. There is a small

overshoot and initial transients in the DC link voltage before settling down to the given reference value as shown in figure 4.9. The performance of the system is very much stable and the controller is following the reference value.

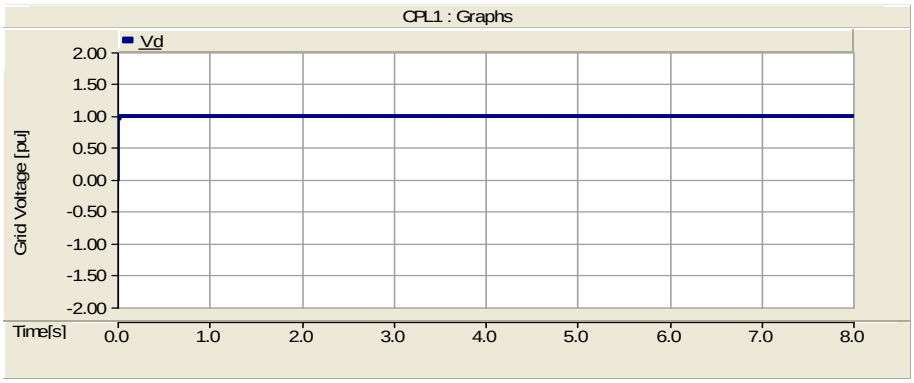

Figure 4.8 –Grid side voltage at steady state

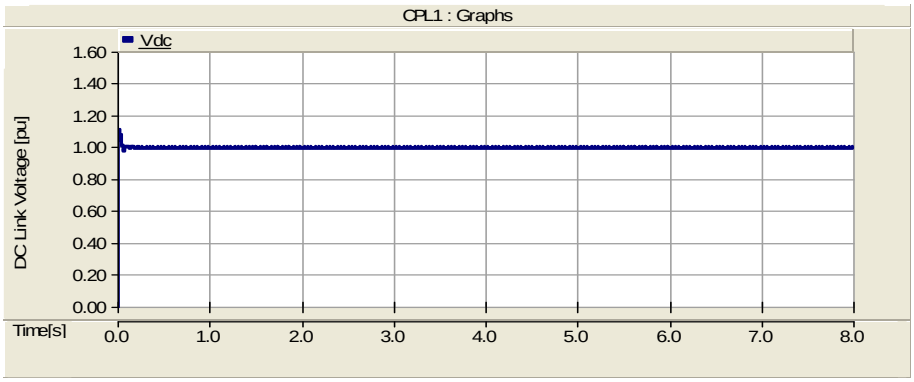

Figure 4.9 –DC link voltage for steady state operation

4.3.2 Simulations for v_d=0.8 pu

The grid voltage is reduced in this case to investigate its impact on the control system. The figure 4.10 shows the reduced value of the voltage and the figure 4.11 shows the DC link voltage under this condition. The results show the effectiveness of the controller tuning method in accordance with the theoretical analysis of section 4.2.2. The system is able to maintain the DC link voltage all the time even for lower value of the AC side voltage.

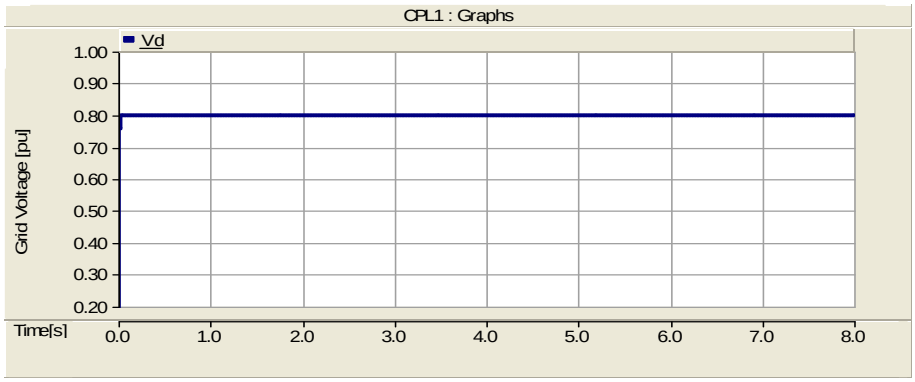

Figure 4.10 –Grid voltage

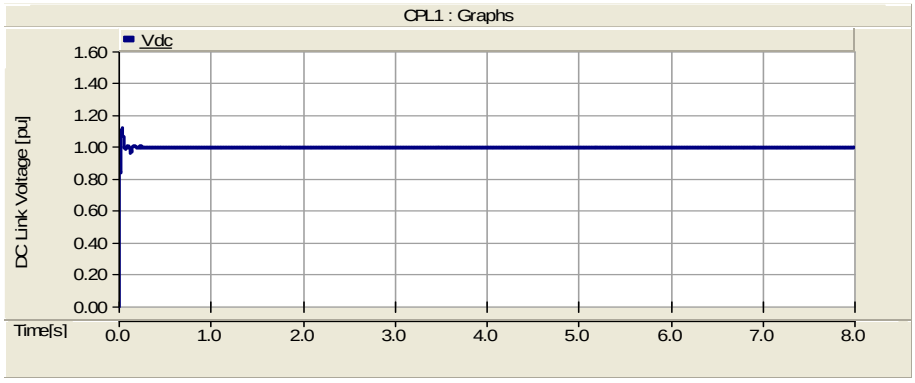

Figure 4.11 –DC link voltage for v_d=0.8 pu

4.3.3 Simulations for v_d =0.6 pu

The AC side voltage is reduced by 40 %. The simulations are carried out and the following figures show the results. Similar to the previous cases for lower values of grid voltage the system seems to be stable for most of the time except for some transients at the start. The analysis of the section 4.2.3 also suggests stable operating condition with a reasonably high value of the phase margin.

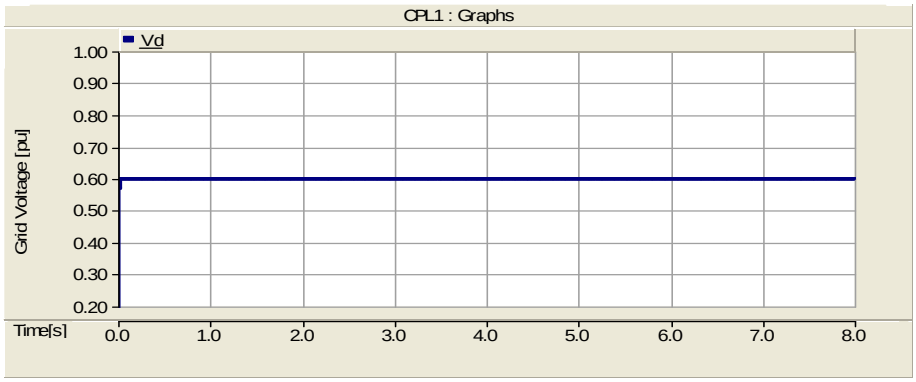

Figure 4.12 –Grid voltage

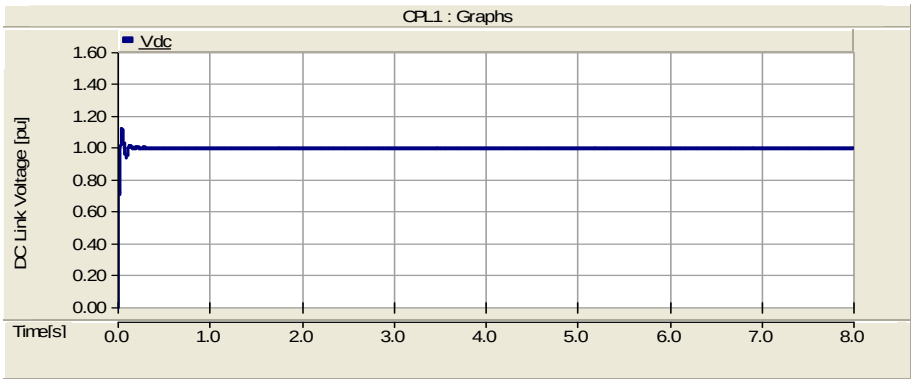

Figure 4.13 –DC link voltage for v_d=0.6 pu

4.3.4 Simulations for v_d =0.4 pu

Simulation results for v_d= 0.4 pu show that the control system is still able to maintain the DC link voltage to the specified value of 1 pu. The simulation results are very much in accordance with the frequency response of the open loop transfer function of the DC link voltage controller.

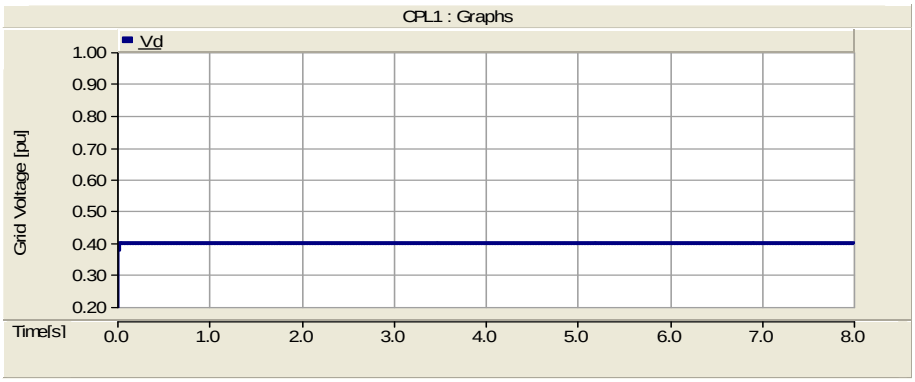

Figure 4.14 –Grid voltage

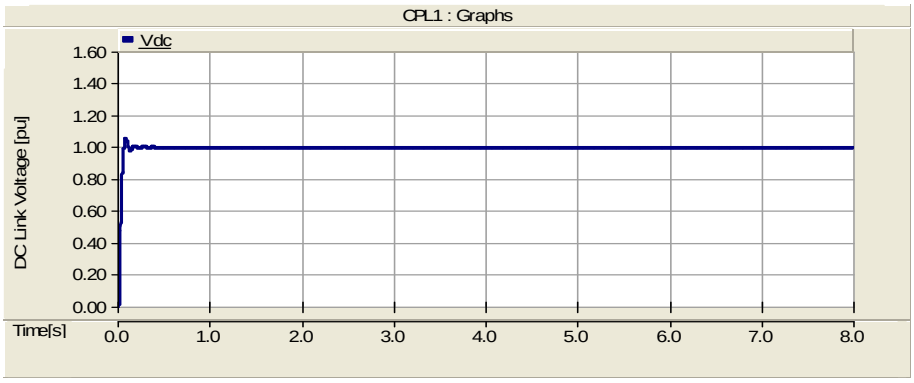

Figure 4.15 –DC link voltage for v_d=0.4 pu

4.3.5 Simulations for v_d =0.3 pu

When the AC side voltage is reduced to 0.3 pu the DC link voltage collapses. At the start of the simulation converter control system tries to maintain the DC voltage to the specified reference value of 1 pu as shown in figure 4.17. However it fails to hold the voltage and a voltage collapse occurs. The DC link capacitor then charges to a value of 0.2 pu for the rest of the simulation. This result is important as the frequency domain analysis of section 4.2.5 also indicate the lower value of the phase margin. This result also confirms that the input AC voltage must always be kept higher than 0.3 pu for the stable operation of the converter control system. This condition however applies only for the system under consideration. The distribution system of figure 3.1 incorporates an induction generator along with a grid with a reasonable value of inductance. The stability limits of this system therefore will be very low compared to the ideal system under consideration.

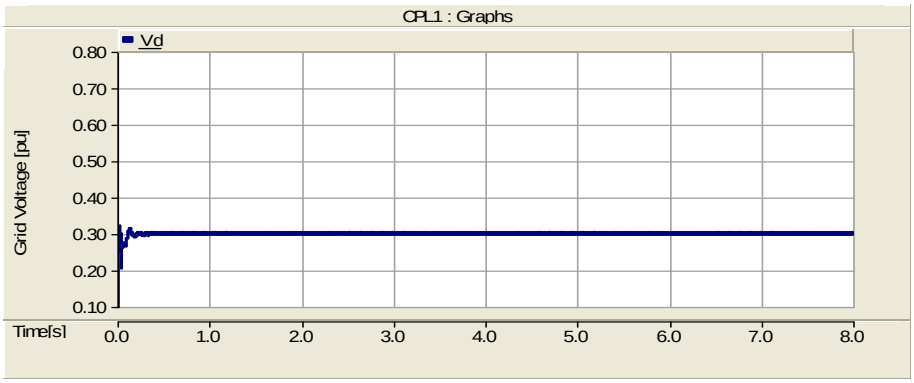

Figure 4.16 –Grid voltage

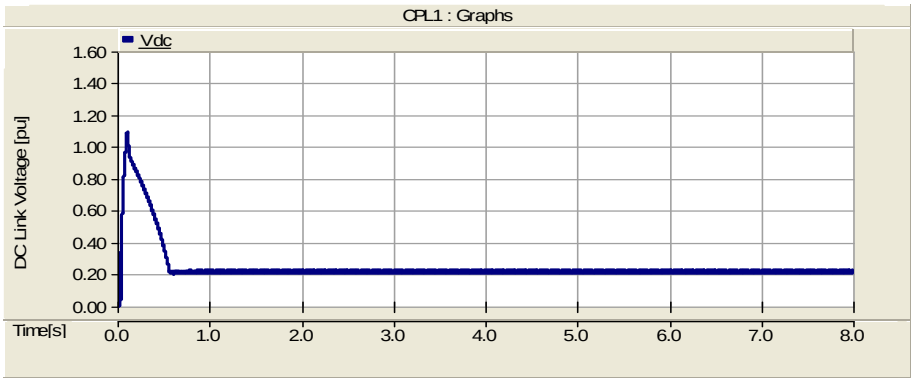

Figure 4.17 –DC link voltage collapse for v_d=0.3 pu

4.4 Simulations for Generation Mode for v_d =0.3 pu

In order to investigate the stability of the converter control when it behaves as a generator or a smart grid the system of figure 4.7 is again used. Simulations are carried out for the condition when the converter is generating 300 kW. This power is being fed to the grid. The grid side voltage is maintained to 0.3 pu. However the generator action of the converter helps to improve the grid voltage by a small amount of 0.015 pu as shown in figure 4.18. This small improvement in the voltage results in a relatively stable system and the DC link voltage is maintained at the given reference value as shown in figure 4.19. This result suggests that the control system is more stable when converter is operating as a generator than the case when it acts as a load under similar operating conditions.

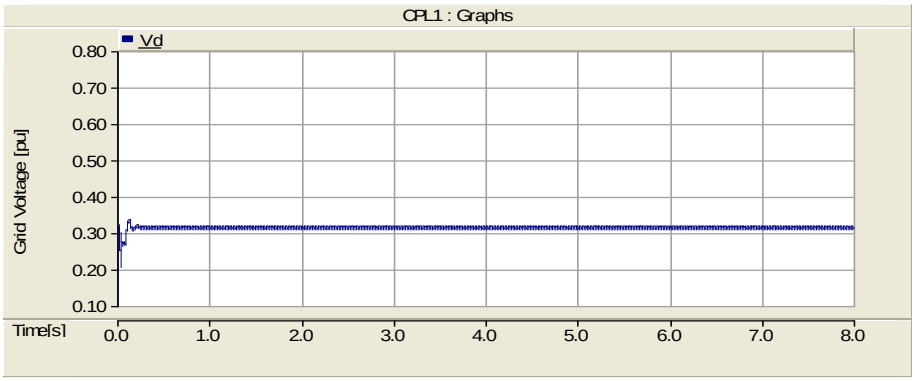

Figure 4.18 –Grid voltage for generator action

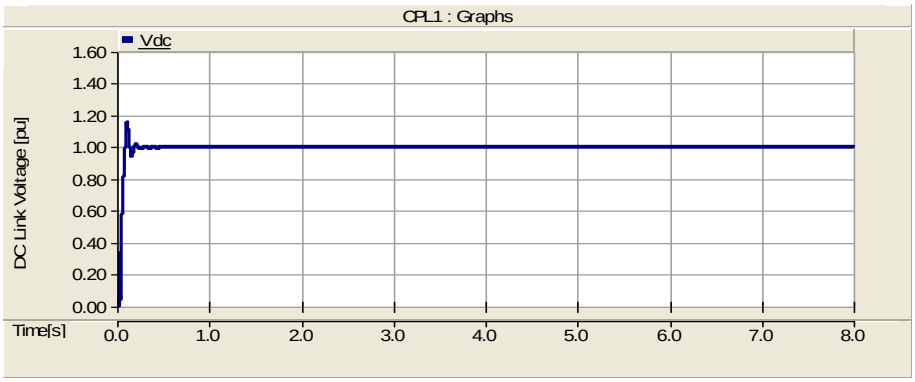

Figure 4.19 –DC link voltage for generator action

4.4.1 Simulations for v_d =0.2 pu

The grid voltage is reduced further to examine the converter control system stability when it acts as a generator. The figure 4.20 shows the gird side voltage and the figure 4.21 shows the DC link voltage for this condition. The converter control system shows a stable behavior even for this very lower value of the grid voltage compared to the stability of the converter when acting as a load where DC voltage collapsed for v_d= 0.3 pu.

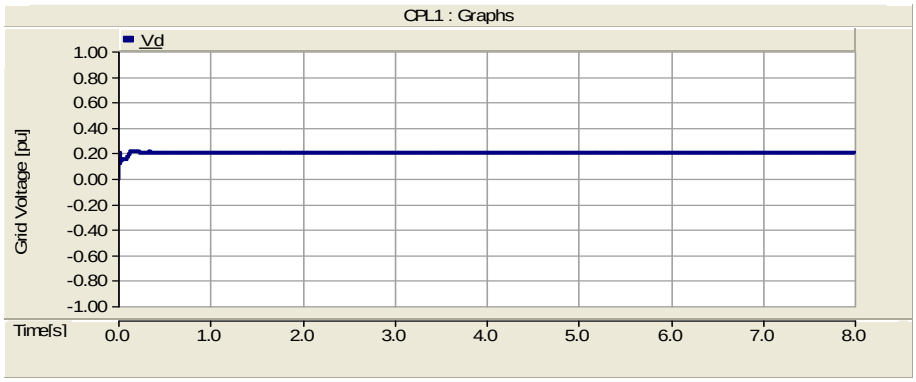

Figure 4.20 –Grid voltage for generator action

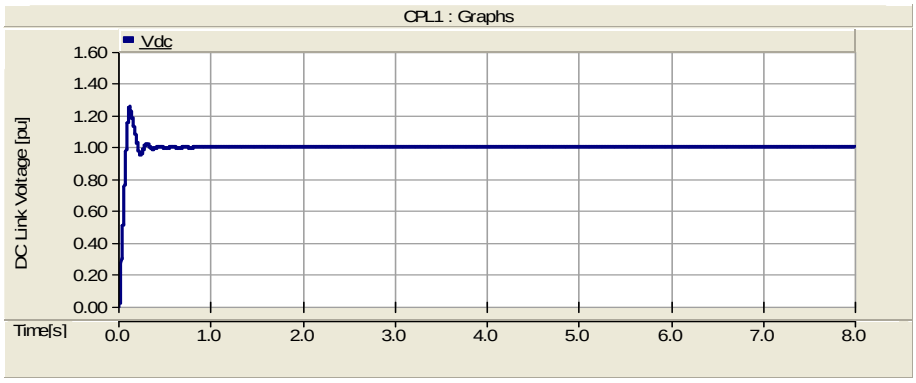

Figure 4.21 –DC link voltage for generator action for v_d=0.2 pu

To find out the unstable voltage condition for generation mode several more simulations are performed and the grid voltage is decreases by a very small amount. The DC link voltage collapse occurs for a value of grid voltage equal to 0.165 pu as shown in the following figures. The generating mode of operation for the converter therefore looks to be very stable compared to the case when converter acts as an interface for the load.

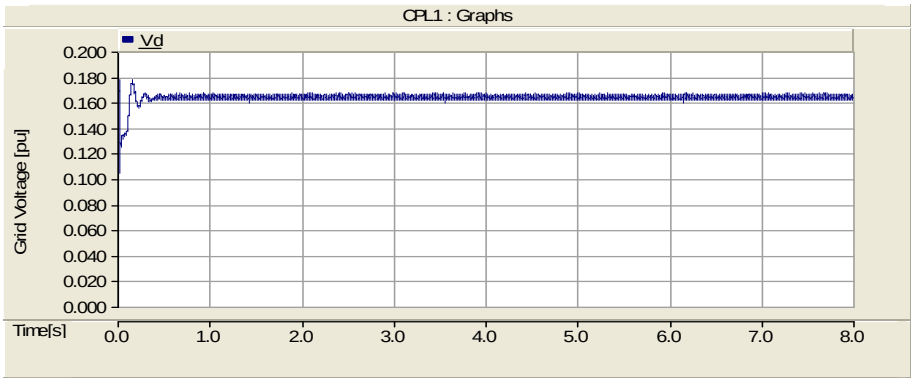

Figure 4.22 –Minimum grid voltage for generator action

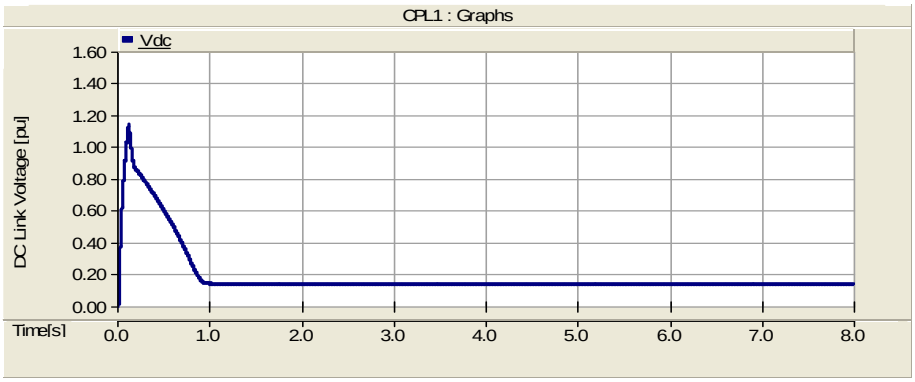

Figure 4.23 –DC link voltage collapse for generator action for v_d=0.165 pu

Grid Voltage (vd)	Phase Margin	(Converter as a Load)	(Converter as a Generator)
		Simulated Voltage Condition	Simulated Voltage Condition
1	53˚	Stable	Stable
0.8	52˚	Stable	Stable
0.6	50˚	Stable	Stable
0.4	46˚	Stable	Stable
0.3	42˚	Unstable	Stable
0.2	36˚	Unstable	Stable
0.165	34˚	Unstable	Unstable

Table 4.1 –Summary of theoretical and simulation results (Active Power= 300 kW)

All the results from the analytical and simulation analysis for the converter control system stability are summarized in the table 4.1. The power consumed or delivered by the converter in all these cases is taken to be 300 kW. The results obtained from the simulations are very much in accordance with the theoretical results. However the converter control system is proved to be more robust for generation mode.

4.5 Effects of DC link Capacitor on Converter Stability

The expressions given in section 4.1 shows that the DC link capacitor does not affect the current controller parameters. However the value of DC link capacitor affects the controller parameters for the DC voltage controller as given in section 4.2. In this analysis the value of the DC link capacitor C is doubled and the values of inductance L_f and resistance R_f are kept the same as given in section 4.1. The new per unit value of the DC link capacitor is 0.67 pu. The new values for the controller parameters are calculated as given below:

$$T_c = \frac{1}{\omega_b.C} = 0.0048$$

Controller Gain, $$K_{pv} = \frac{T_c}{3.K.T_{eq}} = 8$$

$$K_{iv} = \frac{K_{pv,\,pu}}{T_{iv}} = 4444.44$$

Using the calculated controller parameters the open loop transfer function will be the same as shown in the section 4.2 for steady state operating conditions. However by assuming the value of $K_{pv}=4$ from section 4.2 we get the steady state transfer functions as

$$H_{V,\,OL}(s) = \frac{0.0018s + 1}{0.432\times10^{-9}s^3 + 2.16\times10^{-6}s^2}$$

The open loop transfer function for the $v_d = 0.8\ pu$ hence becomes:

$$H_{V,\,OL}(s) = \frac{0.0018s + 1}{0.54\times10^{-9}s^3 + 2.7\times10^{-6}s^2}$$

This is the same transfer function as found in section 4.2.4 for $v_d = 0.4\ pu$ and the phase margin obtained for this condition was 46˚. It shows that the stability of the converter control system is halved by doubling the value of the DC link capacitor and keeping the other controller parameters fixed.

Now for the value of $v_d = 0.6\ pu$ the open loop transfer function is given by:

$$H_{V,OL}(s) = \frac{0.0018s + 1}{0.72 \times 10^{-9} s^3 + 3.6 \times 10^{-6} s^2}$$

This expression is the same as obtained for $v_d = 0.3\ pu$ in section 4.2.5. The value of the phase margin as shown in figure 4.6 is 42˚. It is important now to perform some simulations and find the grid voltage which will result in DC link voltage collapse.

4.5.1 Simulation Analysis

The value of the DC capacitor is doubled in the simulation model and the other controller parameters are kept the same as in the previous simulations. The converter is acting as a load and it consumes 300 kW from the ideal grid. The grid side voltage is reduced by a small amount gradually. The value of the grid voltage which makes the converter control system unstable is found to be 0.57 pu as shown in figure 4.24. The next figure show the DC link voltage collapse. Therefore by increasing the value of the DC link capacitor and keeping the other controller parameters fixed the stability of the system is greatly compromised.

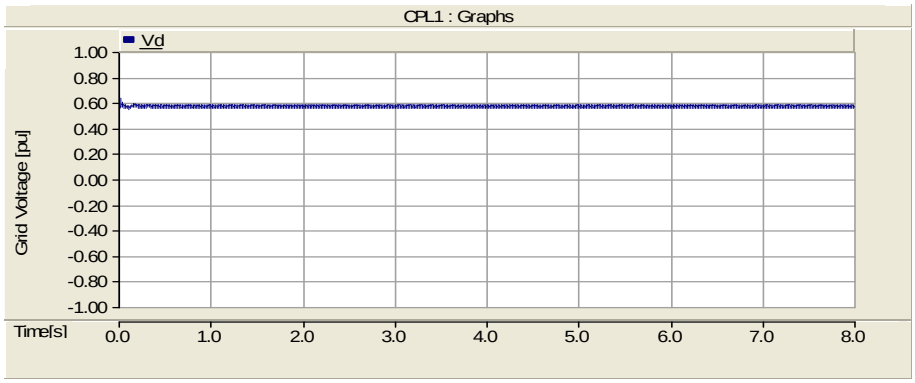

Figure 4.24 –Grid voltage for C=0.67 pu

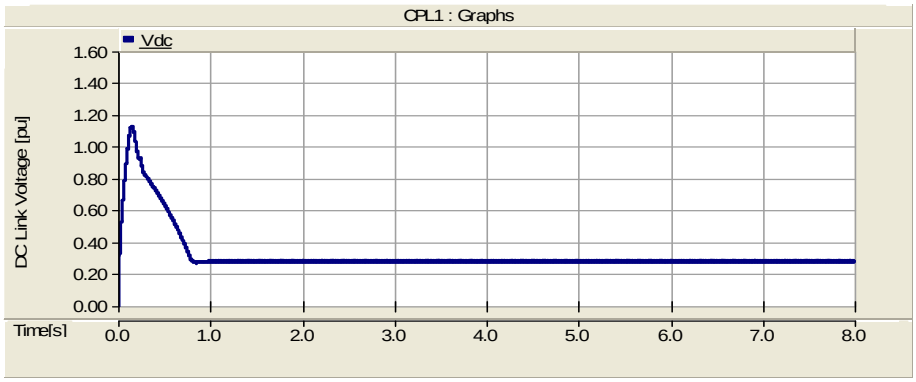

Figure 4.25 –DC link voltage collapse for v_d=0.57 pu

Chapter 5: Transient Stability Analysis of AC Distribution System

This chapter discusses the overall distribution system stability for different types of loads under abnormal voltage conditions. The main focus in this chapter is to avoid the negative resistance instability in a distribution system with large share of constant power load. By allowing injection of reactive current by power electronic interfaces gives the possibility to support the system voltage and increase the transient stability margins. The impact of reactive injection by the controlled power electronic loads on the transient stability margins is first investigated for different load conditions. Then a simulation analysis is done to investigate the increase in current rating of the converter. Finally a comparison is made between the distributed reactive injection by controlled CPLs and the centralized reactive injection by a STATCOM.

5.1 Impact of Reactive Injection on Transient Stability Margins

Transient stability analysis of the AC distribution system has been done by the author in [12]. However some changes in the induction generator parameters are made afterwards and results are modified. The new generator parameters showed significant impact on the transient stability limits of the system. It is observed that a reduction in the value of polar moment of inertia of the induction generator makes the stability margins of the system much lower than with the value used in [12]. For this analysis AC voltage controller of section 3.8.7 is implemented. This controller is active only during the fault and it deactivates automatically when the fault ends. The effect of reactive current injection on the stability margins of the system has been investigated for the following three different shares of loads.

- CPLs are taking 80% of the total generated power. The stability margins of the system are investigated with and without reactive current injection.
- Stability limits of the system are investigated when the amount of load controlled by CPLs and uncontrolled induction motor (IM) is equal.
- Investigation of stability margins of the distribution system is done when the amount of load controlled by CPLs is less than that of uncontrolled IM load.

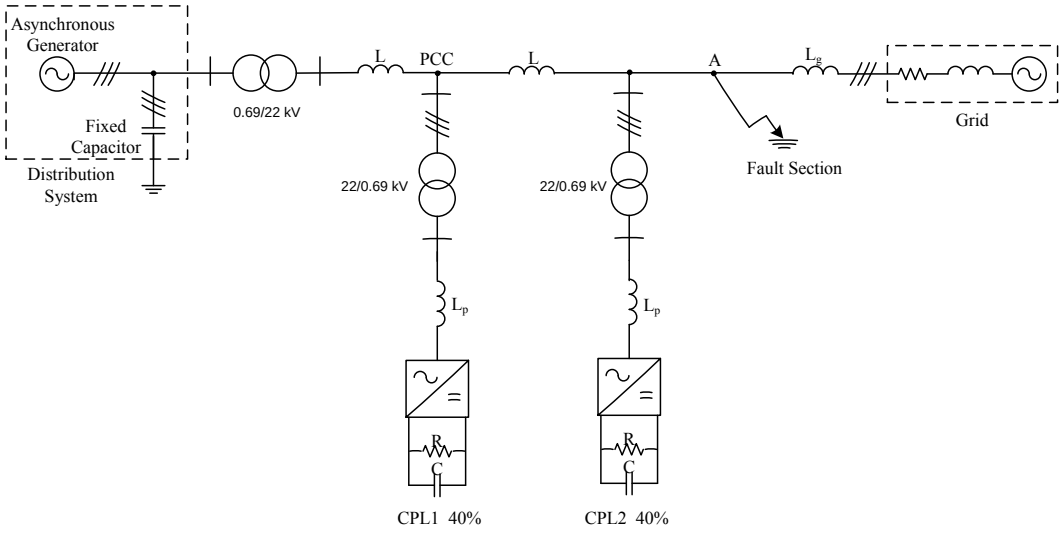

Figure 5.1 –Schematic system with two CPLs and IG

5.1.1 Each CPL is Taking 40% of the Total Generated Power

For this analysis the basic distribution system presented in figure 3.1 is extended to a system with two CPLs as shown in figure 5.1. The parameters of the induction generator are given in section 3.3. The line parameters presented in section 3.6 are used. The length of transmission line between the generator and CPL is taken as 6 km and the distance of the grid from CPL2 is taken to be 50 km. The distribution line length is considered to be 100 m. The resistances of the lines are neglected. The implemented modal in PSCAD/EMTDC is given in figure D.1 in Appendix D.

Case A: AC Voltage Controller is Inactive (Uncontrolled CPLs)

Each CPL is consuming 300 kW which corresponds to 40 % of the total power generated by the induction generator. A three phase line to ground fault is simulated at point A between the grid and the loads. Fault resistance is varied to get a voltage drop equal to 20% of the nominal voltage. The value of the fault resistance found is 110 Ω. Fault occurs at time t=3s seconds during the simulation. Several simulations are carried out under this condition to obtain the critical clearing time (CCT) of the system.

Voltage at the point of common coupling is shown in figure 5.2 when the system becomes unstable. This time the cause of instability is not the converter control system. When the fault occurs the voltage drop is 0.2 pu. However, because of the inductance in the system and lower value of generator inertial constant it goes on decreasing until it collapses as shown in figure

5.2. Figure B.1 in appendix B shows the induction generator (IG) losing the torque control. Figure 5.3 shows the voltage just being able to recover the pre-fault value. Critical clearing time (CCT) is found to be 645 ms. However, the system is very much oscillatory because of lower value of the polar moment of inertia as shown in the figure 5.4 and in figure B.1.

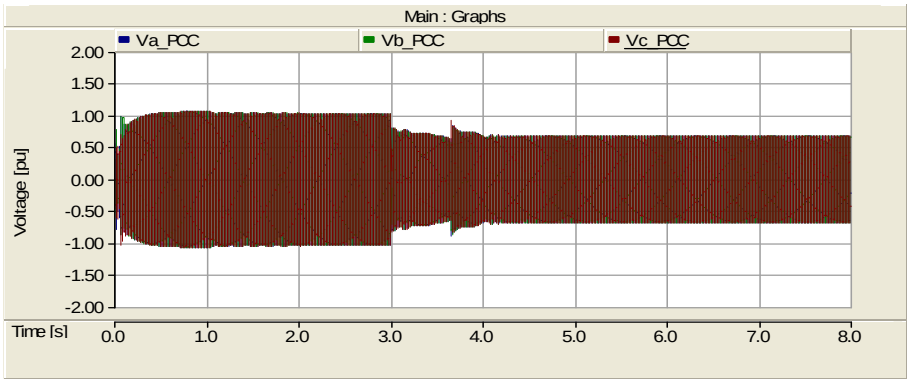

Figure 5.2 –Voltage collapse

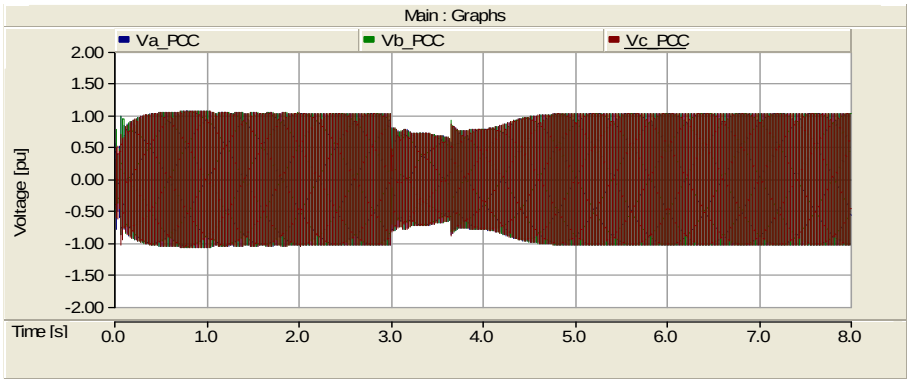

Figure 5.3 –Voltage at the point of common coupling and CCT

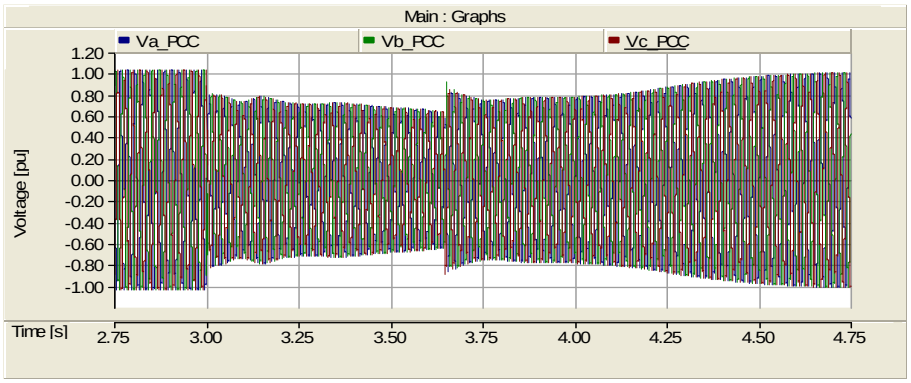

Figure 5.4 –Corresponding zoom of the voltage at PCC

Case B: AC voltage controller is active (Controlled CPLs)

Simulations are carried out under the same load conditions, however this time the AC voltage controller is kept active during the fault the and it injects reactive current to compensate for the voltage drop. The value of fault resistance used is same as in the previous case i.e 110 Ω. Therefore, this time the value of the obtained voltage drop is 0.17 pu. This 3% improvement in voltage is a result of reactive injection by both the CPLs. The amount of injected reactive current is 0.1985 pu for CPL1 and 0.1955 pu for CPL2. This slight difference in current is because of the different distances of the CPLs from the fault location resulting in slightly different voltage drops at the two CPLs terminals. The CPLs reactive currents are shown by figure B.2 and figure B.3 in appendix B. The slope in the current during the fault is due to the PI control action of the controller injecting more reactive current with the decrease in the voltage.

Figure 5.5 shows the voltage recovering back the steady state value. The value of critical clearing time is 1.18 s. The reason for getting this higher value of CCT is that the AC voltage controller injects reactive current during the fault to compensate for the voltage drop and helps the system to tolerate the longer fault. Figure B.4 in appendix B presents the corresponding zoom in the voltage at PCC and figure B.5 shows the generator regaining the torque control at the end of the fault.

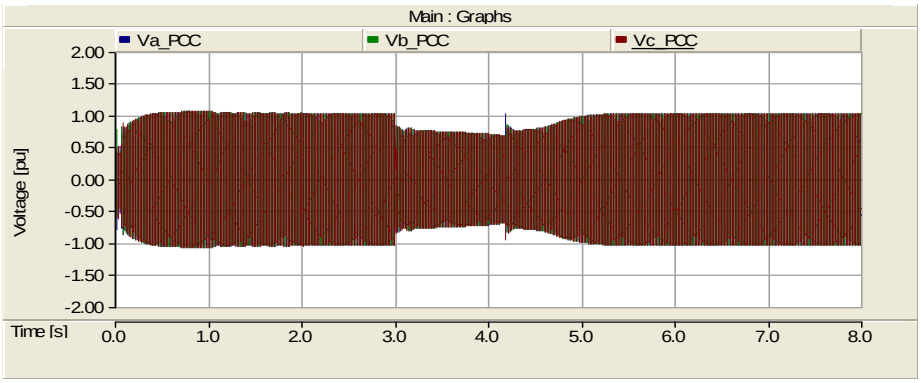

Figure 5.5–Voltage at the point of common coupling and CCT

5.1.2 40% CPLs and 40% Induction Motor

In this section transient stability limits of the distribution system are investigated with the two CPLs and an additional induction motor as a load as shown in the figure 5.6. The amount of load controlled by converters is equal to that of uncontrolled induction motor (IM) load. Total power consumed by the load is 80% of the generated power with each CPL taking 20% (150

kW) and induction motor consuming 40%. The implemented model in PSCAD/EMTDC is shown in figure D.2 in Appendix D.

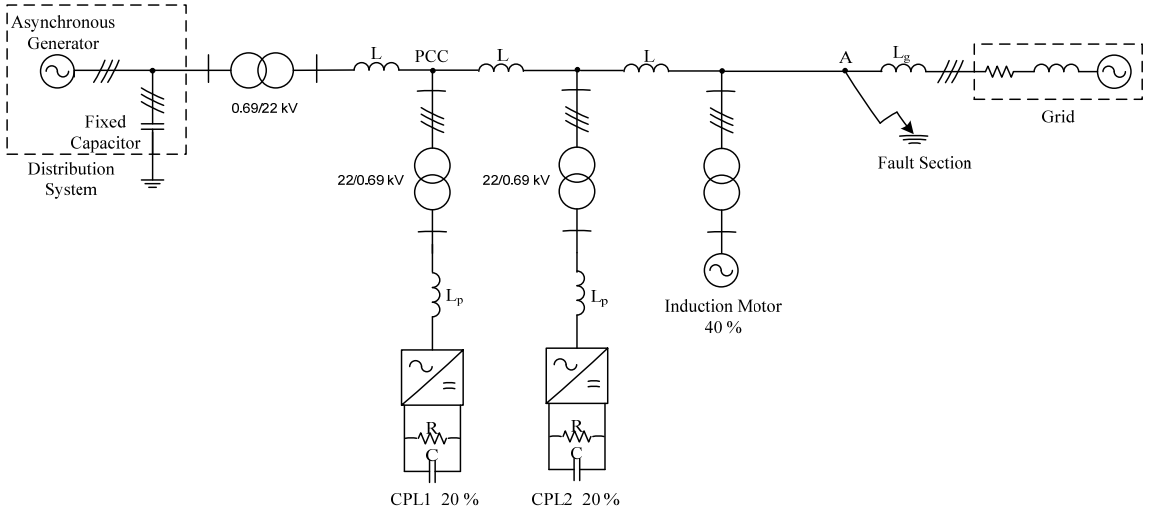

Figure 5.6–Schematic system with two CPLs and an IM Loal

Case A: AC Voltage Controller is Inactive (Uncontrolled CPLs)

A three phase line to ground fault is simulated. The fault resistance remains the same as in the previous sections. Fault occurs at time t=3s during the simulation. Several simulations are carried out under this condition to obtain the critical clearing time. AC voltage controller is kept inactive during the simulation.

The figure 5.7 shows the voltage recovering the pre-fault value of 1.0 pu. The value of critical clearing time is found to be 468 ms. The value is lower as 50% of the load is highly inductive. This increases the overall grid inductance resulting in an early voltage crash during the fault. At the start of the simulation the system takes more time to reach the steady state value compared to the case presented in the previous section. The recovery time after the fault is also higher.

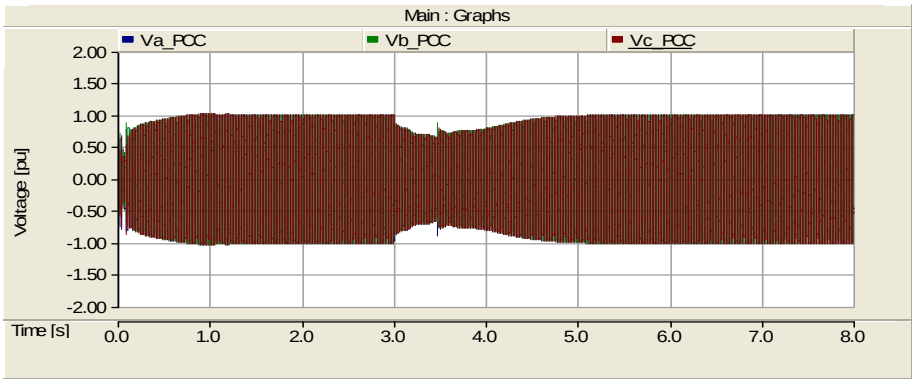

Figure 5.7–Voltage at the point of common coupling and CCT

Case B: AC Voltage Controller is Active (Controlled CPLs)

Simulations are run for the same share of loads, however this time the CPLs are allowed to inject reactive current during the fault. The value of fault resistance is again 110 Ω.

The figure 5.8 shows the voltage recovering back to the pre-fault state. The critical clearing time however is increased this time and is found to be 660 ms. AC voltage controller injects reactive current during the fault. The amount of the reactive current injected is 0.193 pu for CPL1 and 0.191 pu for CPL2. This difference of current corresponds to the effects of the severity of fault on each CPL which increases with the distance from the location of the fault. The value of CCT is higher than the case with two uncontrolled CPL discussed in section 5.1.1. However it looks that with further increase in inductive load the CCT will considerably decrease.

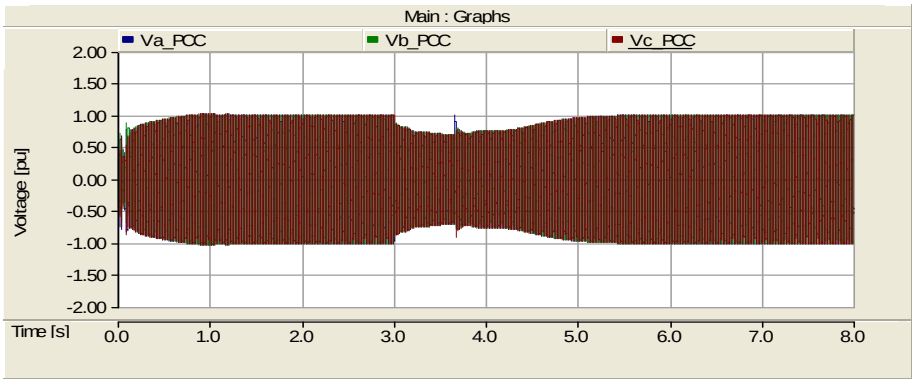

Figure 5.8–Voltage at the point of common coupling and CCT

5.1.3 20% CPLs and 60% Induction Motor

The same model of the distribution system of figure 5.6 is investigated in this section. However the amount of load controlled by CPLs is less than that of uncontrolled IM load. Total power consumed by the load is again 80% of the total generated power with each CPL taking 10% (75 kW) and induction motor consuming 60% (450 kW).

Case A: AC Voltage Controller is Inactive (Uncontrolled CPLs)

A three phase line to ground fault is simulated. The value of the fault resistance is 110 Ω. Fault occurs at time t=3s during the simulation without any reactive current injection by the two constant power loads.

Figure 5.9 shows the voltage at the point of common coupling when the system just recovers back to steady state value. The value of critical clearing time is found to be 340 ms. This is a very lower value justifying highly weak system with very high value of overall inductance. The inertial constant of the induction generator is also very low. A higher value of inertial constant will result in more stable system.

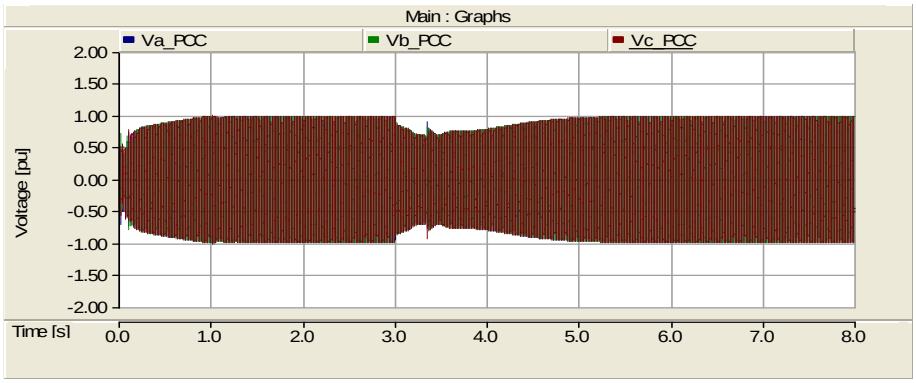

Figure 5.9–Voltage at the point of common coupling

Case B: AC Voltage Controller is Active (Controlled CPLs)

Simulations are run for the same share of load however AC voltage controller is kept active during the fault. The value of fault resistance is same as is used in the previous simulation.

The voltage recovery to the pre-fault value is shown in figure 5.10. The critical clearing time is found to be 480 ms, which is larger than the case without reactive injection of current. Therefore the reactive injection helps to increase the transient stability margin of the

distributed system. The amount of the reactive current injected is 0.187 pu by CPL1 and 0.185 pu by CPL2.

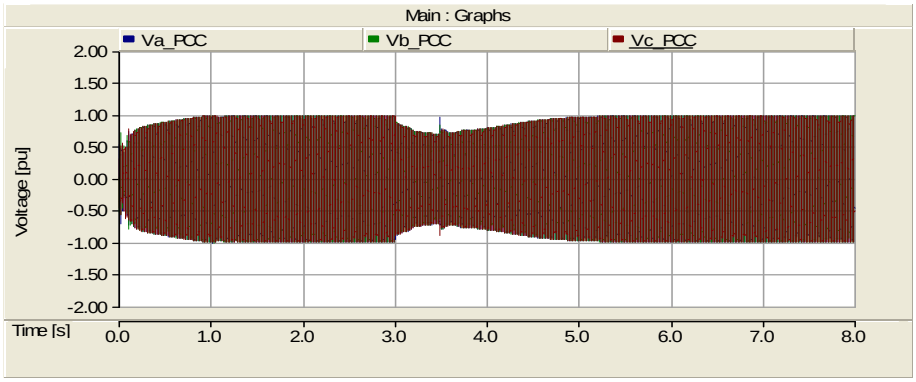

Figure 5.9–Voltage at the point of common coupling and CCT

Results from all the simulations are summarized in table 5.1. The results obtained with the higher value of polar moment of inertia as reported in [12] are presented in table B.1 in appendix B. A big difference in the transient stability limits of the distributed system is observed. The best case is found to be the one with two controlled CPLs in section 5.1.1 while the worst case is reported with 60% IM load without reactive current support during the fault in section 5.1.3. This is obvious because the system will struggle to recover back to its nominal voltage after the fault in the presence of such a high inductive load. Therefore in this case the instability in the system is not provoked by the induction generator only but is also contributed by the IM load.

Type of Loading	Regulation	CCT
Case 1: 80% CPL	*P* constant only	645 ms
80% CPL	*P* constant and *Iq*	1.18 s
Case 2: 40% CPL, 40% IM	*P* constant only	468 ms
40% CPL, 40% IM	*P* constant and *Iq*	660 ms
Case 3: 20% CPL, 60% IM	*P* constant only	340 ms
20% CPL, 60% IM	*P* constant and *Iq*	480 ms

Table 5.1– Summary of the simulation results with J=0.5 [s] and Fault Resistance=110 Ω.

5.2 Incremental Current Rating of the Converter

In this section a simulation investigation is carried out in order to understand the effects of reactive current injection on the total incremental current rating of the converter. Two CPL model of the distribution system of figure 5.1 is considered with each CPL consuming 25% (188kW) of the total induction generator power. Several simulations are carried out for taking different levels of voltage drop and critical clearing time is calculated. Simulations are performed with and without the injection of reactive current by the constant power loads.

Case A: AC Voltage Controller is Inactive (Uncontrolled CPLs)

A three phase to ground fault is simulated between the grid and the load and the fault resistance is decreased to get the desired drop in the grid voltage. The drop in the AC side voltage from 0.2 pu to 0.6 pu is obtained for the different simulations performed. The fault duration is gradually increased to find out the transient stability limits of the distribution system accurately. The instability in the system mainly occurs when the induction generator loses the control of its torque with the increase in the fault duration. It is observed that the critical clearing time of the system is higher for lower values of the voltage drop and lower for the higher values of voltage drop. The total converter current It^* which actually represents only the active component of the AC current increases with the increase in the drop in the grid voltage to keep the power drawn by the load constant. The results from all the simulations for CPL1 are presented in the table 5.2. CPL2 shows the same results also.

Fault Resistance(Ω)	Vd (pu)	Id = It*(pu)	CCT (s)
110	0.8	0.345	1.2
80	0.7	0.42	0.275
60	0.6	0.463	0.12
48	0.5	0.596	0.07
38	0.4	0.82	0.065

Table 5.2– Summary of the simulation results without reactive current injection

Case B: AC Voltage Controller is Active (Controlled CPLs)

Simulations are again carried out to find the critical clearing time of the system for the same levels of voltage drops as done in the previous simulations. In this case however, the AC voltage controller is kept active during the fault and both the converters inject reactive current. The values of the fault resistances are exactly kept the same as in the simulations without

reactive injection. This gives slightly different values of voltage drops during the fault because of the improvement in the voltage as a result of reactive current injection by the CPLs. The value of critical clearing time is also increased for each value of voltage drop compared to the case with no reactive injection. This is due to a small voltage support during the fault enabling the system to tolerate the fault for relatively longer period. Active and reactive components of the current also show an increase with the increase in the voltage drop. The simulation results for CPL1 are shown in table 5.3.

Fault Resistance(Ω)	Vd (pu)	Id (pu)	Iq (pu)	It (pu)	CCT (s)
110	0.835	0.334	0.183	0.380	2
80	0.73	0.367	0.231	0.434	0.328
70	0.64	0.42	0.28	0.505	0.16
48	0.55	0.47	0.321	0.57	0.102
38	0.46	0.646	0.37	0.745	0.085

Table 5.3– Summary of the simulation results with reactive current injection

In the case with no additional injection of reactive current, the total current rating required by the converter are represented by only the active component of current $Id = It^*$. However with reactive current injection the total current is the quadratic sum of active and reactive components of the current given by:

$$I_t = \sqrt{I_d^2 + I_q^2}$$

The increase in the current rating is represented by the difference between the total current with reactive injection It and the total current without reactive injection It^*. The results given in the tables are plotted in figure 5.10. It is obvious from the graph that the value of active component of current Id for the case when CPL injects reactive current is lower than the value of It^* which represents no reactive injection for all the levels of voltage drop. This is because of the slight improvement in the voltage on the converter terminal as a result of reactive current injection. This improvement in the voltage is prominent as the same values of the fault resistance are used for both the cases. Therefore the green curve in the graph is always showing the greater values of the voltage drop compared to the red curve. It can also be noticed that the deeper the voltage drop the higher the amount of reactive current to keep the system stable. However this increase in reactive current is not proportional to the decrease in

the active component of the current. Therefore the required extra current rating of the converter is higher when drop in the voltage is deeper. Upto 60% of voltage drop this increase in the current rating is only 0.07 pu, which can be considered as an acceptable rise.

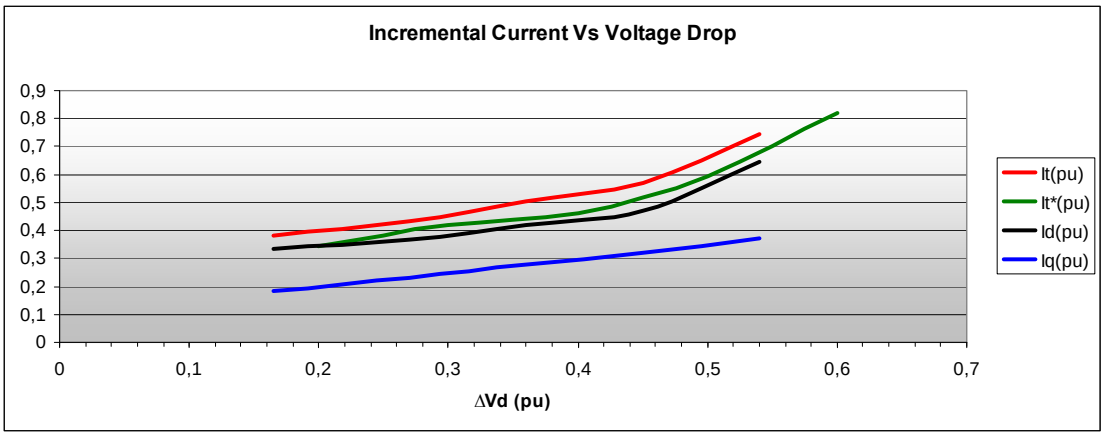

Figure 5.10–Incremental current rating of the CPL as a function of voltage drop

5.3 Distributed Reactive Current Injection by CPLs Vs Centralized Compensation

In this section an investigation is done in order to know whether it is beneficial to implement distributed compensation by CPLs compared to a centralized STATCOM. The model used for this purpose is shown in figure 5.11. A comparison between the system with the STATCOM placed at the terminal of the transformer and two non controlled CPLs is made with the case of two or three CPLs with reactive current control without a centralized STATCOM. A STATCOM operates according to voltage source principle however it differs from the CPL because it does not draw any active power. The implemented control system of the STATCOM is same as in the case of a constant power load described in section 3.8. It provides continuous reactive current in response to grid voltage abnormalities. The PSCAD/EMTDC model is given in figure D.3 in appendix D.

The total power drawn by the loads in all the studied cases is kept to 50% of the total induction generator power. Simulations are performed for different values of fault durations and the fault resistance is decreased upto a value beyond which the system is no more stable.

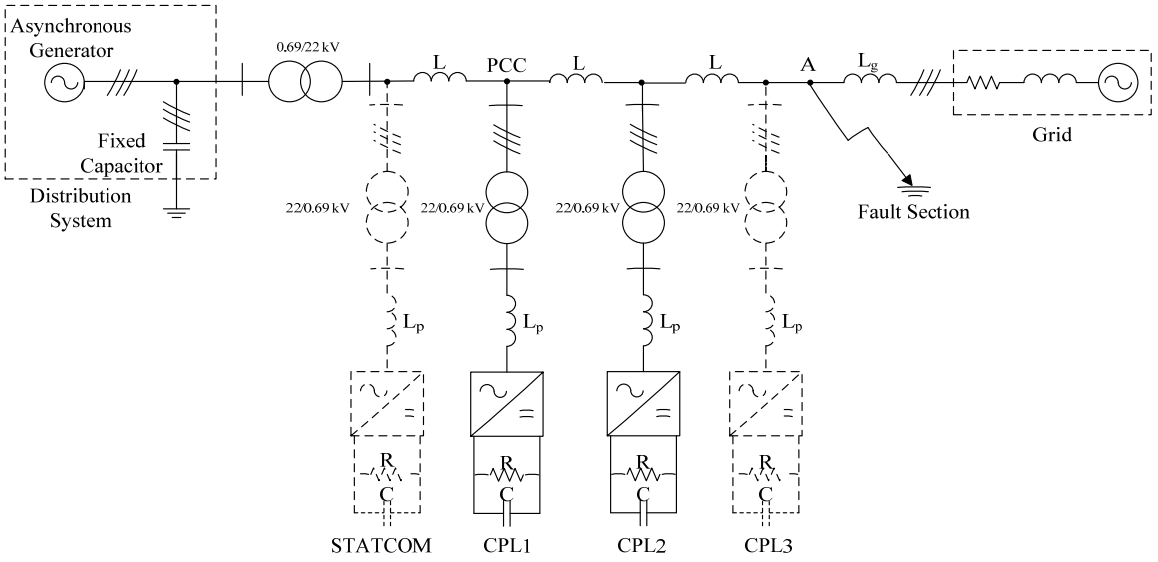

Figure 5.11–Distribution system with two or three CPLs and a STATCOM

The amount of reactive current injected by the centralized STATCOM , two CPLs and three CPLs is measured to achieve a stable system for a specific fault duration. It has been observed that the smaller the value of the fault duration the higher the drop in the voltage to provoke an instability in the system and vice versa. The cause of instability is largely due to the loss of generator torque.

Another important observation is that the reactive current injected by the CPLs is slightly different because of their location from the fault duration. The CPL located closed to the fault experiences slightly lower value of voltage drop at its terminal and therefore the injected reactive current is also slightly smaller. On the other hand the CPL located far from the fault section is faced with relatively higher value of voltage drop at its terminal and injects slightly more current. The sum of the injected reactive current in all the cases is calculated and presented in the table 5.4. The results are then plotted in figure 5.12.

It is clearly indicated in the figure 5.12 that the total injected reactive current by the centralized STATCOM is higher for all the fault durations compared to the sum of reactive current injected by the CPLs. Similarly the sum of reactive current injected by the two CPLs is higher than the sum of reactive current injected by the three CPLs to get a stable system for all the considered fault durations. The total amount of reactive current injected by one CPL belonging to a group of three distributed CPLs is roughly four times lower than the total amount of reactive current injected by the centralized STATCOM for all the simulated cases.

Similarly the sum of reactive current injected by one CPL belonging to a group of two CPLs is nearly 2.5 times lower than the total centralized compensation by a STATCOM. Therefore the implementation of two CPLs proves to be even more efficient and optimal instead of a single centralized STATCOM with higher current rating. In general it can be concluded that the distributed compensation provided by the power electronic loads is always advantageous than centralized compensation.

‘

Fault Duration	Fault Resistance (Ω)	Iq(pu) STATCOM	Iq(pu) 2CPL			Iq(pu) 3CPL			
			CPL1	CPL2	Sum	CPL1	CPL2	CPL3	Sum
0.2	38	0.302	0.139	0.137	0.275	0.0722	0.0716	0.0711	0.215
0.4	55	0.390	0.174	0.172	0.346	0.0935	0.0924	0.0915	0.277
0.6	59	0.517	0.220	0.217	0.437	0.124	0.122	0.120	0.366
0.8	62	0.594	0.263	0.260	0.523	0.164	0.162	0.161	0.487

Table 5.4– Summary of the simulation results

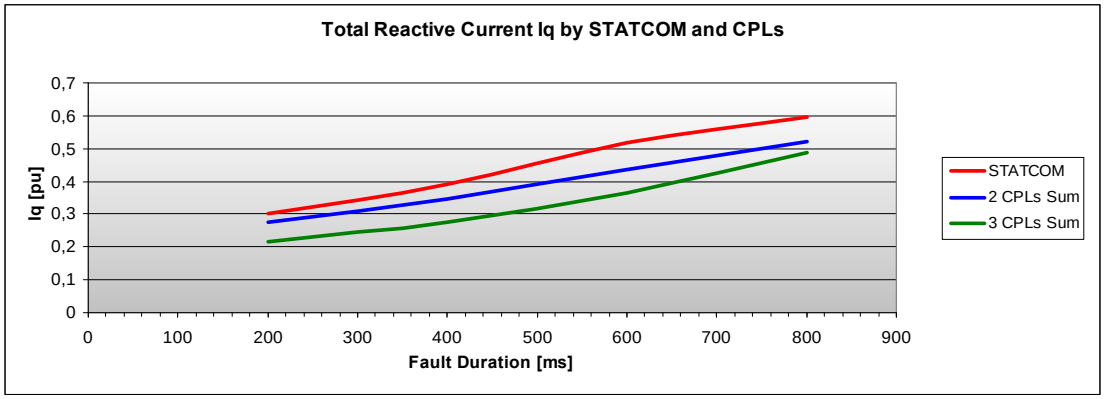

Figure 5.12–Total reactive current Iq by STATCOM and CPLs

Chapter 6: Power Flow Optimization of Distribution System

In this chapter an investigation is done to optimize the distribution system from power flow point of view. The total power losses in the system are the represented by both the distribution level losses and the transmission level losses. A simulation analysis is first done to find the amount of total current flowing in the distribution line which will help in overall reduction in I^2R losses. A methodology is then proposed to optimize the system with the inclusion of distributed energy resources connected to the distribution system through power electronic interfaces. The distributed injection of reactive power from the loads and the power sources is the main feature of this methodology.

6.1 Optimal Amount of Total Current for a Constant Power Load

Simulations are carried out to investigate the amount of reactive current *Iq* corresponding to minimum total current *It* for a constant power load. A model of distribution system is first analyzed with one constant power load as shown in figure 6.1. Controllable power source represents a power electronic interface for distributed energy resource DER located close to the point of power consumption. It is a full power DC/AC converter. DC link of this converter is represented by a Constant DC voltage source. The value of this DC voltage source is kept to 1127 V as given in section 3.2. Therefore the voltage on the AC side of this power source is the same as of the constant power loads. The control strategy for the controllable power source is also the same as given in section 3.8 for a CPL, however there is no DC link voltage controller being used. The manually specified value of the active component of current defines the total generated power. The value of 1.0 pu results in 750 kW of active power generation.

The per meter inductance of the distribution line is assumed to be 1 μH and the resistance is 0.1 mΩ [19]. The length of the distribution line is considered to be 50 meters and the distance between the PCC and the controllable power source or DER is also taken as 50 meters. The

implemented grid and transmission line parameters are the same as given in section 3.5. The length of the high voltage transmission line is taken to be 50 km.

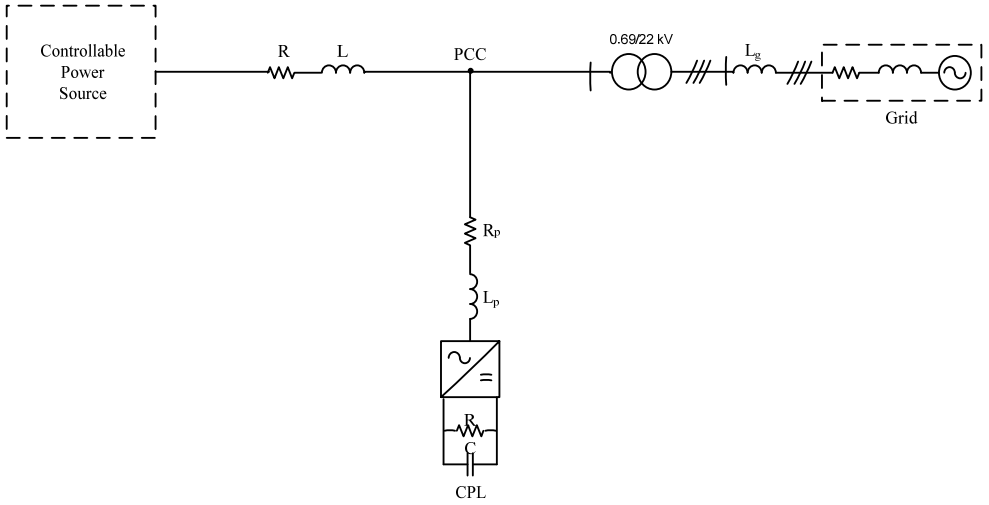

Figure 6.1 – Schematic distribution system with a CPL and DER

Simulations are then carried out for different values of consumed power by a constant power load to know the impact of reactive current on the total current.

6.1.1 CPL Taking 300 kW of Active Power

In this case the constant power load is consuming 300 kW of active power from the system. The DER is kept active therefore this power requirement is being supplied by it. The extra amount of power is being supplied to the grid from the DER. The voltage at the point of common coupling is 1.0 pu under steady state. CPL draws an amount of active component of the current corresponding to the load requirements. Simulations are performed and different amount of reactive current is injected by the converter into the system and the corresponding value of active component of the current is measured. The results are summarized in table 6.1.

The total current is quadratic sum of the active and reactive components of current. As the amount of injected reactive current is increased the value of absorbed active current is decreased slightly and the voltage at PCC is increased keeping the power drawn by the load constant. The results are plotted in the figure 6.2.

As can be observed from the plot that injection of reactive current *Iq* decreases the amount of total current *It* and when the amount reactive current is 0.075 pu the value of total current is minimum. The total current starts increasing from here onwards and reaches to its initial value when the reactive current is nearly 0.125 pu and then it increases rapidly with the further increase in reactive injection. The active component of current *Id* always decreases with the increase in reactive current as shown by the red curve. The impact of reactive current on reduction of total current is not substantial in this case however next simulations will show that as the amount of power consumed by the load will increase the reactive current will have significant effect on the total current for a CPL.

Id (pu)	Iq (pu)	It (pu)
0.405	0	0.405
0.394	0.05	0.397
0.389	0.075	0.396
0.386	0.1	0.399
0.382	0.15	0.41
0.38	0.2	0.43
0.377	0.25	0.452
0.374	0.3	0.48
0.37	0.35	0.51
0.365	0.4	0.541
0.361	0.45	0.577
0.358	0.5	0.615

Table 6.1 – Summary of simulation results for total current for a CPL taking 300 kW

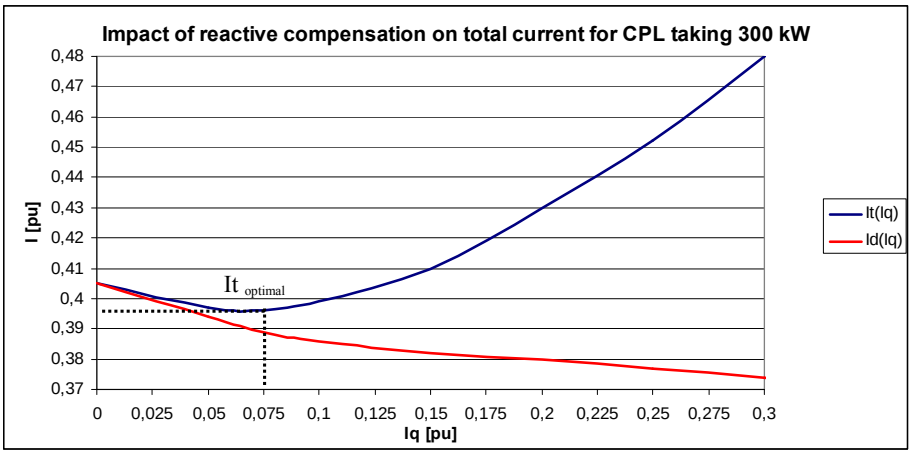

Figure 6.2 – Optimal total current for a CPL taking 300 kW

6.1.2 CPL Taking 500 kW of Active Power

Now the amount of power consumed by CPL is increased and it is now taking 500 kW from the controllable power source or DER. The amount of active component of current is related to the power consumed by the load. For a constant power load, converter must always inject reactive current because when it absorbs reactive current then voltage at its terminal decreases resulting in an increased active current and hence the total current also increases. Therefore it can be stated that the decrease in total current for a CPL comes at a cost of small increase in voltage at its terminal.

In order to find out the amount of reactive current corresponding to minimum attainable total current for the new load condition different amount of reactive current is injected into the system and the decreasing values of active currents are measured and presented in the table 6.2. The results are then plotted in figure 6.3.

Id (pu)	Iq (pu)	It (pu)
0,667	0	0,667
0,66	0,05	0,661
0,652	0,1	0,657
0,647	0,15	0,662
0,642	0,2	0,672
0,638	0,25	0,685
0,632	0,3	0,699
0,627	0,35	0,718
0,621	0,4	0,74
0,617	0,45	0,763
0,613	0,5	0,791

Table 6.2 – Summary of simulation results for total current for a CPL taking 500 kW

The value of total current slightly decreases with the injection of reactive current. It is lowest when the amount of reactive current is 0.1 pu and then increases rapidly with further increase in reactive current. This value of reactive current must always be injected by the converter in order to achieve optimal total current and hence lowest I^2R losses in the distribution line under this load condition. There is a continuous reduction in the active current as a result of reactive injection. The decrease in total current for the converter results in approximately 1.5 % increase in grid voltage at the converter terminal.

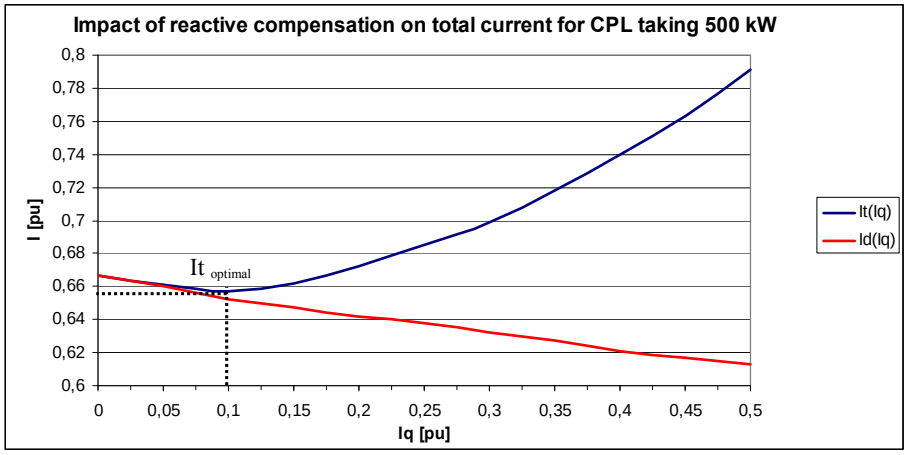

Figure 6.3 – Optimal total current for a CPL taking 500 kW

6.1.3 CPL Taking 750 kW of Active Power

It is interesting to investigate the effect of reactive compensation on the increasing amount of load power. Now the CPL is consuming 750 kW from the DER. Again the simulations are run to find the optimal operating point for the system under these load conditions and the results are presented in table 6.3 and plotted in figure 6.4.

There is about 1.5 % decrease in the total current when 0.2 pu reactive current is injected compared to the case when there is no injection of reactive current. The system is tightly regulated and therefore this is the maximum possible decrease in the total current for the CPL. However compared to the previous cases the optimal operating point for the system has been increased. Beyond this point the total converter current starts increasing rapidly again, suggesting more losses in the distribution line. The decrease in total current is also dependent on the grid parameters. If the grid inductance is increased then the same amount of reactive injection will result in significant increase in the converter terminal voltage. The more prominent effects can therefore be seen in reduction of total current as the reduction in active current will be higher.

Id (pu)	Iq (pu)	It (pu)
0.999	0	0.999
0,994	0,05	0,995
0,986	0,1	0,991
0,977	0,15	0,988
0,966	0,2	0,986
0,957	0,25	0,989
0,95	0,3	0,996
0,943	0,35	1,005
0,935	0,4	1,017
0,929	0,45	1,032
0,922	0,5	1,05

Table 6.3 – Summary of simulation results for total current for a CPL taking 750 kW

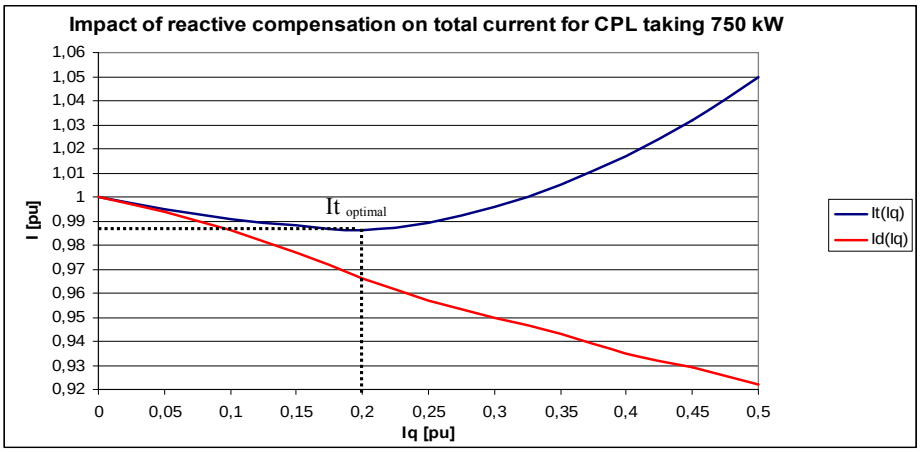

Figure 6.4 – Optimal total current for a CPL taking 750 kW

6.2 Simulations for 2 CPL Model of AC Distribution System

In this section an investigation of optimal operating point of the distribution system with more than one constant power load is done. The system used for this purpose is shown in the figure 6.5. Two constant power loads are being fed from the DER and the grid. The grid only comes into play when the load demand is more than the total capacity of the controllable power source. The parameters of the distribution system are kept same as in the simulations with one CPL. The distance of the DER from the PCC is 50 meters and the distance between the loads is taken to be 25 meters.

As done in the previous sections the simulations are performed for different values of load power to investigate the impact of reactive injection on total distribution line current.

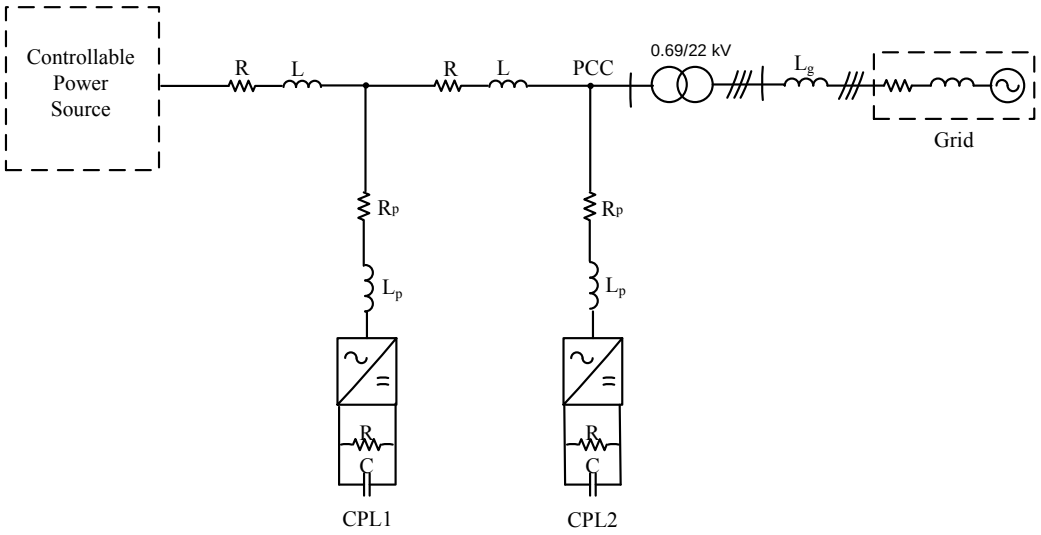

Figure 6.5 – Schematic distribution system with 2 CPLs and DER

6.2.1 Each CPL Taking 500 kW of Active Power

Simulations are carried out for the case when each CPL consumes 500 kW from the system. Controllable power source is supplying 75 % of the load demand. The rest of the power is being supplied by the grid. The voltage at PCC is 1.0 pu.

Each CPL draws an amount of active component of the current corresponding to the load requirements. In order to observe the effect of reactive compensation on the total current different amount of reactive current is injected by each CPL. The simulation results for CPL1 are presented in the table 6.4. Almost the same results are observed for the CPL2. The results are then plotted in the figure 6.6.

Id (pu)	Iq (pu)	It (pu)
0,641	0	0,641
0,633	0,05	0,635
0,624	0,1	0,631
0,616	0,15	0,634
0,609	0,2	0,641
0,602	0,25	0,652
0,595	0,3	0,666
0,586	0,35	0,682
0,575	0,4	0,701
0,568	0,45	0,725
0,561	0,5	0,751

Table 6.4 – Summary of simulation results for total current when each CPL consumes 500 kW

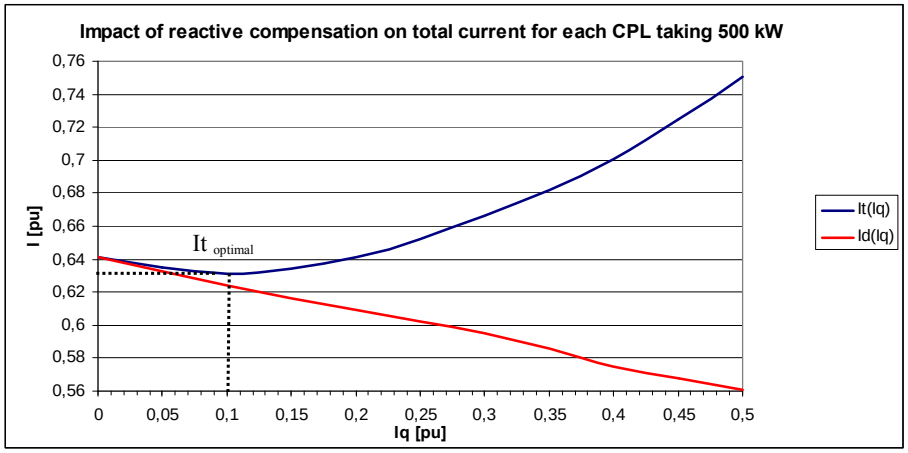

Figure 6.6 – Optimal total current when each CPL consumes 500 kW

There is a slight reduction in the total current as the injected reactive current increases. The total current is minimum when the injected reactive current is 0.1 pu, beyond this point it increases rapidly. Therefore the CPL must always inject this amount of reactive current in order to reduce the overall losses in the distribution system depending mainly on the total amount of current. The result is the same as obtained for one CPL model in section 6.1.2.

6.2.2 Each CPL Taking 750 kW of Active Power

The amount of power consumed by each load has been increased to 750 kW. In this case the power demand is equally shared by both the grid and the DER. With the increase in the load power the active component of the current for a CPL also increases as this is always related to the energy requirements of the system. Simulations are run to find out the reactive component of the current that must be injected in order to find out the minimum attainable total current $It_{optimal}$. The results for CPL1 are summarized in table 6.5 and plotted in figure 6.7.

With the higher share of load power the operating point is further move to the right as shown in figure 6.7. The lowest value of the total current is achieved when the injected reactive current is 0.2 pu. Therefore the CPL must always inject this amount of reactive current in order to reduce the overall losses in the distribution line. If we extend this plot to further left i,e if the converter absorbs reactive current from the system then the voltage at its terminal will decrease and the active component of current will increase to neutralize this effect and to maintain the power being consumed. This will greatly increase the total current.

Id (pu)	Iq (pu)	It (pu)
0,998	0	0,998
0,992	0,05	0,993
0,983	0,1	0,988
0,974	0,15	0,985
0,963	0,2	0,983
0,955	0,25	0,986
0,945	0,3	0,991
0,938	0,35	1,00
0,93	0,4	1,012
0,923	0,45	1,027
0,916	0,5	1,04

Table 6.5 – Summary of simulation results for total current when each CPL consumes 750 kW

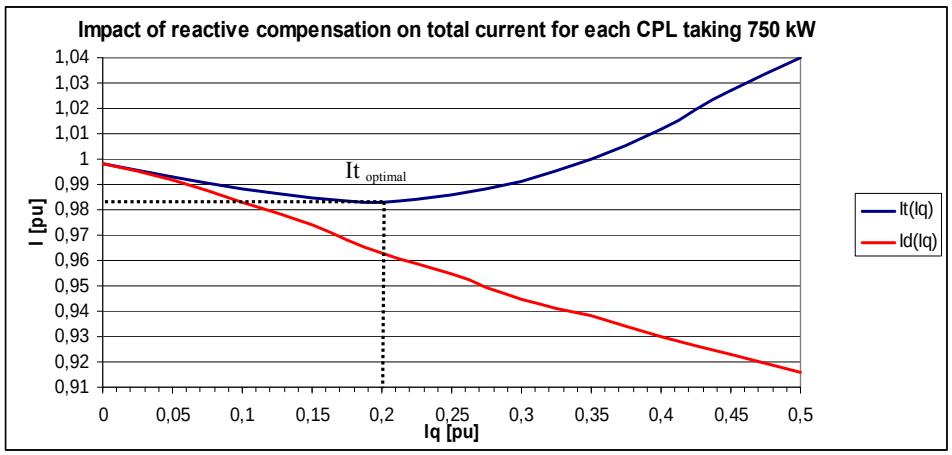

Figure 6.7 – Optimal total current when each CPL consumes 750 kW

6.3 Simulations for 3 CPL Model of AC Distribution System

The model shown in figure 6.8 is used for the investigation of optimal operation of the system with three constant power loads. Before proceeding further for the development of the method for overall distribution loss reduction it is important to investigate for the optimal operating point for the system with three constant power loads. The voltage at PCC is 1 p.u. The parameters of the distribution system are kept same as in the previous simulations. The distance between each load is 25 meters and the distance of PCC from DER is 75 meters. The simulations are performed for different values of load power as explained in the following subsections.

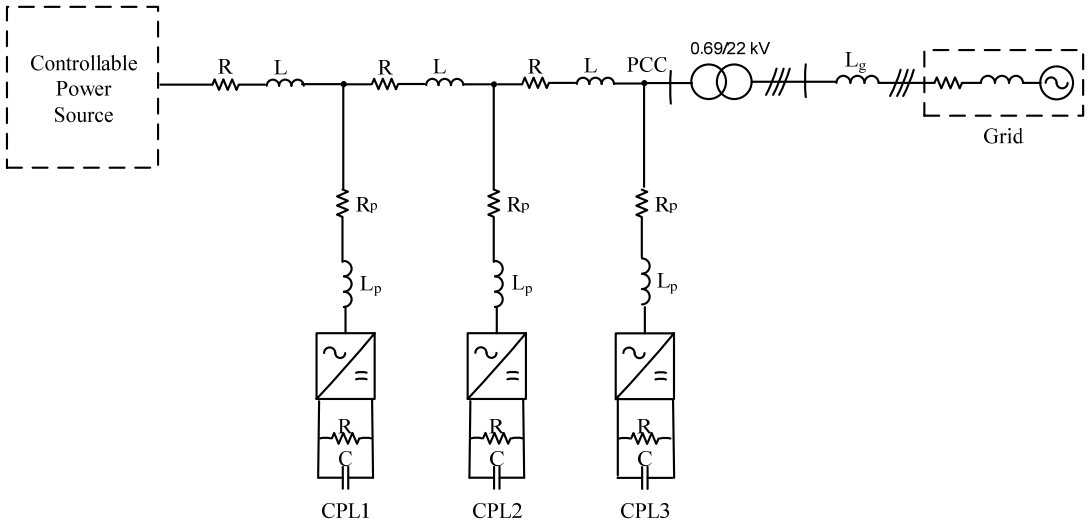

Figure 6.8 – Schematic distribution system with 3 CPLs and DER

6.3.1 Each CPL Taking 500 kW of Active Power

Simulations are carried out for the case when each of the three CPLs consumes 500 kW of the active power. About 750 kW is provided by the controllable power source while 750 kW comes from the grid. The results of the simulations for CPL1 are presented in table 6.6 and then plotted in figure 6.9. The results obtained for the other two CPLs are similar.

Id (pu)	Iq (pu)	It (pu)
0,656	0	0,656
0,646	0,05	0,647
0,637	0,1	0,644
0,628	0,15	0,645
0,619	0,2	0,65
0,612	0,25	0,661
0,604	0,3	0,674
0,596	0,35	0,691
0,588	0,4	0,711
0,581	0,45	0,736
0,574	0,5	0,761

Table 6.6 – Summary of simulation results for total current when each CPL consumes 500 kW

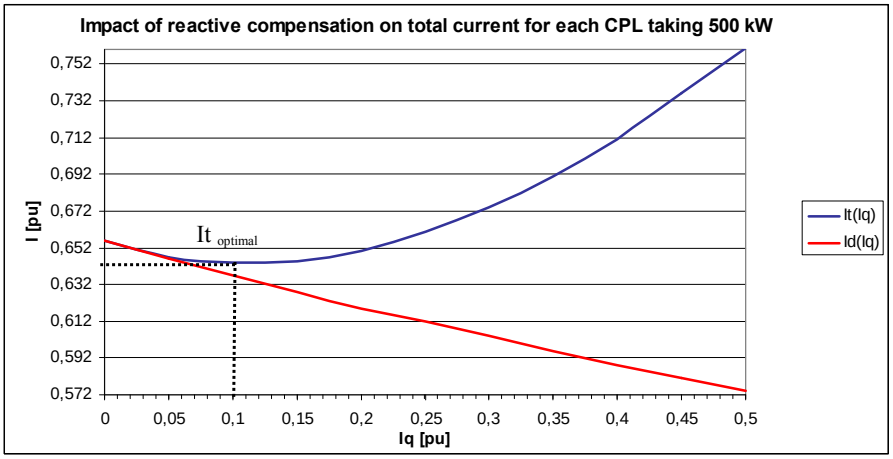

Figure 6.9 – Optimal total current when each CPL consumes 500 kW

In this case too the same amount of reactive current is needed to get the minimum attainable total current as in the case of one and two CPL models for the same load power. This is only point where is system can operate optimally under these load conditions. All the other operating points will result in higher total current and consequently more losses.

6.3.2 Each CPL Taking 750 kW of Active Power

Now each CPL is consuming 750 kW from the system. Almost two third of the power demand is being fulfilled by the grid. Simulations are carried out to find the optimal operating point of the system under these load conditions and the results are presented in table 6.7.

Id (pu)	Iq (pu)	It (pu)
0,998	0	0,998
0,992	0,05	0,993
0,983	0,1	0,988
0,974	0,15	0,985
0,963	0,2	0,983
0,955	0,25	0,986
0,945	0,3	0,991
0,938	0,35	1
0,93	0,4	1,012
0,923	0,45	1,027
0,916	0,5	1,04

Table 6.7 – Summary of simulation results for total current when each CPL consumes 750 kW

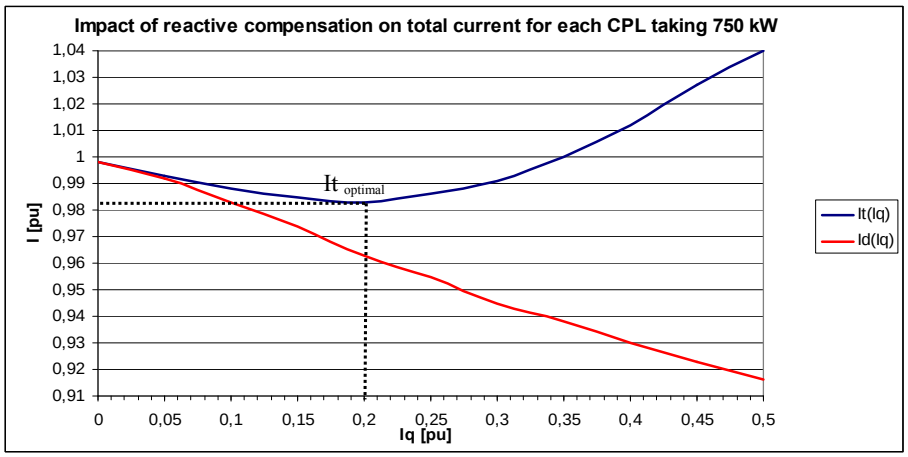

Figure 6.10 – Optimal total current when each CPL consumes 750 kW

As shown in figure 6.10 the operating point is further move to the right with higher share of load power. The optimal operating point is obtained when the injected reactive current is 0.2 pu. This also shows that the power factor does not need to be unity in the distribution line in order the get the minimum losses. The results are in accordance with the simulation analysis performed in section 6.1.3 and section 6.2.2.

6.4 Loss Minimization Methodology for AC Distribution System

The impact of reactive current *Iq* on the overall loss minimization in the distribution system is investigated through simulation. The distribution system is comprised of two DERs and four constant power loads as shown in figure 6.11. Controllable power source represents a switching power interface (SPI) or PE interface for distributed energy resource (DER) as described in section 6.1.

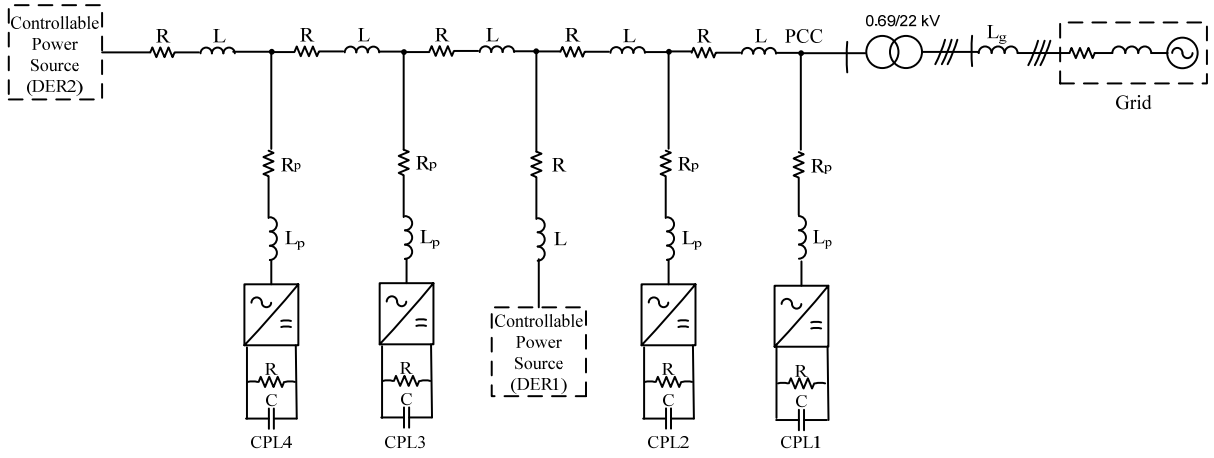

Figure 6.11 – Schematic distribution system with high share of power electronic loads and DERs

It is supposed that the intervention of both the DERs will reduce the overall distribution losses as they are located very close to the point of utilization.

The impedance per meter of the distribution line is chosen to be *0.1 mΩ - 1μH*. The distance between the point of common coupling and DER1 is taken to be 50 meters and the distance between the DER1 and DER2 is also considered to be 50 meters. The length of the distribution line between each load is taken as 25 meters. The length of the distribution branches is 50 meters. The length of the high voltage transmission line is considered as 50 km.

In this distribution system the loss calculation is performed by measuring the input and output powers for the complete system and for each distribution line. The input power is the sum of the powers generated by the grid and the DERs in response to a particular load demand. The load powers are measured at the point of connection to find out the total distribution losses for

a specified load demand. The powers by the controllable power sources are measured to have an idea of how the DER reacts to a particular load demand.

The methodology involves the following three steps:

- Intervention of DERs or controllable power sources located very close to the load centre for load sharing
- Cancellation of grid side reactive power by using the controllable power source located closer to the PCC.
- Injection of reactive current *Iq* by the loads corresponding to minimum total current *It* for a constant power load.

6.4.1 Optimal Total Current for Loads When Each CPL is Taking 500 kW

Some simulations are done in order to find out the amount of reactive current injected by each CPL that will result in the minimum total current in the distribution lines. The DERs are delivering 50 % of their rated power to the loads. The grid is supplying the rest of the load demand. The results are presented in table 6.8.

Id (pu)	Iq (pu)	It (pu)
0,653	0	0,653
0,644	0,05	0,647
0,634	0,1	0,642
0,626	0,15	0,644
0,617	0,2	0,649
0,608	0,25	0,657
0,6	0,3	0,671
0,591	0,35	0,687
0,583	0,4	0,707
0,574	0,45	0,73
0,566	0,5	0,755

Table 6.8 – Summary of simulation results for total current when each CPL consumes 500 kW

In this case the minimum total current is achieved in each branch when the CPL injects 0.1 pu reactive current as shown in figure 6.12. The result is the same as obtained in the previous simulations for one, two and three CPL distribution system models.

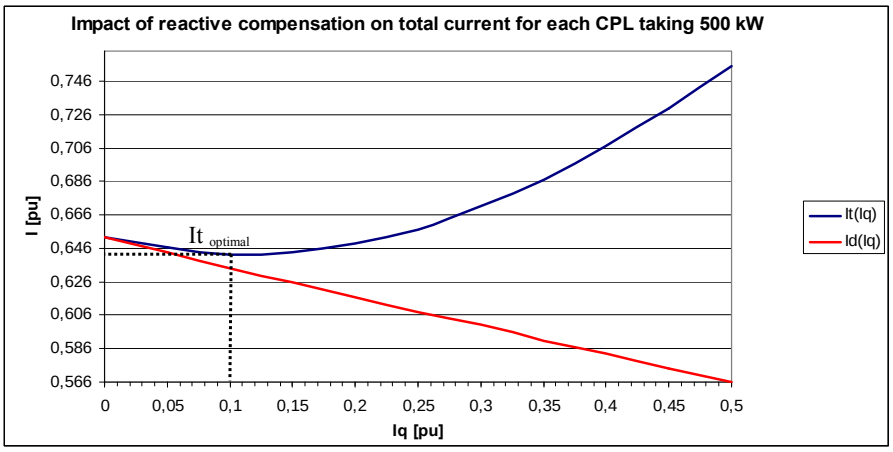

Figure 6.12 – Optimal total current when each CPL consumes 500 kW

6.4.2 Application of Loss Minimization Methodology for Load Power=2000 kW

In order to test the methodology simulations are carried out for the load condition when each CPL is consuming 500 kW of active power from the system. The total power demand is 2000 kW. At the start simulations are run for one second without connecting the loads because of the simulation software limitations. The software PSCAD/EMTDC is time sensitive for complicated models and it is difficult to get the rated voltage when connecting the loads at the very start of the simulation. The loads are therefore connected to the system at time t=1s. Initially only the grid is making sure to fulfill all the load demand. At time t=2s DER_1 is turned on and starts contributing to the local load demand. At time t=3s DER_2 is turned on and results in further decrease in the power supplied from the grid. At time t=4s DER_1 injects reactive power to cancel out the reactive power generated by the grid. At time t=5s each CPL injects reactive current corresponding to the total minimum current. The process is illustrated by the following figures.

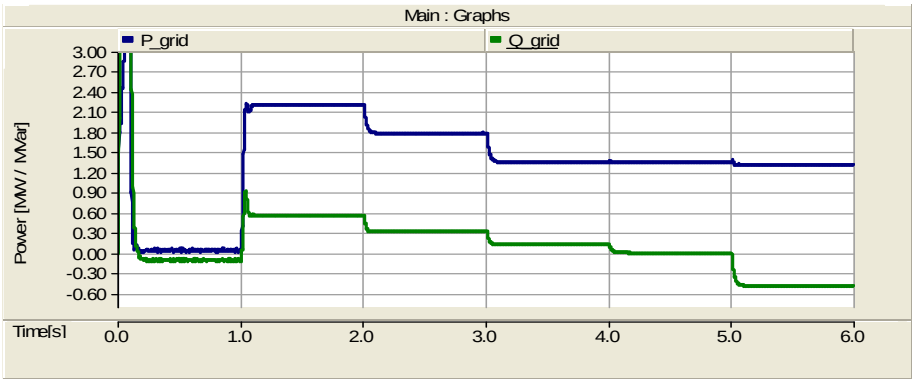

Figure 6.13 – Grid active and reactive power

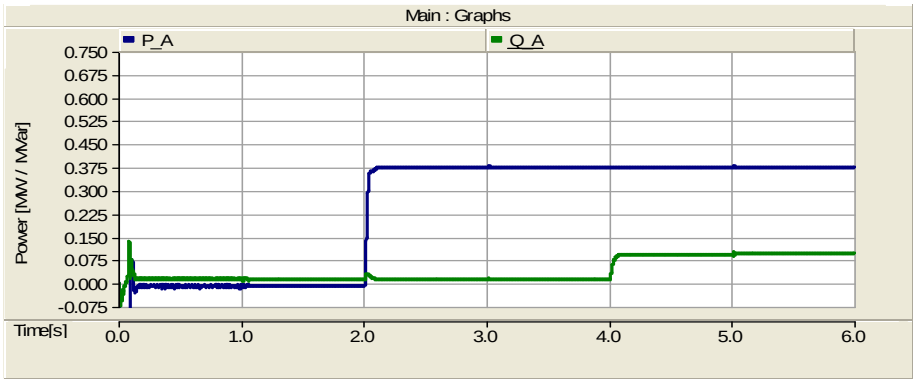

Figure 6.14 – DER1 active and reactive power

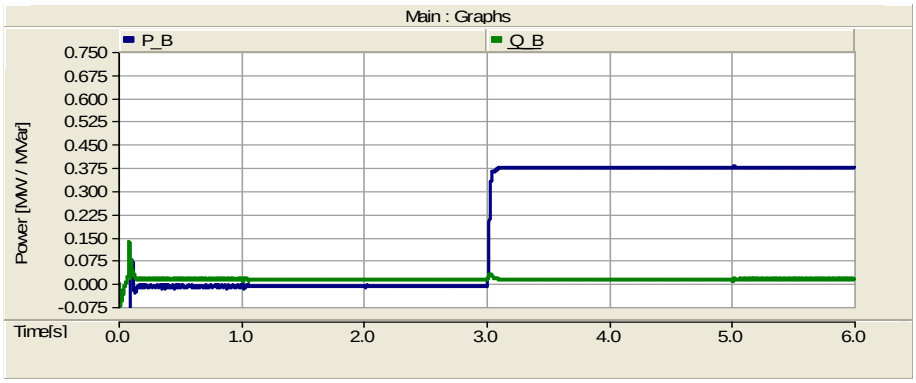

Figure 6.15 – DER2 active and reactive power

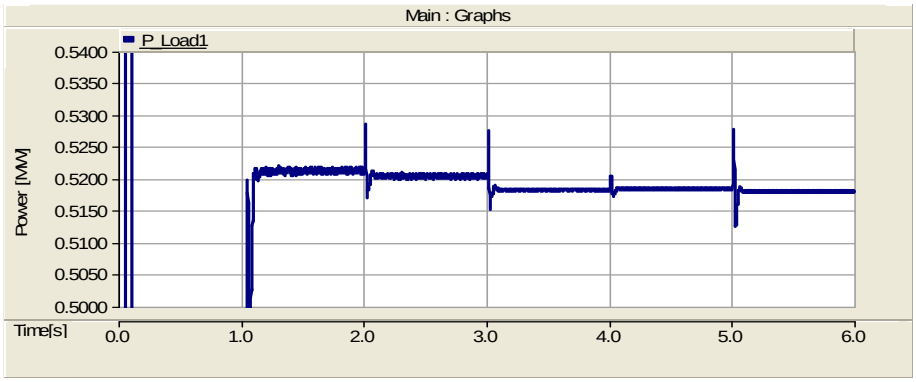

Figure 6.16 – Active power for CPL1

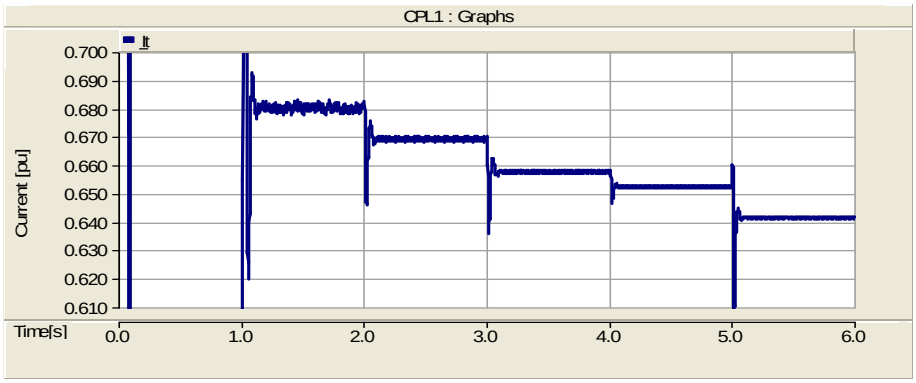

Figure 6.17 – Total current for CPL1

Under the no load conditions for first one second 72 kVar reactive power is supplied to the grid by the capacitive filters of all the converters in the system. When the loads are connected at time t=1s grid supplies 2202 kW of active power in demand to a total load of 2000 kW. The reactive power generated by the grid is 550 kVar. The input power to each distribution line in the system is 522 kW as shown in figure 6.16. At this point the total losses in the system are 202 kW including the losses in the long transmission line.

6.4.2.1 Intervention of DERs

At time t=2s DER_1 is turned on and it starts supplying power to the loads equal to the 50 % of its rated active power as shown in figure 6.14. At this point the power supplied by the grid is 1786 kW while DER_1 supplies 375 kW of active power. The intervention of DER_1 reduces the reactive power to 320 kVar. The total supplied active power is 2161 kW in demand to 2000 kW. The total losses are reduced to 161 kW.

At time t=3s the DER_2 is turned on and its active power reaches to 50 % of its rated value as shown in figure 6.15. The DER units are now supplying 375 kW each. The supplied power from the grid comes down to 1380 kW. The total supplied active power at this stage is 2130 kW. The grid reactive power is reduced to 120 kVar. The total active power losses are 130 kW.

6.4.2.2 Cancellation of Reactive Power

At time t=4s DER_1 unit injects reactive component of the current to nullify the remaining reactive power from the grid. Now there is no flow of reactive power from the grid. Each DER unit supplies 375 kW and the active power supplied by the grid is 1365 kW. The total supplied power comes down to 2115 kW and the losses are reduced to 115 kW.

6.4.2.3 Injection of Reactive Current Iq By CPLs

At time t=5s each CPL injects 0.1 pu reactive current in accordance with the simulation results obtained in section 6.4.1. As a result of reactive injection line losses in each distribution line are reduced by1 kW as shown in figure 6.16. It also helps in stabilizing the voltage at the load

terminals. This methodology helps reducing the total losses in the distribution by 4 kW. The total power input at decreases from 522 kW to 518 kW. Therefore 18 kW is lost in each distribution line which cannot be further decreased as the total current is at its optimal value. The figure 6.17 shows the total current for CPL1 which reduces with the implementation of each step in this methodology.

At the last stage of this methodology the grid is supplying 1356 kW and each DER unit is delivering 375 kW. The total supplied active power is 2106 kW and the losses are reduced to 106 kW or 52 % of the initial value. The total losses in the four distribution lines are still 72 kW as shown in figure 4.16 and 34 kW power loss corresponds to the rest of the system.

The time behavior of distribution losses is plotted in figure 6.18. It shows that the total losses are reduced by 48 %. It also provides the details of the total reduction in losses with the execution of each step of this method.

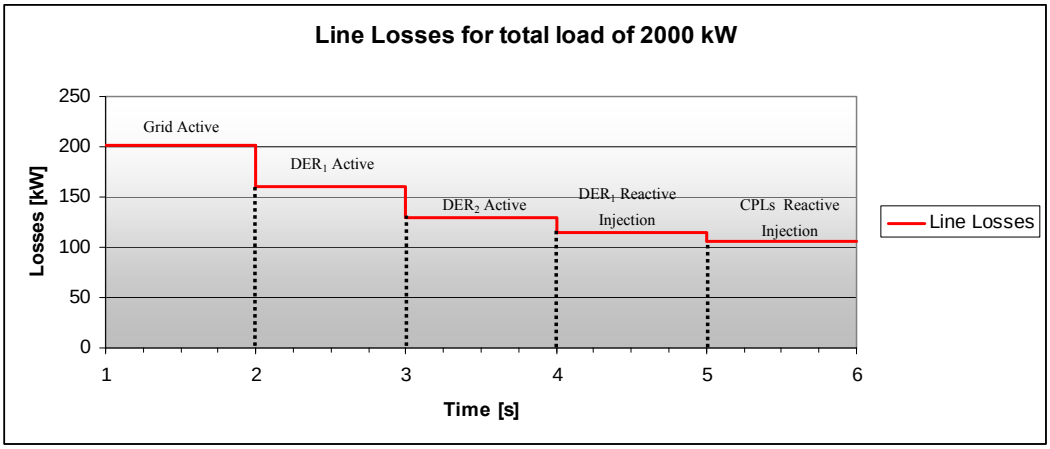

Figure 6.18 – Time behavior of distribution losses

6.4.3 Optimal Total Current for Loads When Each CPL is Taking 750 kW

In this case each CPL is consuming 750 kW. Both the DERs are delivering their rated power to the loads. The grid is supplying for the rest of local load demand. The results for minimum distribution line current are presented in table 6.9.

Figure 6.19 shows that 0.2 pu reactive current must be injected by each CPL in order to minimize the total current in their respective branches resulting in smaller distribution losses.

This also verifies that the amount of reactive current to get the optimal total current is independent of the number of CPLs in the system for a specified amount of load power.

Id (pu)	Iq (pu)	It (pu)
0,987	0	0,987
0,976	0,05	0,977
0,961	0,1	0,966
0,945	0,15	0,956
0,93	0,2	0,951
0,918	0,25	0,953
0,907	0,3	0,956
0,898	0,35	0,963
0,887	0,4	0,973
0,879	0,45	0,988
0,868	0,5	1

Table 6.9 – Summary of simulation results for total current when each CPL consumes 750 Kw

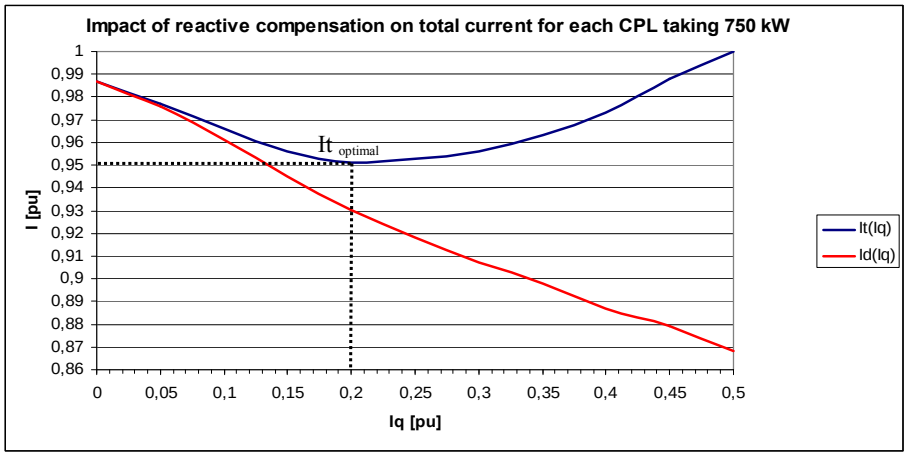

Figure 6.19 – Optimal total current when each CPL consumes 750 kW

6.4.4 Application of Loss Minimization Methodology for Load Power=3000 kW

Simulations are again carried out for the higher load demand and each CPL is consuming 750 kW of active power from the system. The total power demand is 3000 kW. The loads are connected to the system at time t=1s. Initially grid supplies all the power demanded by the loads. DER_1 is turned on at time t=2s. DER_2 is turned on at time t=3s. Both the DERs are operating at their rated active power. At time t=4s DER_1 injects reactive power to cancel out

the reactive power generated by the grid. At time t=5s each CPL injects reactive current corresponding to the total minimum current. Next figures provide the details of this process.

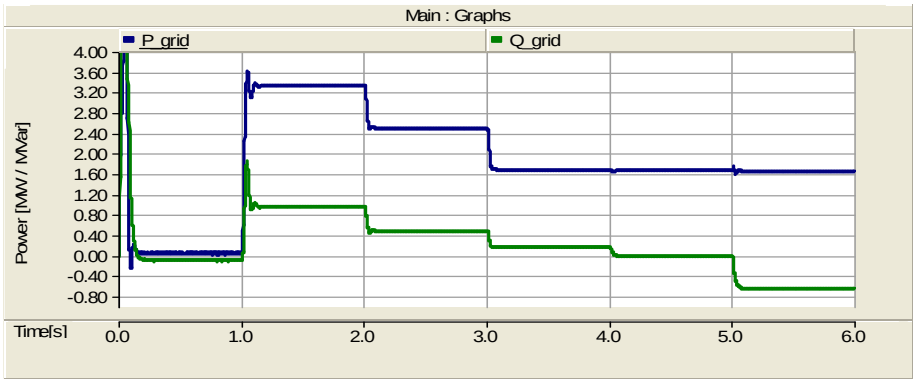

Figure 6.20 – Grid active and reactive power

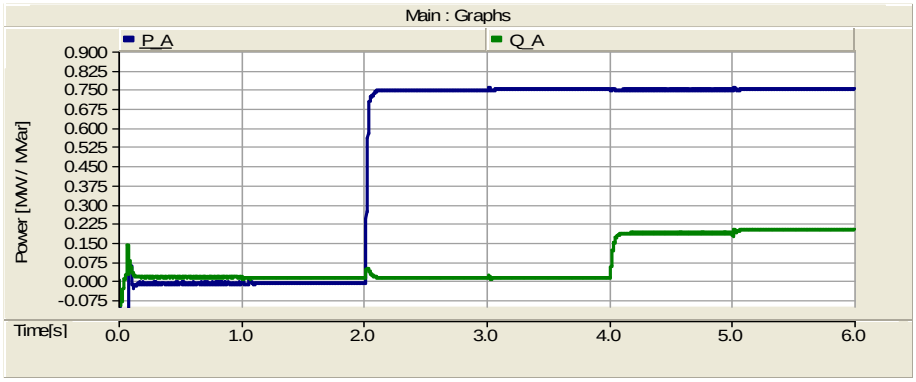

Figure 6.21 – DER1 active and reactive power

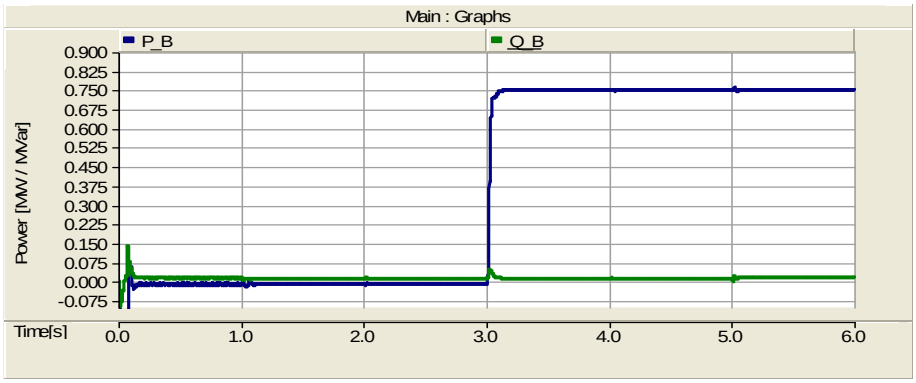

Figure 6.22 – DER2 active and reactive power

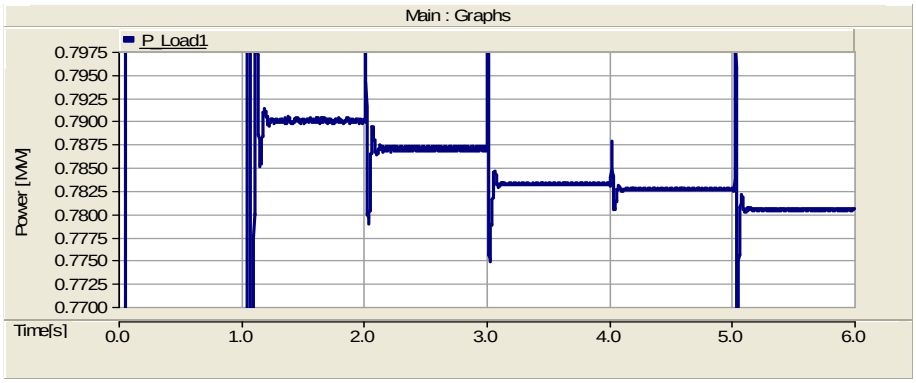

Figure 6.23 – Active power for CPL 1

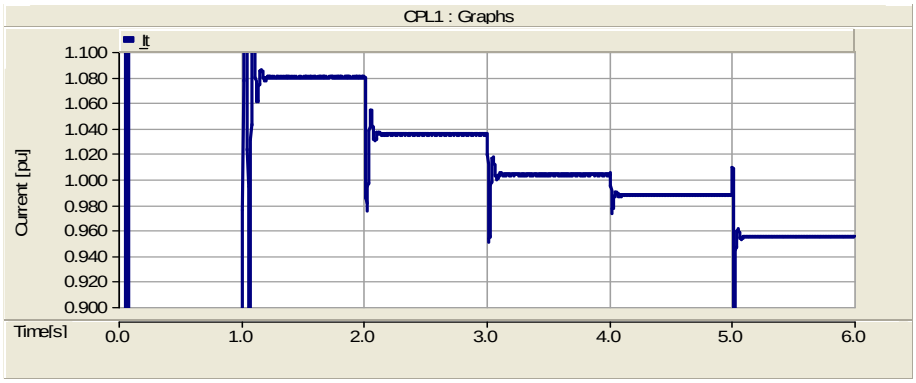

Figure 6.24 – Total current for load 1

When the loads are connected at time t=1s all the power is being supplied by the grid. The amount of active power supplied by the grid is 3320 kW and the total local load demand is 3000 kW. The grid is generating 940 kVar reactive power. At this point the total losses in the system are 320 kW. The power input to each distribution line is 790 kW as shown in figure 6.23.

6.4.4.1 Intervention of DERs

At time t=2s the DER_1 is turned on and it starts supplying 750 kW of power to the loads as shown in figure 6.21. The power supplied from the grid reduces to 2503 kW. The introduction of DER_1 unit also results in the reduction of reactive power from the grid and decreases it to almost half of the initial value. The total supplied power at this point is 3253 kW in demand to 3000 kW. Therefore introduction of DER_1 unit reduces the losses to 253 kW.

At time t=3s the DER_2 is turned on to share the load demand. The DER units are now supplying 750 kW each. The power supplied from the grid comes down to 1702 kW. The

losses are reduced from the initial value of 320 kW to 202 kW. The intervention of DER2 unit also reduces the reactive power from the grid to a value of 178 kVar.

6.4.4.2 Cancellation of Reactive Power

At time t=4s DER_1 unit is allowed to inject reactive current to cancel out the remaining reactive power from the grid. The reactive power from the grid comes down to zero value. At this stage the power calculations are as follows:

$P_{total} = P_{DER1} + P_{DER2} + P_{Grid}$ = 1678 +750+750 = 3178 kW

In this step the total losses in the system are reduced to 178 kW.

6.4.4.3 Injection of Reactive Current Iq by CPLs

At time t=5s each CPL injects 0.2 pu reactive current. As a result of reactive injection line losses in each distribution line are reduced by 3 kW in this step as shown in the figure 6.23. Same results are found for the other three loads. Figure 6.23 also shows that the power input to the distribution line is decreased from 790 kW to 780 kW after implementation of this three step methodology.

Figure 6.24 shows the total current for CPL1. It is obvious that the total current decreases with the implementation of each step in the methodology. In the last step at time t=5s the decrease in current is nearly 4 % in response to reactive current injection. This continuous decrease in current suggests the decrease in the distribution line losses. The losses in the distribution line cannot be further reduced as this is the minimum achievable value of the total current for the power electronic load.

At this last stage the grid is supplying 1649 kW and the power delivered by each DER unit is 750 kW. The total power delivered from the system is 3149 kW .Therefore the losses are reduced to 149 kW. The total reduction in the losses is 171 kW or 53%. The figure 6.23 shows that the total losses in the four distribution lines are still 120 kW and the losses in the rest of the system are 27 kW. The total losses in the system are now only 5% of the total power demand.

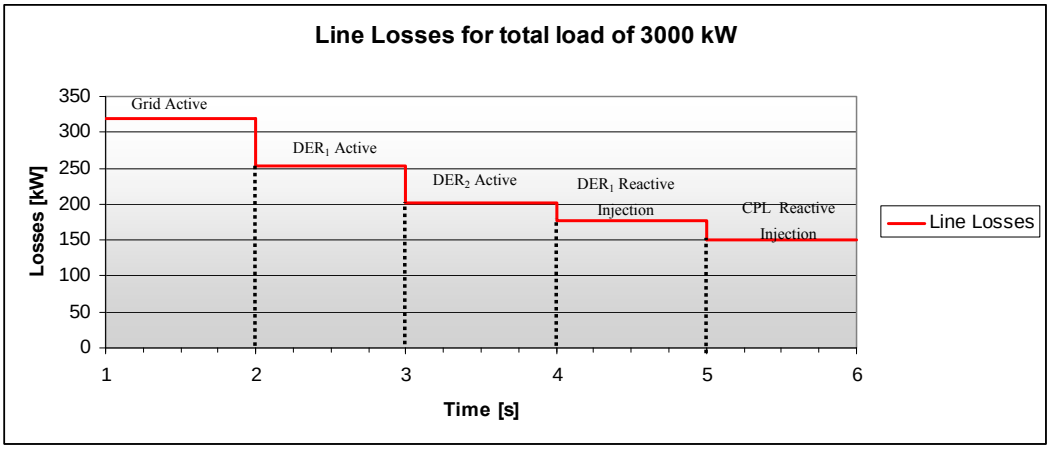

Figure 6.25 – Time behavior of distribution losses

The time behavior of the distribution losses is shown in figure 6.25. The intervention of DER units and reactive injection reduces the losses to 47 % of initial value. This methodology therefore provides the full utilization of the distributed energy resources, voltage support at the load terminals, and lower distribution losses.

Chapter 7: Discussion

This chapter briefly discusses the results achieved in the thesis work. It also describes the accuracy of the obtained results and some limitations and shortcomings of the implemented models. In the first part discussion is made on the investigation of converter stability. The second part discusses the transient stability of the distribution system. Finally a short discussion is done on the optimal power flow and the implemented model.

7.1 Stability of Converter Control System

The tuning of the converter controllers is done based on the methods giving faster response and higher phase margin. The impact of sudden variations in the system parameters on the stability of the control system has been analyzed. The analysis is based on both the theoretical study and the simulation analysis. The frequency domain analysis for steady state operation presented in section 4.2.1 gives the maximum possible value of the phase margin for the given third order system. It has been supposed that in real online situation there will be delays in the system preventing the instantaneous modifications of the controller parameters in response to changes in the grid parameters. However this analysis only provides the information about the instability caused by the low frequency oscillation behavior as a result of drop in the voltage. It is very clear from the theoretical study that the increase in the voltage will give rise to high frequency oscillations and the operating point will move to the further right in the bode plot. This will also result in lower phase margins.

The impact of physical components of the system on the stability of the control system has also been investigated. The investigation involved only the DC link capacitor. By doubling the value of the capacitance in the DC link the time constant will be doubled. The proportionality constant of the controller K_{pv} will also be doubled giving the same value of open loop transfer function. The higher value of the capacitor results in more energy storage and therefore more stable system as described in the literature. However if only the capacitance is increased and the other controller parameters are kept the same then the stability of the converter control system is lowered. The frequency domain analysis confirms that the chosen value of the DC link capacitor provides the maximum phase margin. If the capacitance is increased then the operating point moves to the left on the bode plot giving

lower phase margin and if capacitance is decreased then the operating point will move to the right again resulting in smaller value of the phase margin.

The values of the converter filters L_f and R_f effect the parameters of the current controller only. In this analysis the impedance of the distribution line has been neglected. However for an overall stability analysis of the distribution system the impedance of the line and the grid needs to be incorporated into the control strategy. The stability of the system with a single converter reported in chapter 4 is much higher compared to the stability of the system comprised of several converters with distribution line, transmission line and grid impedances as reported in chapter 5.

Most of the smart grids are not connected to the stiff power network and operate in islanding. In this case they are responsible to maintain the rated frequency. The frequency variation in smart grids is a common problem. If we see the expressions for the controller parameters in chapter 4 the variation in base frequency ω_b will directly influence the physical parameters (C and L_f) of the system. The time constants for both the current controller and the DC link voltage controller are also affected. This will have impact on the stability of the converter control system. The operating point of the bode plot will move either right or to the left giving lower values of phase margin with the variation in system frequency.

The investigation of the converter stability for the generation mode has been identified to be much higher than the case when converter behaves as a load. One of the reasons for this is the small improvement in the grid voltage as a result of injection of active power. However, surprisingly the system is stable even for very lower values of grid voltage. An analytical investigation of the converter control system in generation mode will be very helpful for understanding this phenomenon.

7.2 Transient Stability

The transient stability analysis reported in chapter 5 takes into consideration the impact of grid parameters and IG parameters on the stability of the system. The reactive current injection is introduced to increase the transient stability margins of the system. The activation of AC voltage controller is done only during the contingency. This is a very efficient use of it. However for highly inductive load as discussed in section 5.1.3 the recovery time of the

voltage after the fault is very high. The recovery time can be considerably reduced if the AC voltage controller is kept active until the voltage recovers the steady state value.

The increment in the current rating of the converter when it injects reactive current to support the voltage during contingency is not avoidable. The PI regulator of the AC voltage converter reacts to the AC voltage variations and injects a reactive current in proportional to the drop in the voltage. Therefore the higher voltage drop results in the higher current rating of the converter. Therefore current rating of the converter must always be high enough to provide the required ancillary services to the grid.

The results obtained for the comparison of centralized reactive injection by STATCOM and distributed reactive injection by power electronic loads provide plain indication of the benefits of distributed injection. However these results are obtained by retuning the AC voltage controller parameters for every single case. An intelligent control system with the ability to sense the changes in the system parameters would produce even better results. An example is the droop control for the parallel converters where the communication between the converters is possible. In this case each converter will inject the minimum amount of reactive current required to keep the system stable.

7.3 Power Flow Optimization

The reduction in total current for the power electronic loads in all the investigated cases is not substantive. The reason for this is that the change in the active component of the current and voltage is not large enough in response to the reactive injection. The system with very high overall inductance will show the significant decrease in the total current. The increase in inductance however will again result in more reactive power losses in the system.

The implemented distribution system lacks the information of the type of the DER used. Only the PE interface represents the DER. However this assumption is sufficient enough for this analysis as the implemented DER is fully capable of generating and absorbing the active and reactive powers when required. The implementation of DFIG wind turbine requires a PE interface which is usually a set of rectifier and inverter called switching power interface (SPI). In the presence of several power electronic loads the implementation of two DFIG based DERs would result in high harmonics in the system. On the other hand use of simple IG as a

distributed power source discussed in chapter 5 lacks the capability of reactive power generation. It absorbs reactive power from the grid instead.

Power losses are measured by using the difference between input and output power. In this procedure the value of total losses is correct, but the losses in each phase are unknown. The reduction in the overall power losses is reported to be 50%. The major parts of the remaining losses are the losses in the distribution lines. The distribution line losses include the switching losses in the converter and the losses in the converter filters in addition to the losses in the line resistance. Further decrease in the losses can only be achieved if the physical parameters of the distribution system are changed. Optimal selection of conductors with low per meter resistance in the distribution line will result in significant decrease in the losses.

In addition to the loss reduction another important advantage of the implemented methodology is the local voltage support as a result of distributed reactive injection by the loads. This small improvement in the local voltage will greatly increase the overall stability limits of the system in case of contingency.

Chapter 8: Conclusion and Future Work

This chapter briefly discusses the achievements of the thesis work. The results obtained for all parts of this thesis are summarized. Some suggestions regarding the future work are also given at the end.

8.1 Conclusion

A model of AC distribution system comprised of several power electronic loads is presented in this thesis. The implementation of AC distribution system is done in PSCAD/EMTDC software package and detailed time domain simulations are performed. The first part of this thesis only focuses on the basic control system and tuning rules for the converter controllers. For faster response modulus optimum method is used to derive the parameters of the current controllers and for higher phase margin symmetrical optimum method is used to derive parameters of DC link voltage controller. The focus is mainly put to investigate the stability and robustness of DC link voltage controller.

The stability of the converter control system is theoretically investigated for decreasing values of the grid voltage in frequency domain. Then time domain simulations confirm the validation of the frequency domain analysis. For upto 60% reduction in the grid voltage the DC link voltage controller shows a very stiff control. However when the grid voltage is reduced further then frequency domain analysis shows a low phase margin and a collapse in DC link voltage is observed through simulations. The converter control system has been proved to be more stable and robust in generation mode compared to when it behaves as a load. An analytical and simulation investigation show that the increase in the DC link capacitance results in less stable system if the other controller parameters are not modified accordingly.

The reactive current injection is used to mitigate the negative resistance instability in CPLs and instability caused by the generator and grid parameters in the distribution system. It has been shown that the reactive injection increases the transient stability margins of the system enabling the system to tolerate faults for longer time. However this improvement in stability limits comes at an expense of an increase in current rating of the converter. A simulation analysis is done which proves the advantages of using the distributed reactive injection through CPLs over the centralized reactive injection by a STATCOM in a distribution system.

Finally a power flow optimization of the distribution system is done. It has been identified by several simulations that the reactive injection by a CPL results in a small decrease in total current in the distribution line. The simulations also prove that the amount of reactive injection is independent of the number of CPLs in the system for a specific load power. A methodology is developed for reduction in losses, based on the use of local DERs and distributed reactive injection by the power electronic loads. The simulation results show that a reduction of more than 50% in overall losses in the distribution system is achieved.

The simulation results lead to the conclusion that the reactive injection by the power electronic loads in a distribution system not only increases the stability margins but it also results in reduction in power losses.

8.2 Future Work

In this work an effort is made to optimize the performance of AC distribution system with several power electronic interfaces. However further investigations are required for a good understanding of converter control stability, transient stability and loss reduction in the distribution system. Some of the possibilities to improve the presented work are listed as follows.

- An analytical investigation of the converter control system in generation mode to find out the reasons for higher stability.
- Study and possible extension of the tuning rules for AC voltage controller.
- An analytical investigation of the impact of converter filters on the converter control system stability.
- An analytical investigation of stability of overall distribution system taking into account all the possible factors effecting the stability including the generator and grid parameters.
- Real time modification of controller parameters in online systems using predictive control to eliminate the instability effects caused by the variation in grid parameters.
- An investigation on the role of controlled CPLs for voltage support in relation to Low Voltage Ride Through (LVRT) in AC distribution systems.
- An analytical study of the critical share of CPLs in a distribution system for voltage support.

- Implementation of droop control with a communication mechanism between parallel converters to get better reactive power sharing.
- An investigation of loss minimization in an extended distribution system with combination of active and passive loads.
- Possible extension of the loss minimization methodology to the residential distribution systems.

References

[1] K.J.P. Macken, K. Vanthournout, J. Van den Keybus, G**.** Deconinck, and R.J.M. Belmans. "Distributed control of renewable generation units with integrated active filter". IEEE Transactions on Power Electronics PE, 2004.

[2] R. M. Moreno, J. A. Pomilio, L. C. Pereira da Silva and S. P. Pimentel "Control of Power Electronic Interface for Renewable Energy Sources Under Distorted Grid Voltage". IEEE, 2004.

[3] A. Emadi. "Modeling of Power Electronics Loads in AC Distribution Systems Using the Generalized State-Space Averaging Method". In IEEE Trans. on Industrial Electronics, vol. 51, no. 5, October 2004, pp. 992-1000.

[4] Marta Molinas, Junji Kondoh. "Power Electronic Loads as Providers of Reactive Power Ancillary Service to the Grid: Analytical and Experimental study". In EPE 2009 – Barcelona ISBN: 9789075815009.

[5] M. Molinas, D. Moltoni. G. Fascendini, J.A. Suul, R. Faranda, T.M. Undeland. "Investigation on the role of power electronics controlled constant power loads for voltage support in distributed AC systems". In Proc. of IEEE Power Electronics Specialists Conference, Rodhes, Greece, June 2008.

[6] M. Molinas, D. Moltoni, G. Fascendini, J.A.Suul, T. Undeland. "Constant power loads in distributed AC systems: an investigation of stability". In Proc. of IEEE Industrial Electronics Society Conference ISIE 2008, Cambridge, 2008.

[7] G. Pepermans, J. Driesen, D. Haeseldonckx,W. D'haeseleer and R. Belmans. "Distributed Generation:Definition, Benefits And Issues". IEEE 2003.

[8] A. Bracale, C. Di Pema, M. Mangoni, D. Proto. "Dispersed generators providing ancillary services through power electronic interfaces: A hybrid system". 2008 43rd International Universities Power Engineering Conference [88-89884-09-6] Bracale.

[9] B Kroposki, C Pink, R DeBlasio, H Thomas, M Simoes. "Benefits of power electronic

interfaces for distributed energy systems". 2006 IEEE Power Engineering Society General Meeting [1-4244-0493-2] Kroposki.

[10] Marta Molinas. "The Role of Power Electronics in Distributed Energy Systems". The 5th AIST Symposium on Distributed Energy Systems, Tokyo, Japan, 9 December 2008.

[11] Philip P. Barker, Robert W. de Mello. "Determining the Impact of Distributed Generation on Power Systems: Part 1 - Radial Distribution Systems". IEEE 2000.

[12] Nadeem Jelani. "Transient voltage support in distributer power systems". Specialization Project, Norwegian University of Science and Technology, Jan.2010.

[13] Jan Machowski, Janusz Bialek & Dr. Jim Bumby. "Power System Dynamics, Stability and Control". 2nd Edition Wiley, 2008.

[14] Ali Emadi, Alireza Khaligh, Claudio H. Rivetta, Geoffrey A. Williamson. *"*Constant Power Loads and Negative Impedance Instability in Automotive Systems: Definition, Modeling, Stability, and Control of Power Electronic Converters and Motor Drives*"*. IEEE Transactions on vehicular technology, vol. 55, no. 4, July 2006.

[15] P. J. M. Heskes, J. M. A. Myrzik, W. L. Kling. "Power Electronic Loads With Negative Differential Impedance in a low Voltage Distribution System". 20th International Conference on Electricity Distribution, Prague, 8 – 11 June 2009.

[16] A. B. Jusoh. "The instability Effect of constant power loads". In Proc. of National Power and Energy Conference, Malaysia 2004, pp. 175-179.

[17] Juan Dixon, Luis Morán, José Rodríguez, and Ricardo Domke. "Reactive power compensation technologies: State-of-the-art review". In Proc. of the IEEE, 93(12):2144–2162, December 2004.

[18] M. Elnashar, M. Kazerani, R. El Shatshat, and M. M. A. Salama. "Comparative Evaluation of Reactive Power Compensation Methods for a Stand-Alone Wind Energy Conversion System". Power Electronics Specialists Conference, PESC 2008. IEEE.

[19] Duilio Moltoni and Gabriele Fascendini. “Voltage support in ac distribution systems by power electronic loads”. Masters thesis, Politecnico Di Milano, 2007.

[20] Innocent **E** Davidson, Nelson M ljumba. ”Optimization Model for Loss Minimization in a Deregulated Power Distribution Network”. IEEE Africon 2002.

[21] M. A. Kashem, An D. T. Le, M. Negnevitsky, and G. Ledwich. ”Distributed Generation for Minimization of Power Losses in Distribution Systems”. 1-4244-0493-2006. IEEE

[22] R. J. Sarfi, M. M. A. Salama, A. Y. Chikhanii. “A survey of the state of the art in distribution system reconfiguration for system loss reduction”. 1994, Published by Elsevier Science B.V.

[23] G. CELLI, M. LODDO, F. PILO, A. ABUR. “On-Line Network Reconfiguration For Loss Reduction In Distribution Networks With Distributed Generation”. 18th International Conference on Electricity Distribution, Turin, 6-9 June 2005.

[24] R. F. Arritt, *Member*, R. C. Dugan, D. L. Brooks, T. A. Short, and Karen Forsten. “Techniques for Analyzing Distribution System Efficiency Alternatives”. 978-1-4244-4241. 2009 IEEE.

[25] Jinxiang Zhu, Griff Bilbro, and Mo-Yuen Chow. “Phase Balancing using Simulated Annealing”. IEEE Transactions on Power Systems, Vol. 14, No. 4, November 1999.

[26] Roger Lawrence. “Voltage Optimization, Achieving Regulated Balanced Voltage on 600 V Distribution System”. IEEE Industry Applications Magazine SEP-OCT 2006.

[27] Rakesh Ranjan. Ashvini Chaturvedi, Parmal Singh Solanki and D. Das. “Optimal Conductor Selection Of Radial Distribution Feeders Using Evolutionary Programming” 0-7803-7651- IEEE. 2003.

[28] T. Griffin, K. Tomsovic, and D. Secrest A. Law. “Placement of Dispersed Generations Systems for Reduced Losses”. In Proceedings of the 33rd Hawaii International Conference on System Sciences – 2000.

[29] Richard E. Brown, Lavelle A. A. Freeman. "Analyzing the Reliability Impact of Distributed Generation". 0-7803-7173-9/01.2001 IEEE.

[30] Carmen L. T. Borges and Djalma M. Falcao. "Impact of Distributed Generation Allocation and Sizing on Reliability, Losses and Voltage Profile". 2003 IEEE Bologna PowerTecb Conference, June 23-26, Bologna, Italy.

[31] N. Mohan, T. Undeland, W. Robbins. "Power Electronics: Converters, Applications, and Design" J. Wiley & Sons, 2003.

[32] Jorun Irene Marvik. "Nettstabilitet i vindpark med asynkrongeneratorer". Master Thesis, Norwegian University of Science and Technology, June 2004.

[33] Ned Mohan. "Advanced Electric Drives: Analysis, Control and Modeling Using Simulink" MINPERE.

[34] S. K. Chung. "Phase-locked loop for grid-connected three-phase power conversion systems". IEE Proc-Electr. Power Appl., Vol. 147, No. 3, May 2000.

[35] Ruihua Song et al. "VSC based HVDC and its control strategy". IEEE/PES Trans. And Distrb. Conference and Exhibition, 2005.

[36] Chandra Bajracharya. *"*Control of HVDC Light for Wind Power*"*. Masters thesis Norwegian University of Science and Technology, June. 2008.

[37] Chandra Bajracharya, Marta Molinas, Jon Are Suul, Tore M Undeland. "Understanding of tuning techniques of converter controllers for VSC-HVDC". NORPIE-2008, June 9-11, Helsinki.

[38] Ned Mohan. "Electric Drives: An Integrative Approach". MINPERE.

[39] Katsuhiko Ogata. "Modern Control Engineering". (4th Edition).

Appendix A

A.1 Clark and Inverse Clark Transformation

α -axis is aligned with the three phase a-axis to simplify the analysis. The matrix for clark transformation is

$$\begin{pmatrix} v_\alpha \\ v_\beta \\ v_0 \end{pmatrix} = \frac{2}{3}. \begin{pmatrix} 1 & -\frac{1}{2} & -\frac{1}{2} \\ 0 & \frac{\sqrt{3}}{2} & -\frac{\sqrt{3}}{2} \\ \frac{1}{2} & \frac{1}{2} & \frac{1}{2} \end{pmatrix} \cdot \begin{pmatrix} v_a \\ v_b \\ v_c \end{pmatrix} \qquad \text{(A.1)}$$

Where v_0 is the zero sequence voltage. It has non zero value only when there is any unbalanced condition. For $v_0 = 0$ equation A.1 becomes

$$\begin{pmatrix} v_\alpha \\ v_\beta \end{pmatrix} = \frac{2}{3}. \begin{pmatrix} 1 & -\frac{1}{2} & -\frac{1}{2} \\ 0 & \frac{\sqrt{3}}{2} & -\frac{\sqrt{3}}{2} \end{pmatrix} \cdot \begin{pmatrix} v_a \\ v_b \\ v_c \end{pmatrix} \qquad \text{(A.2)}$$

The matrix for Inverse-Clark transformation is therefore written as

$$\begin{pmatrix} v_a \\ v_b \\ v_c \end{pmatrix} = \frac{2}{3}. \begin{pmatrix} 1 & 0 \\ -\frac{1}{2} & \frac{\sqrt{3}}{2} \\ -\frac{1}{2} & -\frac{\sqrt{3}}{2} \end{pmatrix} \cdot \begin{pmatrix} v_\alpha \\ v_\beta \end{pmatrix} \qquad \text{(A.3)}$$

A.2 Park and Inverse Park Transformation

The matrix for park transformation is

$$\begin{pmatrix} v_d \\ v_q \end{pmatrix} = \begin{pmatrix} \cos\theta & \sin\theta \\ -\sin\theta & \cos\theta \end{pmatrix} \cdot \begin{pmatrix} v_\alpha \\ v_\beta \end{pmatrix} \tag{A.4}$$

The inverse park transformation represented equation A.5 is

$$\begin{pmatrix} v_\alpha \\ v_\beta \end{pmatrix} = \begin{pmatrix} \cos\theta & -\sin\theta \\ \sin\theta & \cos\theta \end{pmatrix} \cdot \begin{pmatrix} v_d \\ v_q \end{pmatrix} \tag{A.5}$$

Same equations are used for phase currents.

Appendix B

B.1 Transient Stability Analysis

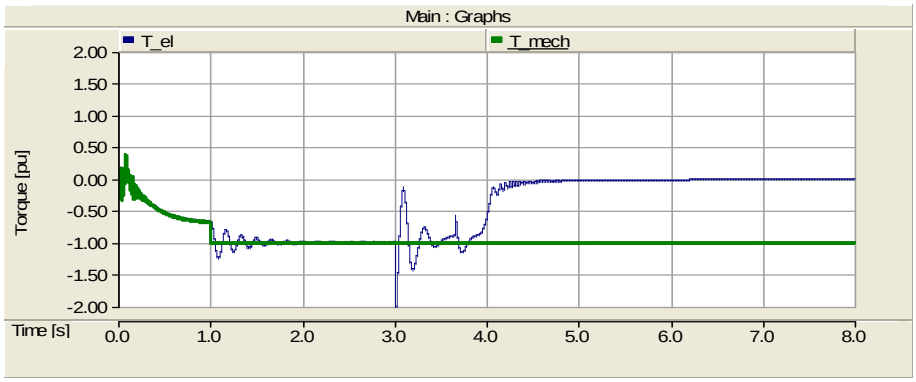

Figure B.1–Induction generator losing control of electromagnetic torque

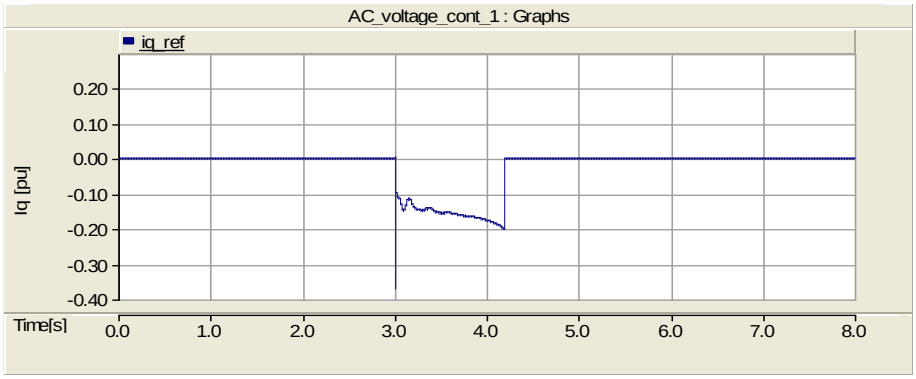

Figure B.2–Injected reactive current from CPL1 during the fault

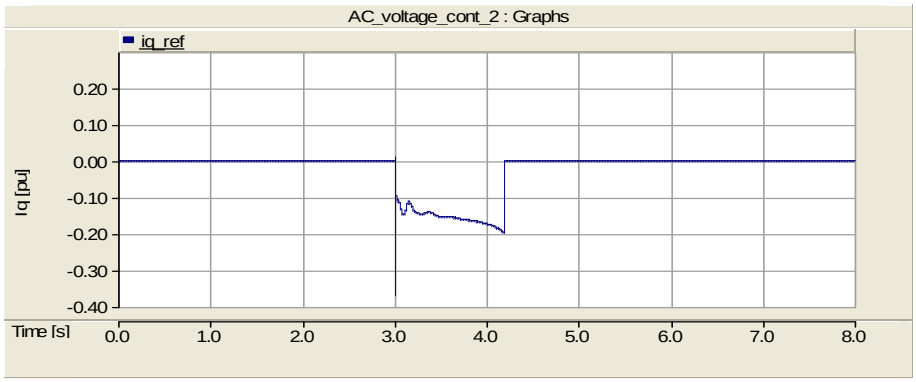

Figure B.3–Injected reactive current from CPL2 during the fault

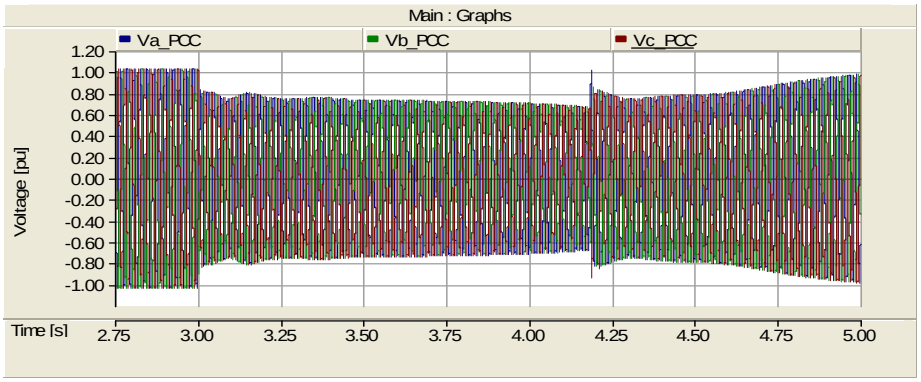

Figure B.4–Corresponding zoom of the voltage at PCC

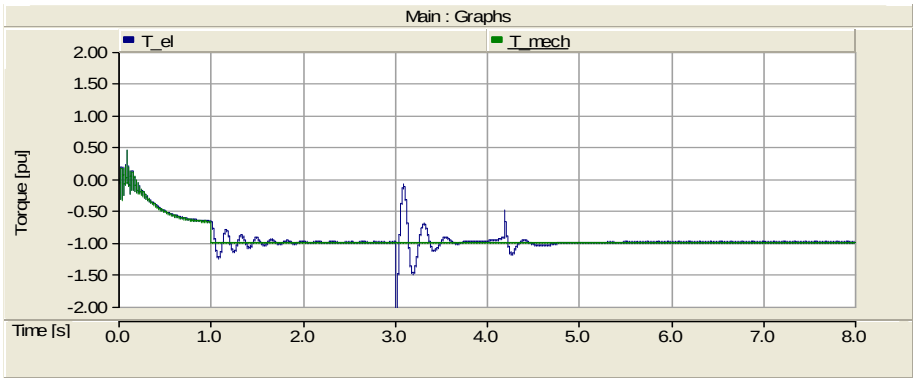

Figure B.5–Generator regaining the torque control

Type of Loading	Regulation	CCT
Case 1: 80% CPL	*P* constant only	2.95 s
80% CPL	*P* constant and *Iq*	4.3 s
Case 2: 40% CPL, 40% IM	*P* constant only	2.1 s
40% CPL, 40% IM	*P* constant and *Iq*	3.1 s
Case 3: 20% CPL, 60% IM	*P* constant only	1.4 s
20% CPL, 60% IM	*P* constant and *Iq*	1.9 s

Table B.1– Summary of the simulation results reported in [12] with J=10 [s]

Appendix C

C.1 PSCAD Models for Converter Control System Stability

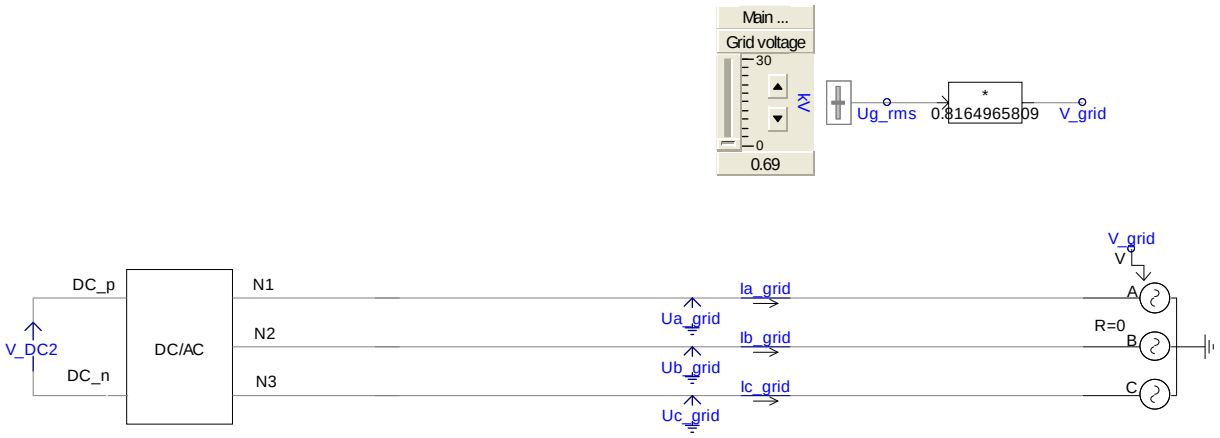

Figure C.1– Model for Converter Control System Stability

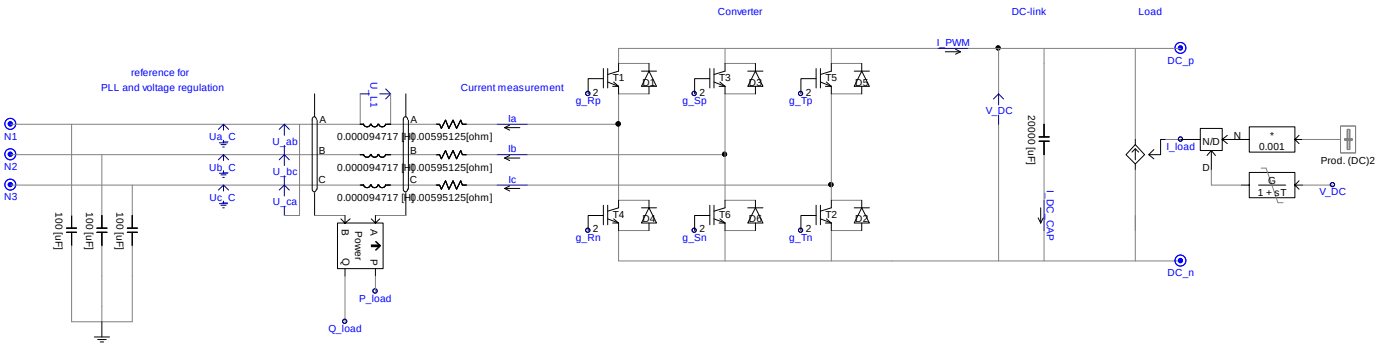

Figure C.2– Implemented Converter

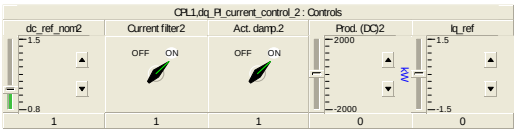

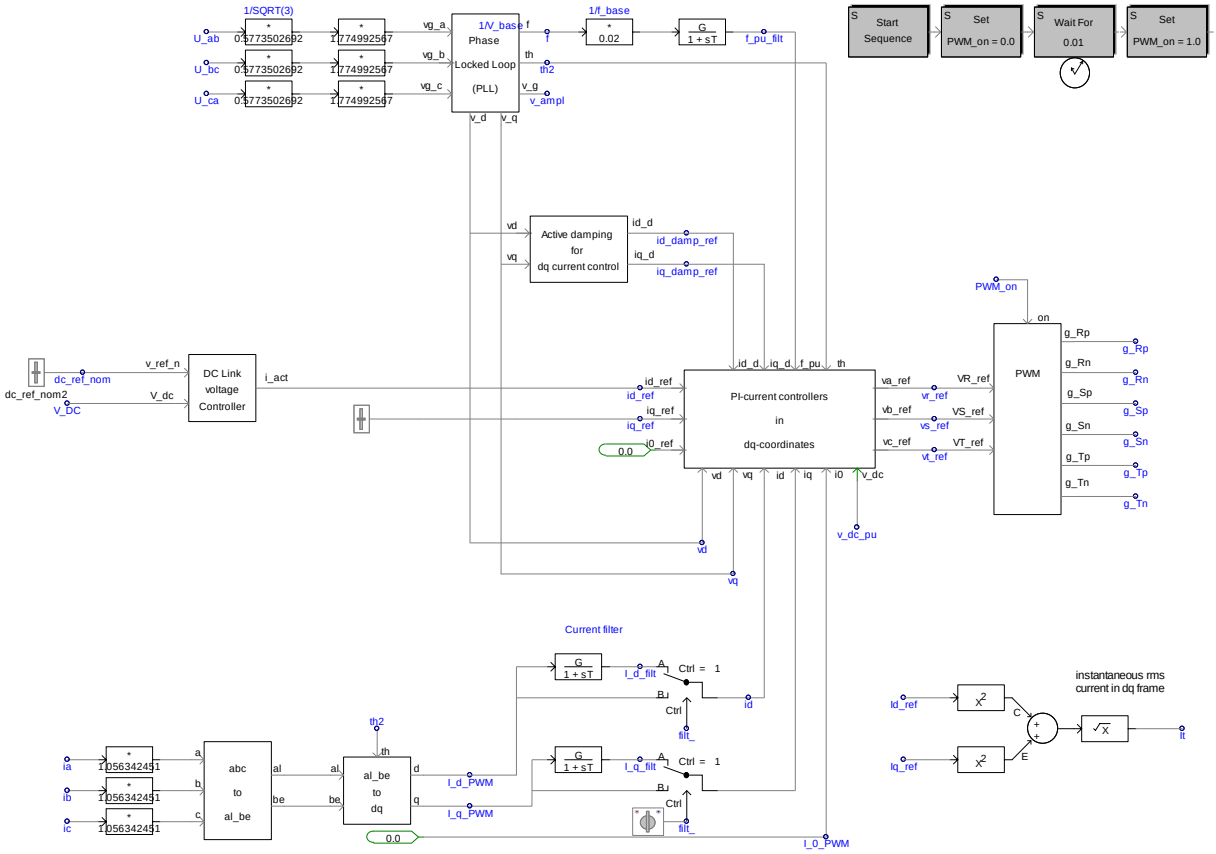

Figure C.3– Implemented Converter Control System

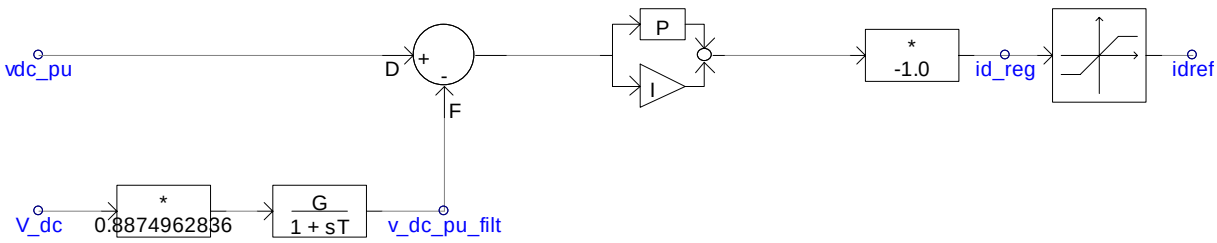

Figure C.4– DC Link Voltage Controller

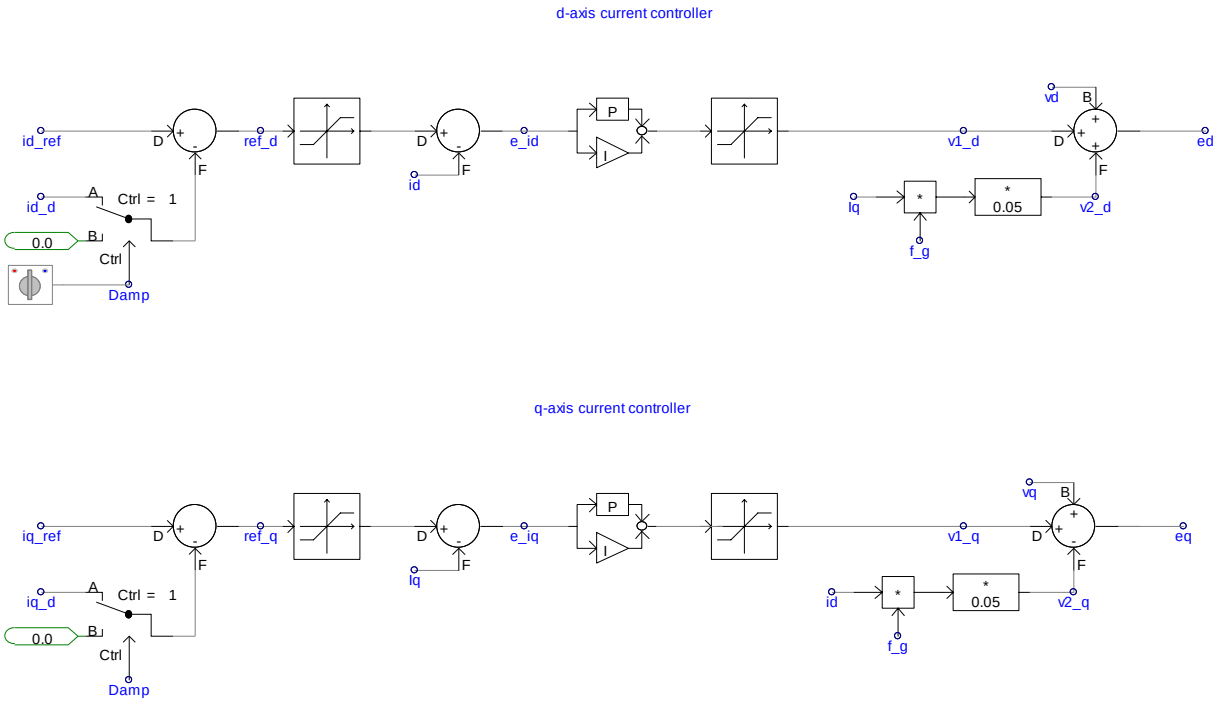

Figure C.5– Current Controllers

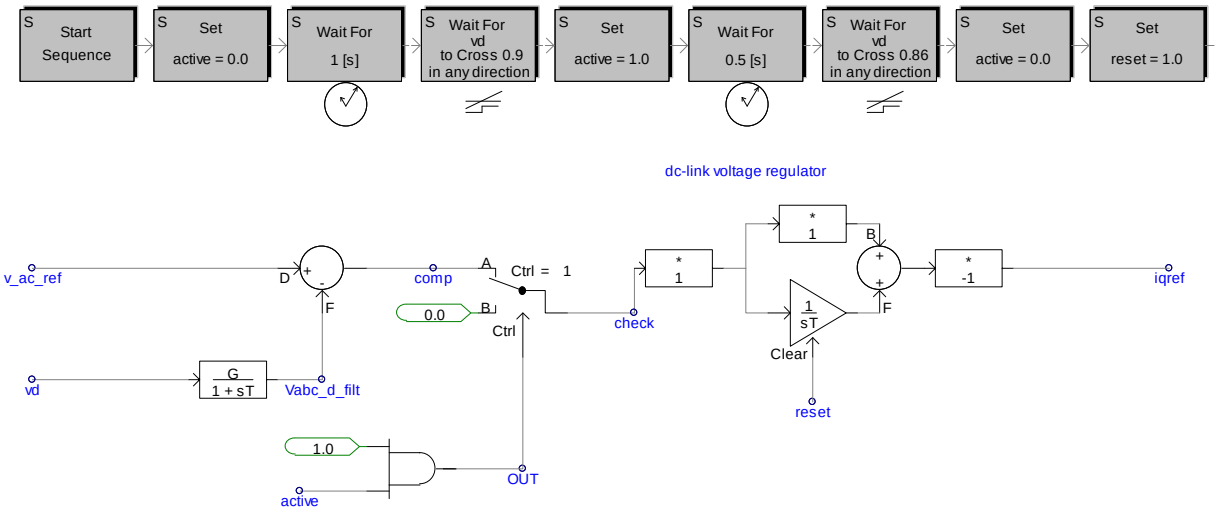

Figure C.6– AC Voltage Controllers

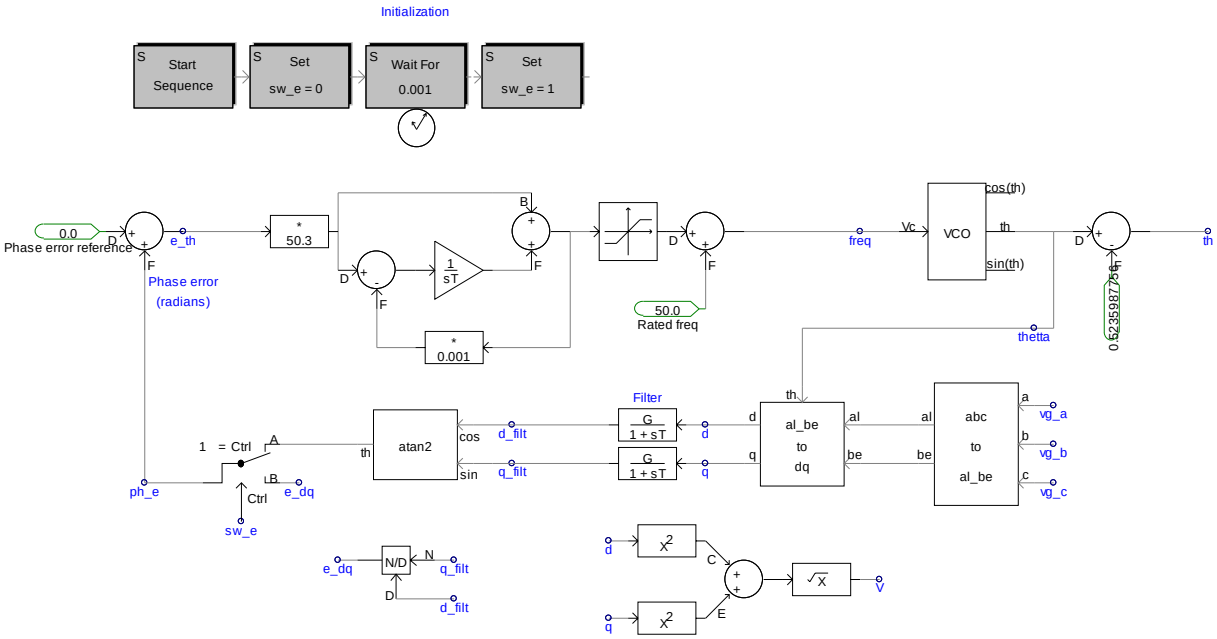

Figure C.7– Phase Locked Loop

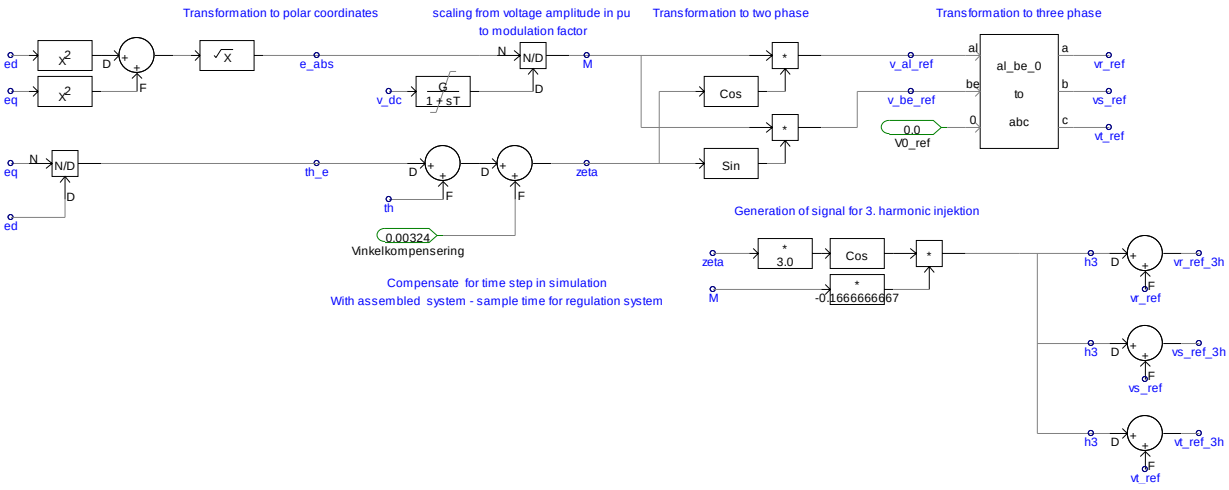

Figure C.8– Third Harmonic Injection for PWM

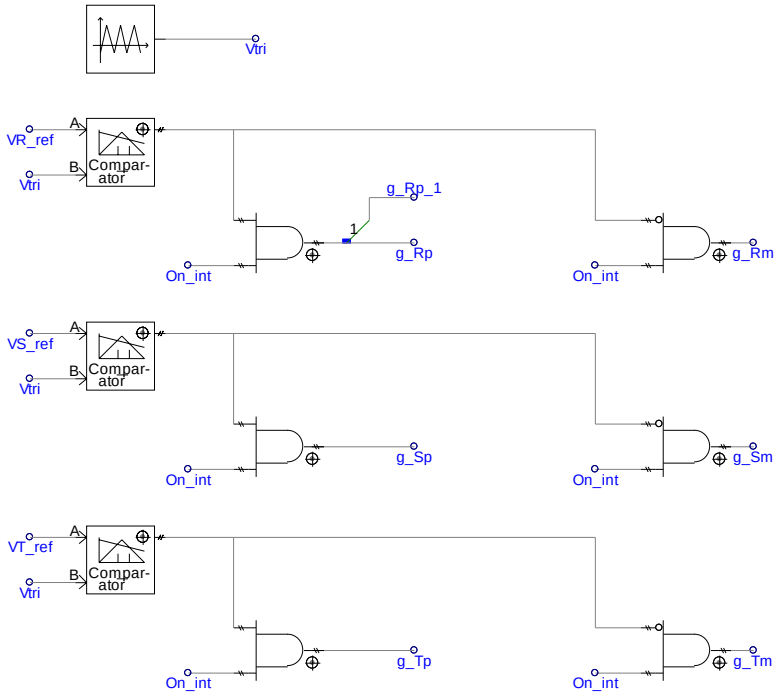

Figure C.9– Pulse Width Modulation

Appendix D

D.1 Transient Stability Models

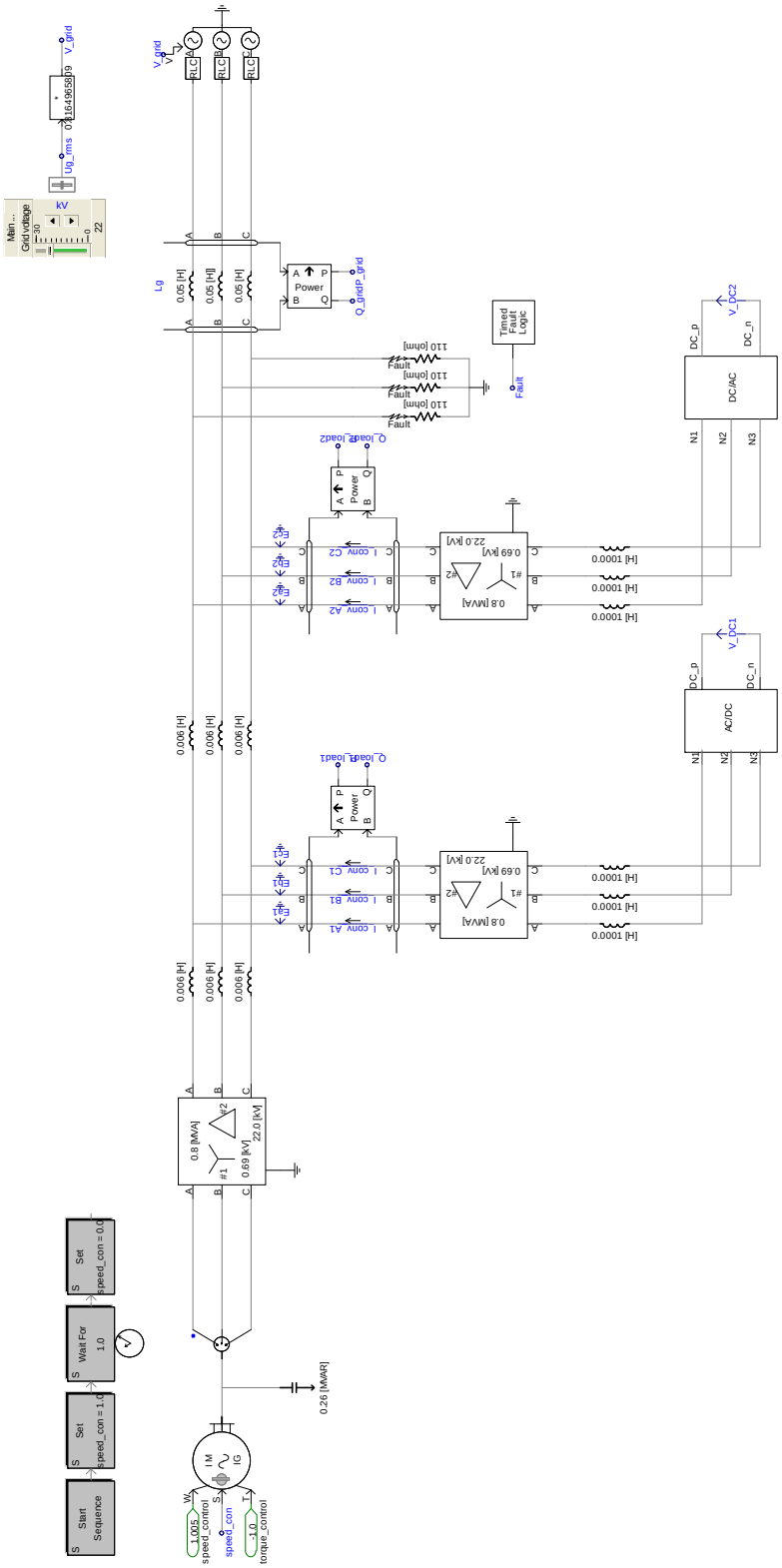

Figure D.1 – Distribution System with Two CPLs and an IG

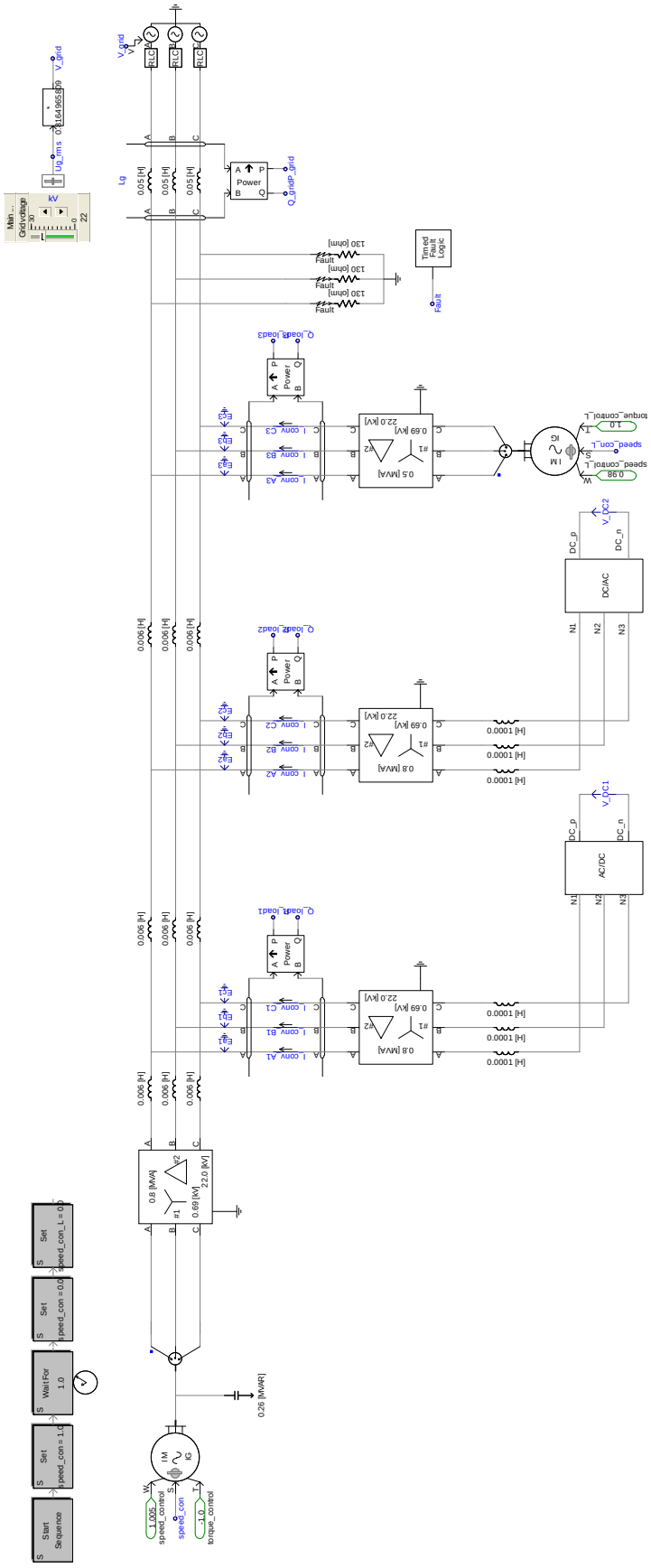

Figure D.2 – Distribution System with Two CPLs and an IM

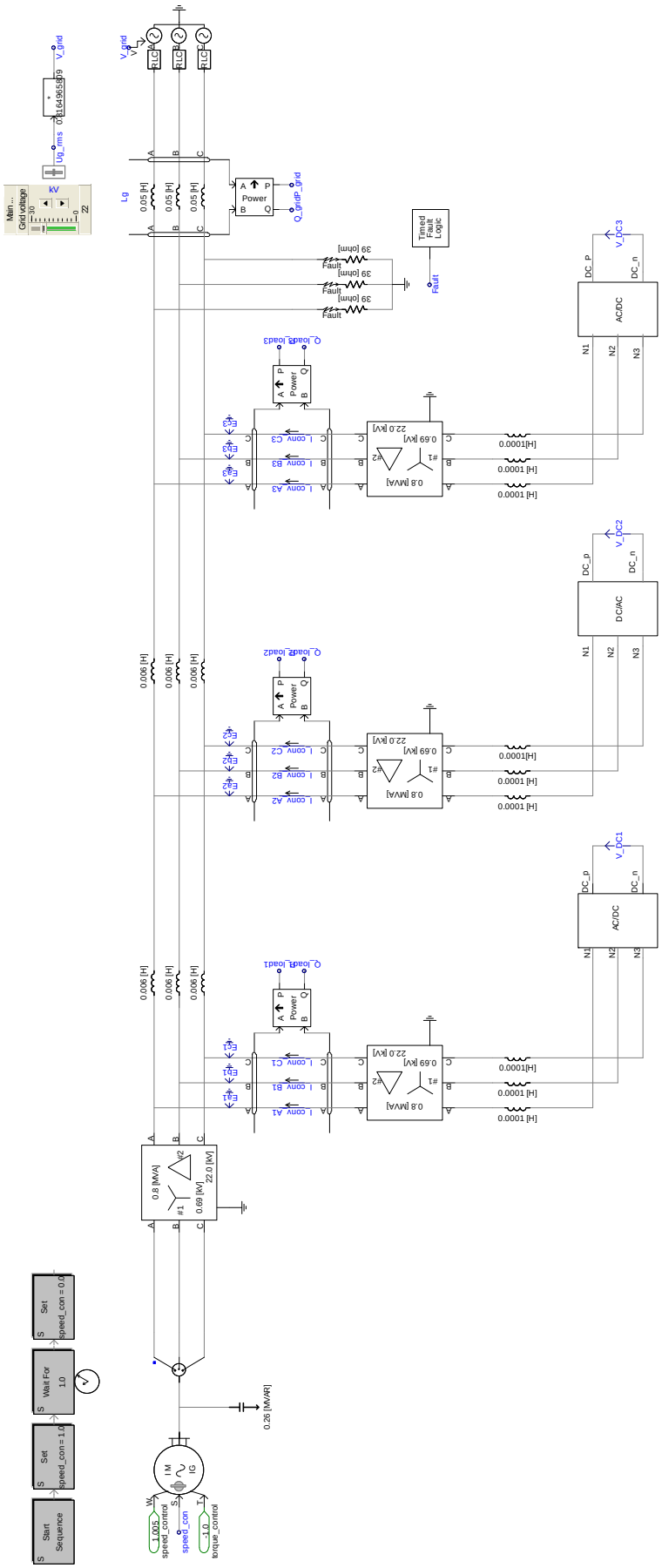

Figure D.3 – Distribution System with a STATCOM and CPLs

Appendix E : Paper presented in IEEE-ISIE July 4-7 ,2010 Bari, Italy

Optimal use of power electronic interfaces for loads in distributed systems

Nadeem Jelani, Marta Molinas
Norwegian University of Science and Technology
Department of Electric Power Engineering
Trondheim, Norway
Email: jelani@stud.ntnu.no

Abstract- **This article investigates how power electronic interfaces for loads provide reactive power in case of abnormal voltage conditions. An evaluation of voltage support is done for different values of voltage sags when the power electronic interface provides with reactive current. The stability margins of the distributed system are investigated for different types of loads and it is proved that the higher the share of controlled constant power loads in the system the higher the critical clearing time of the voltage. The incremental current rating of the converter when providing additional reactive current is investigated. Comparison is made between a centralized STATCOM and distributed reactive current compensation implemented in the form of controlled constant power loads, it is observed that it is always advantageous to use distributed compensation because the amount of reactive current injected is lower for achieving the same stability margins of the system.**

Keywords: Distributed Energy Systems, Constant Power Loads, Voltage Source Converters, STATCOM

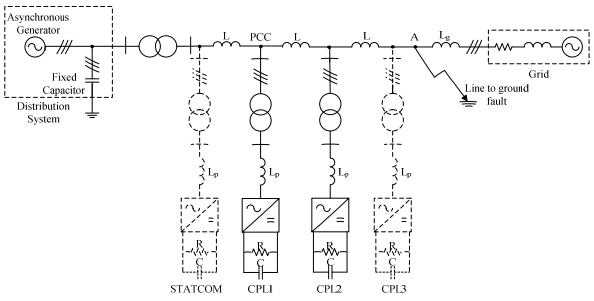

Fig. 1. PSCAD/EMTDC model of the AC distribution system under investigation

I. INTRODUCTION

Unlike the large traditional electric power system, the distributed energy system is a small or medium scale power generation system. Being close to the load centre this scheme has the advantage of having small transmission distances and transmission voltages and therefore low transmission losses [1]. An increasing practice these days is to connect loads and sources to the three phase AC system through the power electronic interfaces. Different ways of handling these interfaces greatly affect the operation and compensation of these power systems. By allowing injection of reactive current by power electronic interface would give the possibility to support the system voltage [2]. Operating margins of the electric grid stability, reliability and efficiency can be substantially improved [1]-[2]. Among electric loads, Constant Power Loads (CPLs) interfaced to the grid by active rectifiers, are one of the most destabilizing types of loads under abnormal voltage conditions [1]-[5]. CPL is a load which draws a constant amount of active power irrespective of any drop in the system voltage. The behaviour of CPL during different levels of fault is simulated in PSCAD/EMTDC software package. A drop in the voltage results in an increase in the active component of current and vice versa, leading to negative incremental resistance. This phenomenon is discussed in this paper and the results show that the injection of the reactive current by the controller could be an effective remedy for this. Simulation results presented in the paper show how the voltage stability margins can be greatly improved with different shares of controlled constant power loads. Distributed reactive current compensation has been investigated and is proved to be more advantageous compared to the centralized compensation by a STATCOM.

II. SIMULATION MODEL

The schematic representation of the investigated system is shown in Fig.1, it represents a real distributed generation connected to the grid and three constant power loads connected along the line. The line is connected to the main grid through the inductance Lg, and there is an inductance L corresponding to the line between the three different loads. The constant power load is a tightly regulated Voltage Source converter (VSC) absorbing constant power and is able to inject reactive power into the network and thereby providing ancillary service to the grid. DC side is supposed to behave as a constant DC power source. Fig. 2 shows the CPL from converter filter to DC-link and load. The voltage source

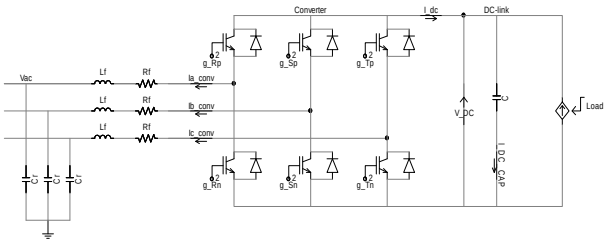

Fig. 2. The implemented converter with load as an example of interface for constant power loads (CPL) in AC distribution system

converter consists of IGBT switches with anti-parallel diodes that will conduct reverse current. Switching of IGBT is done by a pulse width modulation (PWM) technique at a frequency of 5 [kHz]. The load is modelled as a dependent current source that use a manually specified value of power divided by measured dc voltage [6]. Vector control technique is used for the regulation of AC/DC converter. In this way an independent control of active and reactive component of the current can be achieved. If we are able to control the DC link voltage to a constant value the active input voltage to the controller can be kept as constant [3]. This is achieved by the implementation of a DC link controller in the control strategy. The controlled DC voltage produced by these PWM rectifiers is much higher than that produced by the diode rectifiers[7],[8]. PWM converters have the inherent capability to compensate for the voltage drop by injecting reactive component of the current [9]. For a CPL to behave as an active front end converter and to be able to inject an additional reactive component of the current, an AC voltage controller is also implemented. It works in a way that it injects the reactive power into the network under abnormal voltage conditions and becomes inactive at the end of the fault. The next section will illustrate the negative input resistance exhibited by the load in this simulation model.

III. IMPACT OF CONSTANT POWER LOAD ON VOLTAGE

Negative resistance or negative differential resistance (NDR) is a characteristic of electrical circuit element during which at a specific range of voltage the current decreases as a function of voltage [5]. For a CPL an increase in voltage will result in a decrease of the active component of the current and a decrease in voltage will result in an increased active component of current. The input resistance *Rcpl* is defined by the ratio of small-signal changes in input voltage over the small-signal input current:

$$Rcpl \simeq \frac{\Delta V}{\Delta I}$$

and this value will depend on the converter operating point. The negative input resistance can be calculated by considering that the input power and output power of a CPL are equal, that is;

$$P_{in}=P_o=v \cdot i \text{ and } v=\frac{P}{i}.$$

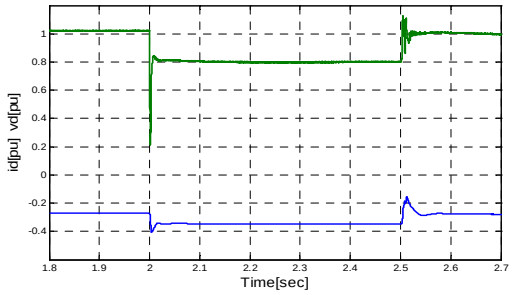

Fig. 3. d-axis current and voltage without reactive current injection

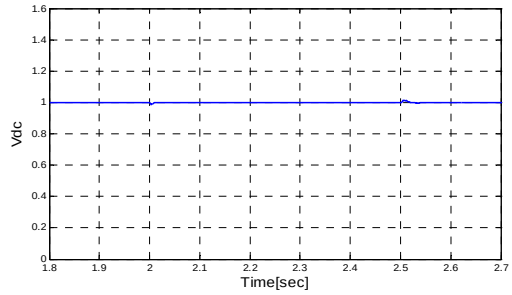

Fig. 4. DC link voltage when there is 20 % voltage drop in AC voltage

Differentiating the voltage with respect to the current yields:

$$\frac{dv}{di}=-i^{-2}\cdot P=-\left|\frac{P}{i^2}\right|=-\left|\frac{V^2}{P}\right|=R_{cpl}$$

Above expressions are used to calculate the small-signal input resistance of a constant power load; the resistance is negative and is also non linear, depending upon the current and voltage [5]. In order to observe the relationship between converter terminal voltage and the active component of the current, a resistive three phase to ground fault is simulated in the grid between the converter and grid inductance Lg for a period of 0.5 sec as shown in Fig.1. By decreasing the value of the fault resistance, reduced values of the converter terminal voltage can be obtained. In this simulation model only one CPL is used taking 30% of power generated by the induction generator. Fig.3 shows the values of d-component of voltage and current on the AC side of the converter when a voltage drop of 20% compared to nominal voltage is simulated with no injection of the reactive current. Because of the presence of DC link voltage controller, there is no drop in it as shown in Fig.4. Now the automatic control of AC voltage controller is disabled and manual control is enabled to inject a specified amount of reactive current for observing its effects on the voltage during fault.Fig.5, and Fig6, represent the same situation with 0.2 pu and 0.4 pu reactive current injection respectively during the fault, evidencing 3% and 6% increase in the voltage for both the cases. Moreover

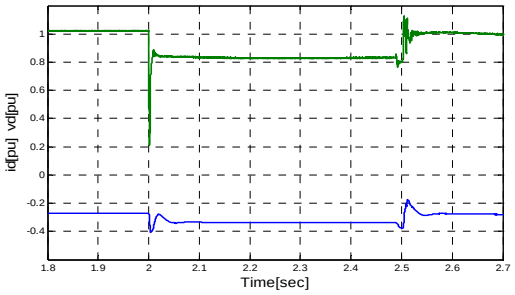

Fig. 5. d-axis current and voltage with 0.2 pu iq- injection

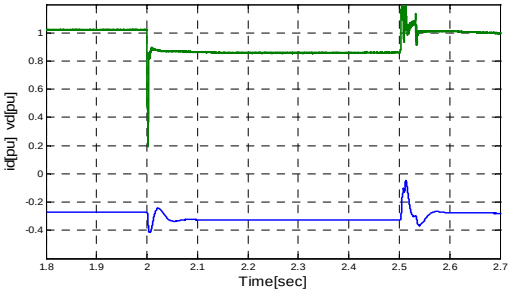

Fig. 6. d-axis current and voltage with 0.4 pu iq- injection

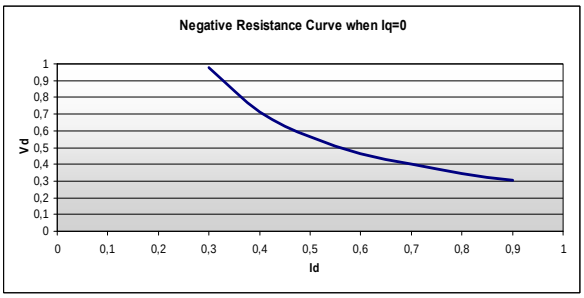

Fig. 7. Negative incremental resistance behaviour of the CPL with no reactive. compensation

a reduction of 1.2 % and 2.2 % in the active component of current can be seen which is because of a slight improvement in the voltage thereby keeping the power of the CPL constant. The curves in Fig.7 and Fig.8 demonstrate the negative resistance characteristics of the CPL for all the studied cases confirming the inverse relation between voltage and current. However there is a small improvement in the negative resistance curve when more reactive current is injected which is vital for the improvement of the stability margins of the system as it will be explained in subsequent sections.

IV. IMPACT OF REACTIVE CURRENT INJECTION ON STABILITY MARGINS

To understand the effects of controlled CPLs on the stability margins of the system, simulation model presented in Fig.1 is considered. The load is modelled as a dependent current source that use a manually specified value of power divided by measured DC voltage [6]. A DC link voltage

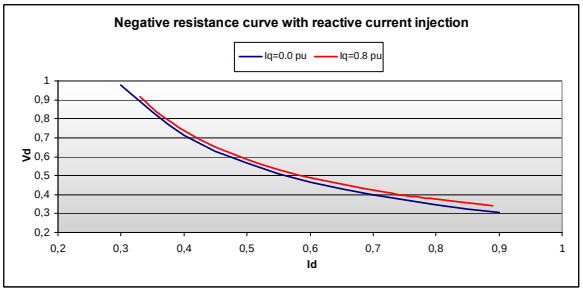

Fig. 8. Negative incremental resistance behaviour of the CPL with reactive compensation

controller is implemented to keep the DC voltage constant thereby ensuring a constant power being fed into the load. An AC voltage controller is implemented in the control design to inject the reactive power into the network. Three cases with different load conditions are investigated and the effect of controlled CPL is observed on the stability limits of the system.

Case 1: 80% CPL

Two CPL models are used, with each CPL taking 40% of the power generated by the induction generator. A three phase line to ground fault is simulated at point A. Fault resistance is varied to get a voltage drop equal to 20% of the nominal voltage. Several simulations are carried under this condition to obtain the critical clearing time (CCT) which is the maximum time before the system becomes unstable due to voltage collapse. In the first simulation AC voltage controller is kept inactive and CCT is measured. Fig. 9a shows the simulation result. In the second simulation AC voltage controller is kept active, only during the fault and 0.2 pu reactive current is allowed to be dispatched into the network to compensate for the voltage drop. Fig. 9b presents the simulation result. A considerable difference in the CCT can be observed. When the AC voltage controller is active the CCT is 1.18 seconds compared to the previous case with CCT 645 ms when no reactive current compensation is allowed.

Table1
CCT for the studied cases

Type of loading	Regulation	CCT
Case 1: 80% CPL	P constant only	645 ms
80% CPL	P constant and Iq	1.18 s
Case 2: 40% CPL, 40% induction motor	P constant only	468 ms
40% CPL, 40% induction motor	P constant and Iq	660 ms
Case 3: 20% CPL, 60% induction motor	P constant only	340 ms
20% CPL, 60% induction motor	P constant and Iq	480 ms

Case 2: 40% CPL and 40% Induction motor

Stability of the system is investigated when the amount of load controlled by converters (CPLs) and that of uncontrolled one is equal. Two CPL are taking 40% of the total power generated by the induction generator and the third CPL is replaced with an induction motor also taking 40%

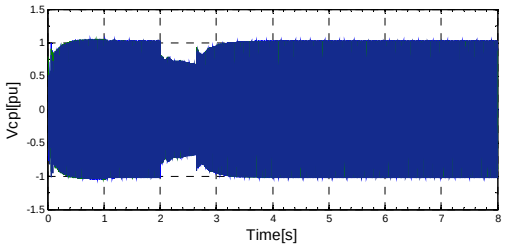

Fig. 9a. CCT for 80% share of CPL without reactive current control

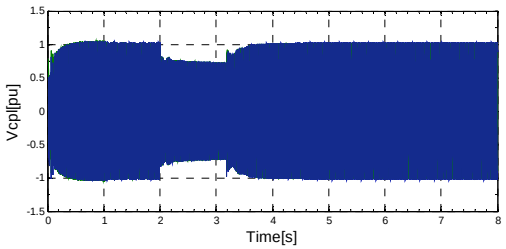

Fig. 9b. CCT for 80% share of CPL with reactive current compensation

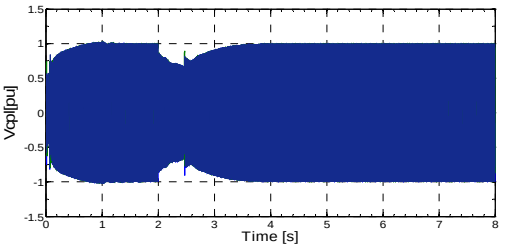

Fig. 10a. CCT for 40% CPL and 40% induction motor without reactive current control

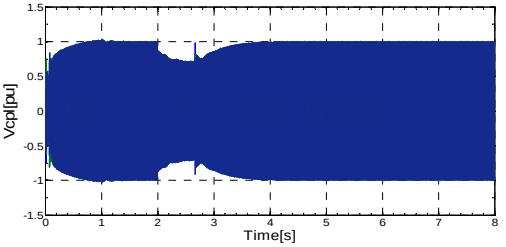

Fig. 10b. CCT for 40% CPL and 40% induction motor with reactive current compensation

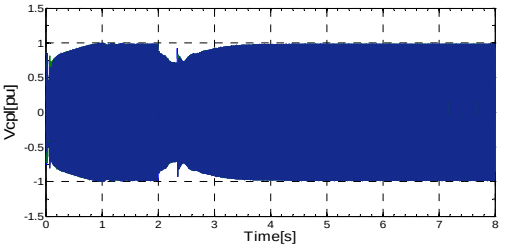

Fig. 11a. CCT for 20% CPL and 60% induction motor without reactive current control

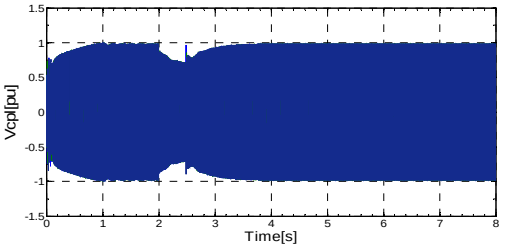

Fig. 11b. CCT for 20% CPL and 60% induction motor with reactive current compensation

of the induction generator power A three phase line to ground fault is simulated to obtain a voltage drop equal to 20% of the nominal voltage and critical clearing time (CCT) is observed. In the first simulation AC voltage controller is kept inactive and the CCT is measured. Fig. 10a shows the simulation result. In the second simulation AC voltage controller is set active only during the fault and 0.2 pu reactive current is allowed to be dispatched into the network to compensate for the voltage drop by both the CPLs. Fig. 10b presents the simulation result. Again a big increase in the CCT is observed for the case when controlled CPLs are used.

Case 3: 20% CPL and 60% Induction motor

In this case the amount of load controlled by converters (CPLs) is less and that of uncontrolled one is high. Two CPLs are taking 20% of the power generated by the induction generator and the third CPL is replaced with an induction motor taking 60% of the power generated. In the first simulation AC voltage controller is kept inactive and the CCT is measured. Fig.11a shows the simulation result. In the second simulation AC voltage controller is kept active during the fault and 0.2 pu reactive current is injected by both the CPLs. Fig 11b presents the simulation result. A big improvement in the stability margins is obtained for the later case. Fig.11c shows the induction generator completely losing control of its torque when the system becomes unstable.

The results from all the studied cases are presented in table 1 and signify the role of controlled CPL in improving the stability margins of the system. The best case is when the share of controlled CPLs is higher and the worst case is when the induction motor load is higher and the share of uncontrolled CPLs is lower. Therefore, the more the amount of load being controlled by CPLs the higher the stability limits of the system. However this improvement in the stability margins of the system comes at a cost of an increased current rating of the converter.

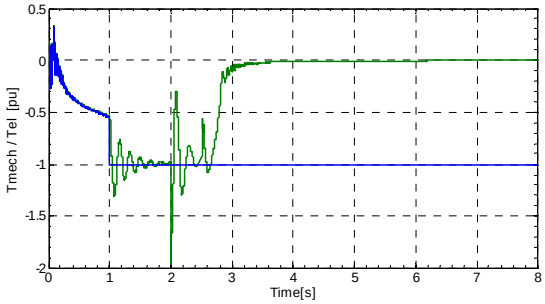

Fig. 11c. Induction generator losing its toque control when system became unstable

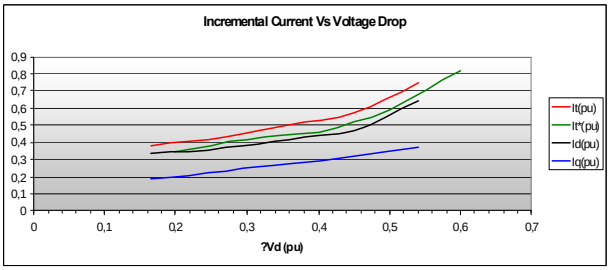

Fig. 12. Incremental current rating of the CPL as a function of voltage drop

V. INCREASE IN THE CURRENT RATING OF THE CONVERTER FOR PROVIDING REACTIVE CURRENT TO THE GRID

For investigation of the increased current rating of the CPL, two CPL model is considered, each taking 25% of the total induction generator power. Several simulations are carried out for taking different levels of voltage drop. During the fault the voltage cannot be kept constant and CPL injects maximum amount of reactive current to make the system stable. Fig.12 presents the simulation results. If there is no additional injection of reactive current, the total current rating required by the converter are represented by only the active component of current It*. When there is injection of reactive current by the converter the additional rating required is represented by the difference between It* when there is no injection of reactive current and the total current It in case of injection of reactive current. The total current It represents the quadratic sum of active and reactive components of current. For all levels of voltage drops the value of It* is higher than the value of only active component of current Id when converter injects the reactive current. This is because of the slight improvement in the voltage on the converter terminal as a result of reactive compensation, keeping the power drawn by the CPL constant. This improvement in the voltage is prominent as the same values of the fault resistances were used for both the cases It can also be seen that the deeper the voltage drop the higher the amount of reactive current injected to keep the system stable. However this increase in reactive current is not proportional to the decrease in the active component of the current. Therefore the required extra current rating of the converter are higher when drop in the voltage is deeper. Upto 60% of voltage drop this increase in the current rating is only 0.07 pu, which could be considered as an acceptable rise. This to a large extent also depends upon the control strategy implemented. However this rise in the current ratings of the converter could be compensated by an increase in the number of CPL producing reactive current connected to the line. Then a small amount of injected reactive current would be quite sufficient to achieve the same stability limits as would have achieved by lower number of CPLs injecting higher amount of current. In the next section simulations are carried out to compare the total reactive current injected by a centralized STATCOM with the case when the system is loaded with distributed CPLs with reactive current control.

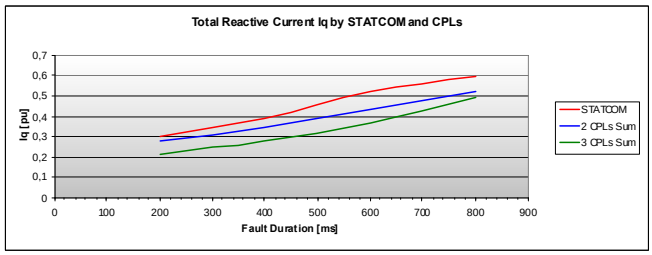

Fig. 13. Total reactive current Iq by STATCOM and CPLs

VI. DISTRIBUTED INJECTION Vs CENTRALIZED COMPENSATION

In this section an investigation is done in order to know whether it is advantageous to implement distributed compensation by CPLs compared to a centralized STATCOM. For this, different simulations are performed for different values of fault durations and the fault resistance is decreased upto a value beyond which the system is no more stable. Therefore, a comparison between the system with the STATCOM placed at the terminal of the transformer and two non controlled CPLs is made with the case of two or three CPLs with reactive current control without a centralized STATCOM. The total power taken by the load in all these cases is kept to 50% of the induction generator power. Fig.13 shows the results of these simulations. It is quite evident that the total reactive current injected by the centralized STATCOM is higher for all the fault durations simulated than the sum of reactive current injected by the CPLs. In fact the sum of reactive current injected in the case of three CPLs is even lower than the sum of reactive current by the two CPLs for all the fault durations to keep the system stable. For a fault duration of 100 ms, total amount of reactive current injected by one CPL belonging to a group of three distributed CPLs is almost four times lower than the total amount of reactive current injected by the centralized STATCOM. Therefore, it

can be concluded that the higher the number of controlled CPL the lower the total amount of current rating of the installed converters. Also implementation of two CPLs looks to be more efficient and optimal instead of a single centralized STATCOM with higher current rating. This lower current capacity can however be at the expense of an increase in the cost of the installed equipment.

VII. CONCLUSIONS

Efficient use of constant power loads interfaced through power electronic converters is demonstrated. Simulations are done in PSCAD/EMTDC software to verify the typical negative resistance behaviour associated with constant power loads and it is shown how this destabilizing effect can be reduced by the injection of reactive current and by reduction of the active component of current when the voltage is slightly improved by injecting reactive current. The stability limits of the system has been investigated under different load conditions and critical clearing time of the voltage is measured. It is demonstrated that the stability margins of the systems are higher for a case when there is an injection of reactive component of current by the CPL than the case when there is no reactive compensation. The higher the number of controlled CPL acting as a load the higher the critical clearing time of the system. The incremental current rating of the converter is studied and it is concluded that the deeper the drop in the voltage the higher the current rating required for the converter to keep the system stable. Finally, a comparison is performed between the total reactive current capacity of a centralized STATCOM and distributed compensation by the CPLs. The comparison proves advantages to the distributed reactive current compensation by the CPLs connected through power electronic converters rather than one centralized compensating device.

REFERENCES

[1] Marta Molinas "The Role of Power Electronics in Distributed Energy Systems" The 5th AIST Symposium on Distributed Energy Systems, Tokyo, Japan, 9 December 2008

[2] Marta Molinas, Junji Kondoh"Power Electronic Loads as Providers of Reactive Power Ancillary Service to the Grid: Analytical and Experimental study" in EPE 2009 - Barcelona ISBN: 9789075815009

[3] M. Molinas, D. Moltoni. G. Fascendini, J.A. Suul, R. Faranda, T. Undeland, "Investigation on the role of power electronics controlled constant power loads for voltage support in distributed AC systems," in *Proc. of IEEE Power Electronics Specialists Conference*, Rodhes, Greece, June 2008

[4] M. Molinas, D. Moltoni, G. Fascendini, J.A.Suul, T. Undeland, "Constant power loads in distributed AC systems: an investigation of stability," in *Proc. of IEEE Industrial Electronics Society Conference ISIE 2008*, Cambridge, 2008

[5] D. Moltoni, G. Fascendini, "Voltage Support in AC Distribution Systems by Power Electronic Loads," Master Thesis, Politecnico di Milano, Dec. 2007

[6] Bjørn Erik Strand, "Voltage Support in Distributed Generation by Power Electronics," Master Thesis, Norwegian University of Science and Technology, Jun. 2008

[7] Jaakko Antero Ollila, "A Novel Space Vector Control Strategy for reversible PWM-Rectifiers" IEEE /KTH Stockholm Power Tech conference June 1995

[8] S.N.Klachinikov, H.Berger "AC-Drive with Three Phase PWM Rectifier as a Reactive Power Compensator" IEEE /KTH Stockholm Power Tech conference June 1995

[9] Leopoldo Rossetto, Paolo Tenti, "Using Ac-Fed PWM Converters as Instantaneous Reactive Power Compensators" IEEE transactions on power electronics ISSN 0885-8993 CODEN ITPEE8, Jan 1992.